REMARKS/ARGUMENTS

Status of the Claims

Claims 1-8, 13-16, 19-20, and 22-23 were withdrawn from consideration by the Examiner in the Office Action. Claims 12 and 18 were canceled without prejudice or disclaimer by Applicant in this reply. Applicant reserves the right to pursue these claims in subsequent and pending applications. Claims 9-11, 17, 21, and 24 are pending and under consideration.

Amendment of Claims

Claim 9 was amended to more clearly define the "determining" step of the claimed method. The "determining" step is a contacting step that specifies contacting integrin alpha10 with an antibody. This contacting step finds support throughout the specification (for example, paragraph 112) and in now canceled claim 12.

Claim 17 was amended by including steps involved in the claimed method. These steps find support throughout the specification, for example, in paragraphs 27-30, 33, 97-90, and 95. None of the amendments added new matter.

Rejection under 35 U.S.C. § 112, second paragraph

Claims 9-12, 17-18, 21, and 24 were rejected under 35 U.S.C. § 112, second paragraph, as being indefinite. The Examiner objected to claim 9 as being indefinite for failing to include a "contacting step in which the reaction of the sample with the reagents necessary for the assay." Office Action, page 3. In response, Applicant has amended claim 9 to better define the "determining" step of the claimed method. This "determining" step is defined in the specification (for example, paragraph 112) and in now canceled claim 12 as a "contacting" step in which integrin alpha10 chain is

contacted with a binding agent having a binding site specific for the integrin alpha10

chain. Because this contacting step is now included in claim 9, claim 12 has been

canceled.

The Examiner objected to claim 17 as being indefinite for failing to "set forth any

steps involved in the claimed method/process." Office Action, page 3. In response,

Applicant has amended claim 17 to include such steps. These steps find support

throughout the specification, for example, in paragraphs 27-30, 33, 97-90, and 95.

Claim 18 has been cancelled.

By the above amendments and cancellations Applicant has addressed all

rejections raised under 35 U.S.C. § 112, second paragraph, and Applicant thus

respectfully requests that these rejections be withdrawn.

Rejection under 35 U.S.C. § 112, first paragraph

Claims 9-12, 17-18, 21, and 24 were rejected under 35 U.S.C. § 112, first

paragraph, as lacking enablement. The Examiner stated that the most relevant factors

for this rejection were "the scope of the claims, the amount of direction or guidance

provided, the lack of sufficient working examples, the unpredictability in the art and the

amount of experimentation required to enable one of skill in the art to practice the

claimed invention." Office Action, page 4. Applicant respectfully traverses.

Specifically, the Examiner questioned the clinical value of Applicant's strategies

because the specification allegedly fails to demonstrate a differential expression or a

correlation of the alpha10 chain in an atherosclerotic artery compared to a normal

artery. Office Action, page 4. Applicant respectfully disagrees with this assertion.

The specification clearly demonstrates differential expression of integrin alpha10 in the cells of atherosclerotic plaque and the cells of the normal artery tissue (see paragraphs 42 and 163, and Figure 2A). The staining in Figure 2A shows that expression of the integrin alpha10 chain is detected only on the surface of the cells in the atherosclerotic plaque, but not in the cells of the underlying normal artery tissue, including the smooth muscle cells of the media. A graphic illustration of the tissue structure of normal artery and artery containing an atherosclerotic plaque is provided to clarify this point. The illustration is taken from the widely used textbook "Molecular Cell Biology", Lodish et al., 5th Edition, W.H. Freeman and Company, New York, page 768. The tissue structure adjacent to the stained atherosclerotic plaque on the lower right side of the plaque in Figure 2A of the instant application comprises the media and adventitia of the normal artery wall, containing smooth muscle cells and connective tissue cells. Furthermore, the tissue structure adjacent to the stained atherosclerotic plaque on the lower left side of Figure 2A comprises the intima of the normal artery wall, containing smooth muscle cells. As evident from Figure 2A, the cells of the normal artery wall do not express detectable levels of integrin alpha10 chain. Hence, the specification shows differential expression of the integrin alpha10 chain in atherosclerotic plaque and normal artery tissue, with integrin alpha10 being expressed in the plaque but not the normal artery tissue.

The Examiner cited Lehnert et al. as teaching that integrin alpha10 is widely expressed in a panel of 24 tissue types. Office Action, page 4. Applicant notes that Lehnert et al. determined only expression of integrin alpha10 mRNA but did not investigate expression of integrin alpha10 protein. It is widely accepted, however, that

mRNA expression does not necessarily correlate with protein expression. In addition, Lehnert et al. observed two major transcripts of integrin alpha10, one of which, a 1.8 kb transcript, is too short to encode a full length integrin alpha10 protein (see first paragraph of Discussion, page 243). While it may encode a "truncated variant with an altered function", as speculated by Lehnert et al., it has not been demonstrated that this truncated transcript expresses any functional integrin alpha10 fragment. Moreover, Figure 5 of Lehnert et al. (referred to by the Examiner) shows the PCR amplification of an about 500 bases long fragment from the integrin alpha10 transcripts in various tissues. Since this amplified fragment may only reflect the presence of the truncated transcript described above, it is unclear how this fragment relates to integrin alpha10 protein expression.

The Examiner also cited WO99/51639 as teaching that integrin alpha10 is expressed in aorta (normal nonatherosclerotic artery). Office Action, page 4. Applicant notes that this study also analyzed exclusively integrin alpha10 mRNA levels but not integrin alpha10 protein levels. Hence, for the reasons outlined above the described results may not correlate to integrin alpha10 protein expression in aorta.

Furthermore, Applicant notes that the formation of atherosclerotic plaque is a process that starts very early in life, i.e. in childhood (see, for example, McGill et al., Am. J. Clin. Nutr. 72(5 Suppl):1307S-1315S (2000) (provided herewith); see also the website of the National Heart, Lung and Blood Institute at http://www.nhlbi.nih.gov/health/dci/Diseases/Atherosclerosis/Atherosclerosis_WhatIs.ht ml and the website of the American Heart Association at http://www.americanheart.org/presenter.jhtml?identifier=4440). Therefore, the aortic

tissue used for the assessment of integrin alpha10 mRNA expression in Figure 12 of WO99/51639 is likely to have contained atherosclerotic plaque. When isolating mRNA from arterial/aortic tissue it is not possible to separate the mRNA of the normal artery/aorta tissue from the mRNA of the plaques. Hence, the strong expression of integrin alpha10 mRNA in aorta, as shown in Figure 12 of WO99/51639, is likely due to integrin alpha10 expression in atherosclerotic plaques.

The fact that the formation of atherosclerotic plaque is a slow, progressive process starting already in childhood also means that there is no such negative control for detection of atherosclerotic plaque in an individual as another individual that is free of atherosclerotic plaque (the "healthy normal control individual'). Rather, the negative control for detection of atherosclerotic plaque is the normal artery tissue within the same individual. As discussed above, the normal artery tissue does not express integrin alpha10 protein while the atherosclerotic plaque does. The detection of integrin alpha10 protein, as disclosed in the instant application, therefore has significant value for the detection and diagnosis of clinical atherosclerosis.

In conclusion, Applicant respectfully submits that the specification discloses the differential expression of integrin alpha10 protein in atherosclerotic plaque and the adjacent normal artery tissue, and that the disclosed strategy of scoring the amount of integrin alpha10 chain in an artery has significant value for the detection of atherosclerotic plaque and the diagnosis of clinical atherosclerosis. In light of this, Applicant respectfully requests that these rejections regarding differential expression or correlation of integrin alpha10 chain in normal artery tissue and atherosclerotic plaque tissue be withdrawn.

The Examiner further objected that except for anti-alpha10 specific antibodies, the specification provides no guidance as to how to make and use any "binding agent" for *in vitro* and *in vivo* detection of atherosclerotic plaques. Office Action, page 4. Applicant respectfully disagrees with this assertion.

The specification clearly provides guidance on how to use polypeptides (other than antibodies) that bind specifically to integrin alpha10 for the *in vitro* or *in vivo* detection of integrin alpha10 (see, for example, paragraph 92). The disclosed methods for such detection are essentially similar to those disclosed for the antibodies. The specification further discloses the use of other binding agents, for example, nucleic acids that hybridize any nucleic acid encoding integrin alpha10, including polynucleotides and oligonucleotides (see, for example, paragraphs 72-76). The detailed protocols on how to make and use such nucleic acids for the detection of a gene of interest, in this case integrin alpha10, were well known to the skilled artisan at the time of the invention, as these were commonly used standard protocols (see, for example, Sambrook et al., Molecular Cloning: A Laboratory Manual, Cold Spring Harbor Laboratory Press).

However, in an effort to speed up the prosecution of the instant application Applicant now limits the claims currently under consideration to antibodies and fragments thereof that specifically bind to integrin alpha10 chain. This limitation is reflected in the amended claims 9 and 17. Claim 12, the only pending claim under consideration containing the expression "binding agent", has been cancelled. Applicant, therefore, respectfully requests that the above rejection be withdrawn.

The Examiner further contends that (1) it is unclear what imaging device and imaging tag can be used to detect atherosclerotic plaque *in vivo* using the claimed binding agent; (2) it is unclear what is the control for the *in vivo* method; (3) no animal model is used to detect atherosclerotic plaque *in vivo*; and (4) it is unclear that the *in vitro* studies accurately reflect the relative human detection strategy. Office Action, page 5. Applicant respectfully disagrees with these assertions.

With respect to objection (1), Applicant directs the Examiner to paragraph 92 of the specification. This paragraph discloses the imaging techniques and imaging tags that can be used to detect atherosclerotic plaque *in vivo*. At the time the instant application was filed, these methods were considered "standard techniques" for the assessment of atherosclerotic vessels. See, for example, Fayad and Fuster, Circ. Res. 89:305-316 (2001) (cited in paragraphs 78 and 98 of the specification and provided herewith). The combination of such imaging techniques with the detection of a specific biological activity within atherosclerotic plaques is today considered "the most interesting imaging modality" for the early identification of atherosclerotic lesions (see http://www.touchcardiology.com/atherosclerosis-plaque-imaging-characterization-a574-1.html). The disclosed expression of integrin alpha10 protein in atherosclerotic plaque provides such a specific biological activity.

With respect to objection (2), Applicant submits that one skilled in the art knew at the time of the invention that the formation of atherosclerotic plaque is a slow, progressive process starting in childhood and that therefore there is no such control as a "healthy normal control individual" (see above). Furthermore, paragraphs 97-98 of the specification describe the prior art understanding of arterial histology and the correlation

between different types of atherosclerotic lesions and particular disease stages of clinical atherosclerosis. The review article cited in paragraph 97 (Stary et al., Circulation 92:1355-1374 (1995)) and references therein spell out in great detail the differences between normal artery tissue and atherosclerotic plaques of various stages. One skilled in the art would have understood from this disclosure -- in consideration of the non-existence of a "healthy normal control individual" -- that the control in the claimed method is the normal artery tissue from the same individual that harbors the atherosclerotic plaques to be detected.

With respect to objections (3) and (4), Applicant notes that the Examiner acknowledged that the specification provides guidance how to make and use anti-alpha10 antibodies for *in vitro* or *in vivo* detection of atherosclerotic plaques. Office Action, page 4, third paragraph. Because Applicant has now limited the scope of the claims currently under consideration to anti-alpha10 antibodies as the only binding agent (see above), the objections (3) and (4) are no longer relevant.

In sum, Applicant has addressed objections (1) to (4) and hence respectfully requests that in light of the above remarks these objections be withdrawn.

In further support of the specification being enabled, Applicant makes the following comments. Applicant notes that at the time of the invention a variety of antibodies had been developed against the extracellular domain of integrins and successfully applied *in vivo* in animal model studies and human clinical trials. See, for example, Shimaoka and Springer, Nat. Rev. Drug Discov. 2(9):703-16 (2003) (provided herewith), and references therein. These included monoclonal antibodies directed against the I-domain of integrin alpha chains. As a case in point, phase III clinical trials

for treatment of psoriasis were successfully conducted using a monoclonal antibody against the I-domain of integrin alphaL. Cather et al., Expert Opin. Biol. Ther. 3(2):361-70 (2003).

Therefore, one skilled in the art at the time of the invention would have known how to make and use an antibody against an integrin alpha chain *in vivo*. "Detailed procedures for making and using the invention may not be necessary if the description of the invention itself is sufficient to permit those skilled in the art to make and use the invention." MPEP § 2164. Hence, a description of how to apply the methods of the invention *in vivo* beyond what is provided in the specification is not required to enable the invention.

Further, it was well established in the art at the time of the invention that administration of an antibody against the extracellular domain of an integrin alpha chain into the vascular system leads to detectable and effective binding of the antibody to integrin alpha chains *in vivo*. See, for example, Shimaoka and Springer, Nat. Rev. Drug Discov. 2(9):703-16 (2003), and references therein. The art considered the binding of a molecule, such as an anti-integrin antibody, to integrins *in vivo* as "straightforward". Id. at 713. Furthermore, animal models for atherosclerosis were routinely used for many years prior to the filing date of this application. See, for example, Breslow, Science 272(5262):685-8 (1996). Hence, the art at the time of the invention was highly developed and there was a high degree of skill regarding *in vivo* binding to integrin of an administered anti-integrin binding agent such as an anti-integrin antibody.

The fact that the specification does not contain more working examples describing the use of anti-integrin alpha10 antibodies *in vivo* does not by itself support a

rejection based on non-enablement. In fact, a specification need not contain <u>any</u>

working example to be enabled. "The specification need not contain an example if the

invention is otherwise disclosed in such manner that one skilled in the art will be able to

practice it without an undue amount of experimentation." MPEP § 2164.02. In weighing

the underlying factual findings in an enablement determination, the absence of a

working example is not a strong factor if the art involved is predictable and well

developed, as is the case here.

Together, considering the developed state of the prior art, the manifold prior

success *in vivo* of anti-integrin antibodies, and the *in vitro* studies of the specification, no

undue experimentation would be required to practice the invention. In light of all the

above remarks, Applicant respectfully requests that the rejections under 35 U.S.C. §

112, first paragraph, as lacking enablement be withdrawn.

Claims 9-12, 17-18, 21, and 24 were rejected under 35 U.S.C. § 112, first

paragraph, as lacking possession of the claimed invention. The Examiner

acknowledged that Applicant has disclosed anti-alpha10 antibodies, but indicated that

no other binding agents were disclosed. Office Action, page 5. Applicant respectfully

traverses for reasons outlined above. However, since Applicant has limited the scope

of the claims currently under consideration, this rejection should be withdrawn.

Rejection under 35 U.S.C. § 102(b)

Claims 17-18 were rejected under 35 U.S.C. § 102(b) as being anticipated by

WO99/51639. Applicant respectfully traverses. Applicant notes that the section of

WO99/51639 cited by the Examiner only relates to the use of <u>polynucleotides or</u>

<u>oligonucleotides</u> for determining the differentiation-state of certain cells. The reference

does not relate to the use of antibodies that can bind integrin alpha10 protein expressed on the cell surface. Because claim 17 has now been amended to relate only to the use of anti-integrin alpha10 antibodies as binding agents, and claim 18 has been cancelled, the reference is no longer relevant.

In addition, the reference does not relate to the use of any binding agent for the detection of atherosclerotic plaques or the diagnosis of atherosclerosis. WO99/51639 does not disclose if and how expression of integrin alpha10 is altered in atherosclerosis, and WO99/51639 simply makes no mention of atherosclerotic plaques or the utility of integrin alpha10 for diagnostic purposes. There is no disclosure that integrin alpha10 could be used as a marker for detection of atherosclerotic plaque or the diagnosis of atherosclerosis. Since the diagnosis of atherosclerosis is a distinct element of claim 17, WO99/51639 can not anticipate this claim. To anticipate a claim, the reference must teach every element of the claim. MPEP § 2131.

In light of the above, Applicant respectfully requests that the rejection under 35 U.S.C. § 102(b) as being anticipated by WO 99/51639 be withdrawn.

Rejection under 35 U.S.C. § 103(a)

Claims 9, 11-12, and 21 were rejected under 35 U.S.C. § 103(a) as being obvious over WO99/51639 in view of US Patent No. 6,458,590. Applicant respectfully traverses.

As discussed above, the cited section on page 9 of WO 99/51639 only relates to the use of polynucleotides or oligonucleotides for determining the differentiation-state of certain cells. It does not contemplate the use of antibodies that can bind integrin

alpha10 protein expressed on the cell surface. However, claim 9 has now been amended to be limited only to anti-integrin alpha10 antibodies as binding agents.

Moreover, WO99/51639 does not disclose the use of any binding agent for the detection of atherosclerotic plaques or the diagnosis of atherosclerosis. WO99/51639 does not disclose if and how expression of integrin alpha10 is altered in atherosclerosis, and WO99/51639 simply makes no mention of atherosclerotic plaques or the utility of integrin alpha10 for diagnostic purposes. There is also no disclosure that integrin alpha10 could be used as a marker for detection of atherosclerotic plaque or the diagnosis of atherosclerosis.

The section on page 7 of WO99/51639 cited by the Examiner relates to the use of binding entities against integrin alpha10 as markers of cells expressing integrin alpha10. The examples 6 and 11 of WO99/51639 cited by the Examiner relate to the preparation of an anti-integrin alpha10 antibody and to the use of such an antibody for the immunohistochemical staining of integrin alpha10 in fascia around tendon and skeletal muscle and in tendon structures in heart valves. However, these examples do not disclose the use of anti-integrin alpha10 antibodies for the detection of integrin alpha10 in either normal artery tissue or atherosclerotic plaques.

The teachings of the '590 patent cited by the Examiner relate to a comparison of OPN expression in coronary artery tissue from patients with severe atherosclerosis in coronary arteries who underwent directional coronary atherectomy (DCA) and from individuals with no evidence of atherosclerosis who did not undergo DCA. Thus, the tissues of two very distinct, distinguishable groups of individuals are compared: one group that underwent DCA, and another group that did not. Hence, in this experimental

setup there is a defined group of individuals, i.e. those who did not undergo DCA, who can serve as a control for those individuals who underwent DCA. This is very different from the experimental setup in the instant invention and is also not suitable for individual diagnosis. Here, the disclosed methods are aimed at detecting atherosclerotic plaque in individuals who did not undergo DCA. The purpose is to detect the development of atherosclerotic plaque which occurs in all individuals to varying degrees. Hence, the control group used in the '590 patent would not be a suitable control group for the methods of the instant invention. Rather, in the instant methods the control is the normal artery tissue that is spatially separate from atherosclerotic plaque but within the same individual in whom the atherosclerotic plaques are to be detected. As discussed above, integrin alpha10 protein expression is detected in the atherosclerotic plaque but not in the normal artery tissue.

In conclusion, the WO99/51639 reference relates to the use of polynucleotides or oligonucleotides but not to the use of antibodies that can bind integrin alpha10 protein expressed on the cell surface. WO 99/51639 also does not disclose the use of any binding agent for the detection of atherosclerotic plaques or the diagnosis of atherosclerosis, and the control taught by the '590 patent is not a suitable control for the methods disclosed in the instant application. Hence, by combining the teachings of WO99/51639 and the '590 patent one of skill in the art does not derive at the instant invention. Based on these considerations, Applicant respectfully requests that the rejection under 35 U.S.C. § 103(a) as being obvious over WO 99/51639 in view of US Patent No. 6,458,590 be withdrawn.

In summary, in view of the foregoing amendments and remarks, Applicant respectfully requests reconsideration and reexamination of this application and the timely allowance of the pending claims. If the Examiner believes a telephone conference would be useful in resolving any outstanding issues, the Examiner is invited to call the undersigned at (202) 408-4173.

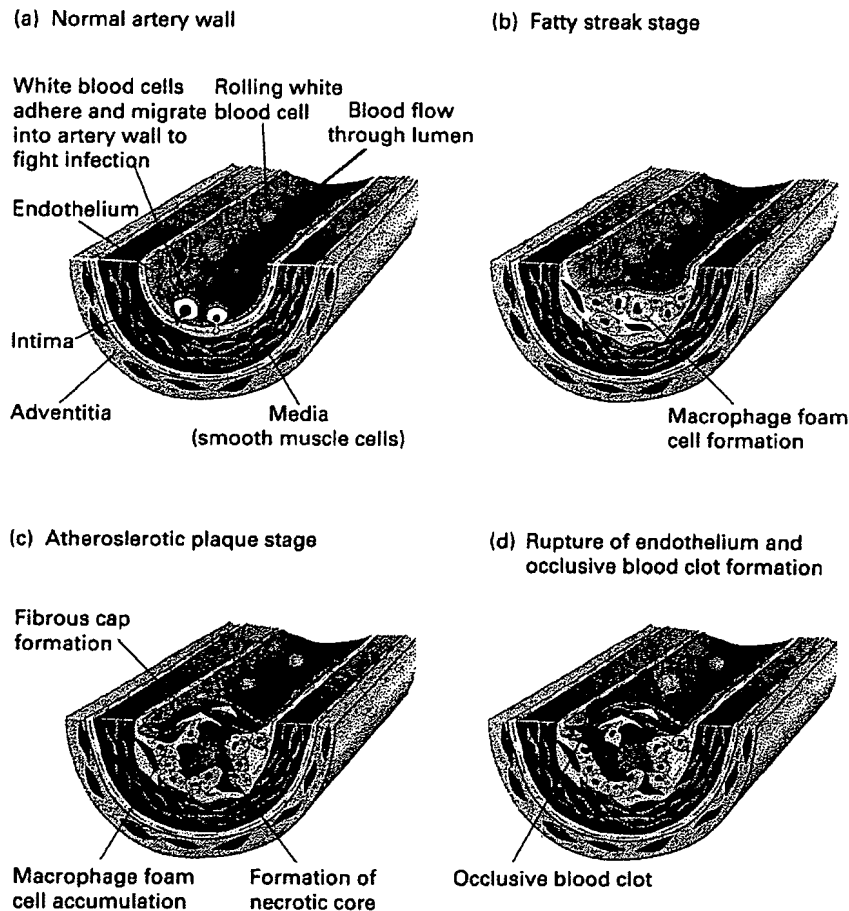Please grant any extensions of time required to enter this response and charge any additional required fees to our deposit account 06-0916.

Respectfully submitted,

FINNEGAN, HENDERSON, FARABOW, GARRETT & DUNNER, L.L.P.

Dated: June 6, 2007   By

Anthony C. Tridico
Reg. No. 45,958

(a) Normal artery wall

(b) Fatty streak stage

White blood cells adhere and migrate into artery wall to fight infection

Rolling white blood cell

Blood flow through lumen

Endothelium

Intima

Adventitia

Media (smooth muscle cells)

Macrophage foam cell formation

(c) Atheroslerotic plaque stage

(d) Rupture of endothelium and occlusive blood clot formation

Fibrous cap formation

Macrophage foam cell accumulation

Formation of necrotic core

Occlusive blood clot

▲ FIGURE 18-19 Major stages in the onset and progression of atherosclerosis in the artery wall. (a) The anatomy of a normal artery wall, which is composed of concentric layers of cells and extracellular matrix, is shown. White blood cells adhere to the endothelium, roll along it, and then migrate into an artery wall to fight infection (see Figure 6-30). (b) When plasma LDL is high or plasma HDL is low, or both, macrophages in the intima can accumulate lipoprotein cholesterol, generating foam cells filled with cholesteryl ester droplets (see Figure 18-20). Accumulation of foam cells produces a fatty streak in the vessel wall that is only visible microscopically. (c) Continued generation of foam cells and migration of smooth muscle cells from the media into the intima is followed by cell death, producing advanced atherosclerotic plaque. This plaque consists of a necrotic core of lipids (including needlelike cholesterol cry and extracellular matrix overlain by a fibrous cap of smooth muscle cells and matrix. (d) As an atherosclerotic plaque g into the lumen of the artery, it disrupts and reduces the flo blood. In some cases, the plaque alone can fully occlude t artery. In many cases, the fibrous cap ruptures, inducing formation of a blood clot that can fully occlude the artery [Adapted from R. Ross, 1999, *N. Engl. J. Med.* **340**(2):115.]

that directly attack bacteria and other pathogens. The cells also secrete proteins that help recruit additional monocytes and other immune cells (e.g., T lymphocytes) to join in the fight. Macrophages also engulf and destroy pathogens, damaged macromolecules, and infected or dead body cells. When the infection has been cured, damaged tissue is repaired and the remaining macrophages and other leukocytes move out of the artery wall and reenter the circulation.

As we will see, atherosclerosis is an "unintended" consequence of this normal physiological *inflammatory response*, which is designed to protect against infection and tissue damage. For this reason and because atherosclerosis most often strikes late in life after the prime reproductive years, there appears to have been little evolutionary selec-

tive pressure against the disease. Thus, although ather rosis has an enormous negative influence on modern h populations, its high incidence in well-fed, long-lived p is not surprising.

Arterial Inflammation and Cellular Import of Cholesterol Mark the Early Stages of Atherosclerosis

During an inflammatory response, macrophages in flamed artery wall can endocytose substantial amou cholesterol from lipoproteins, which accumulate wit artery wall under some circumstances (Figure 18-20 macrophages convert the imported cholesterol into th

Circulation Research

Clinical Imaging of the High-Risk or Vulnerable Atherosclerotic Plaque

Z. A. Fayad and V. Fuster

The online version of this article, along with updated information and services, is located on the World Wide Web at:
http://circres.ahajournals.org/cgi/content/full/89/4/305

This Review is part of a thematic series on **Inflammatory Mechanisms in Atherosclerosis**, which includes the following articles:
Anti-Inflammatory Mechanisms in the Vascular Wall

Clinical Imaging of the High-Risk or Vulnerable Atherosclerotic Plaque

Innate and Adaptive Immune Mechanisms in Atherosclerosis
CD40 Signaling and Plaque Instability
Novel Clinical Markers of Vascular Wall Inflammation   *Andreas Zeiher, Guest Editor*

Clinical Imaging of the High-Risk or Vulnerable Atherosclerotic Plaque

Z.A. Fayad, V. Fuster

Abstract—The study of atherosclerotic disease during its natural history and after therapeutic intervention will enhance our understanding of disease progression and regression and aid in selecting appropriate treatments. Several invasive and noninvasive imaging techniques are available to assess atherosclerotic vessels. Most of the standard techniques identify luminal diameter, stenosis, wall thickness, and plaque volume; however, none can characterize plaque composition and therefore identify the high-risk plaques. We will present the different imaging modalities that have been used for the direct assessment of the carotid, aortic, and coronary atherosclerotic plaques. We will review in detail the use of high-resolution, multicontrast magnetic resonance for the noninvasive imaging of vulnerable plaques and the characterization of plaques in terms of their various components (ie, lipid, fibrous, calcium, or thrombus). (***Circ Res.** 2001;89:305-316.*)

Key Words: atherosclerosis ■ magnetic resonance imaging ■ ultrasound ■ computed tomography ■ lipid-lowering

Atherosclerosis is a systemic disease of the vessel wall that occurs in the aorta and in the carotid, coronary, and peripheral arteries.[1] The main components of the atherosclerotic plaques are (1) connective tissue extracellular matrix, including collagen, proteoglycans, and fibronectin elastic fibers; (2) crystalline cholesterol, cholesteryl esters, and phospholipids; and (3) cells such as monocyte-derived macrophages, T lymphocytes, and smooth muscle cells.[2] Varying proportions of these components occur in different plaques, thus giving rise to a spectrum of lesions.[1,3,4]

Atherosclerotic Plaques and Need for Imaging

The high-risk or vulnerable plaque has different characteristics depending on the arterial regions (ie, coronaries, carotids, or aorta).

Coronary Artery Vulnerable Plaques

Rupture-prone plaques in the coronary arteries, the so-called "vulnerable plaques," tend to have a thin fibrous cap (cap thickness ≈65 to 150 μm) and a large lipid core. Acute coronary syndromes (ACSs) often result from rupture of a modestly stenotic vulnerable plaque,[3,4] not visible by x-ray angiography.[3]

According to the criteria of the American Heart Association Committee on Vascular Lesions, lesion types depend in part on the phase of progression as shown schematically in Figure 1.[1,4] Coronary "vulnerable" type IV and type Va lesions (phase 2) and the "complicated" type VI lesions (phase 4) are the most relevant to ACS. Type IV and Va lesions, although not necessarily stenotic at angiography, are prone to disruption (see the Figure in the online data supplement available at http://www.circresaha.org), with
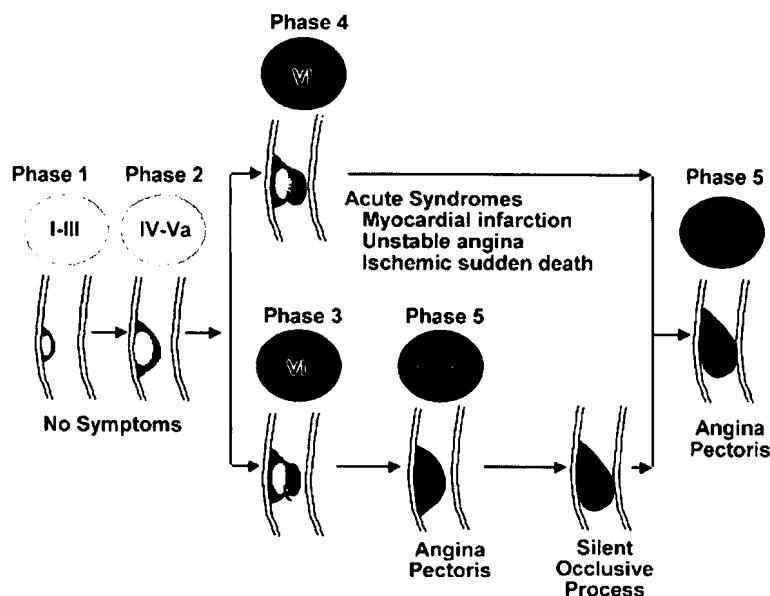
Figure 1. Phase and lesion morphology of coronary atherosclerosis. Progression is based on gross pathological and clinical findings. An early lesion (phase 1) can become a fibrolipid plaque (phase 2). Phase 2 can progress into an acute phase (phase 3 or 4). Formation of thrombosis or hematoma may cause angina pectoris (phase 3) or an ACS due to occlusive thrombosis (phase 4). Phase 3 and 4 lesions can evolve into a fibrotic phase (phase 5) characterized by more stenotic plaques that may progress to occlusive lesions. Yellow indicates lipid accumulation; red, thrombosis and hemorrhage; and green, fibrous tissue. Roman numerals indicate lesion types, as follows: I to III, early lesions with isolated macrophage-foam cells (I), multiple foam-cell layers (II), and isolated extracellular lipids (III); IV to Va, advanced lesions (fibrolipid plaques with confluent extracellular lipid pools [IV] and fibromuscular tissue layers and atheroma [Va]); VI, advanced lesions (complicated plaques with surface defects, hemorrhage, or thrombus deposition); and Vb to Vc, advanced lesions with calcifications (Vb) and those with fibrous tissue (Vc). Modified from Fuster.[4]

macrophage-dependent release of proteolytic enzymes such as metalloproteinases.[2,5] Type IV lesions consist of extracellular lipid intermixed with fibrous tissue covered by a fibrous cap, whereas type Va lesions possess a predominant extracellular lipid core covered by a thin fibrous cap. Disruption of a type IV or Va lesion leads to the formation of a thrombus or "complicated" type VI lesion. The lipid core is highly thrombogenic as a result of the presence of tissue factor.[1,6] The type VI lesion associated in ACS, rather than being characterized by a small mural thrombus, consists of an occlusive thrombus.

Relatively small type IV and Va coronary lesions may account for as many as two-thirds of cases of unstable angina or other ACSs.[3] These relatively nonstenotic plaques with large lipid cores are more vulnerable and at higher risk of rupture and thrombosis; the caps are often thinnest at the shoulder region where macrophages[7] and mast cells[8] accumulate and disruption tends to occur.[5] In contrast, the most severely stenotic plaques at angiography, which have a high content of smooth muscle cells and collagen, and little lipid, are less susceptible to rupture.

Carotid Artery High-Risk Plaques

In contrast to coronary artery vulnerable plaques characterized by high lipid content and a thin fibrous cap, high-risk plaques in carotid arteries are severely stenotic. The term "high-risk" is used rather than the classic term "vulnerable," which only implies the presence of a lipid-rich core. High-risk carotid plaques are heterogeneous, very fibrous, and not necessarily lipid-rich. Rupture often represents an intramural hematoma or dissection, probably related to the impact of blood during systole against the resistance of such stenotic lesion.[9] Imaging and plaque characterization of carotid arteries are simpler than those of coronary arteries because the former are superficial and not subject to significant motion.[10] This is also true for the assessment of lower-extremity atherosclerotic disease, in which the pathobiology is similar to that of carotid disease. However, compared with peripheral

vascular lesions, more information about carotid plaques and their imaging is available.

Aortic Vulnerable Plaques

Postmortem[11] and transesophageal echocardiography (TEE)[12] studies have shown that thoracic aortic atherosclerosis is a significant marker for coronary artery disease (CAD).[13] Parameters such as aortic wall thickness, luminal irregularities, and plaque composition are strong predictors of future vascular events.[14,15] Using TEE, the French Aortic Plaque in Stroke investigators determined increased risk of all vascular events (stroke, myocardial infarction, peripheral embolism, and cardiovascular death) for patients who had noncalcified aortic plaques >4 mm thick.[14,15] Such noncalcified plaques, relatively easy to assess and characterize by imaging methods, are thought to be lipid-laden plaques (types IV/Va),[15] which are prone to rupture and thrombosis in coronary arteries.

Imaging of Atherosclerotic Plaques

Direct visualization of plaques may enhance understanding of the natural history of atherosclerotic disease. Currently, a number of invasive and noninvasive imaging modalities are used to study atherosclerosis (Table 1); most identify luminal diameter or stenosis, wall thickness, and plaque volume.

Invasive Imaging

X-Ray Angiography

The x-ray angiogram reflects luminal diameter and provides a measure of stenosis with excellent resolution or irregular luminal surface implying the presence of atherosclerotic disease. But this imaging method does not image the vessel wall or provide information about the composition of the atherosclerotic plaque such as the vulnerable lipid-rich plaques or other histopathological features.[16] This technique, however, has become the gold standard for diagnosis of coronary, carotid, and peripheral artery lesions. Nevertheless, angiography may reveal advanced lesions, plaque disruption,

TABLE 1.   Clinical Imaging of the High-Risk or Vulnerable Plaque

	Luminal Percentage Stenosis	Wall	Lipid	Fibrous	Thrombus	Calcium
X-ray angiography	●○◉	...	...	...	?	?
IVUS*	●	●	?	●	?	●
Angioscopy	...	...	●	...	●	...
Thermography/OCT†/Raman spectroscopy/NIR	...	?	?	?	?	?
US‡	○◉	○◉	...	...	...	...
UFCT	?○◉	...	...	...	...	●○◉
Nuclear scintigraphy	...	...	◉	...	○◉	...
MRI	?○◉	?○◉	?○◉	?○◉	?○◉	?○◉

● indicates coronary artery; ○, carotid artery; and ◉, aorta.
*IVUS in carotid arteries or aorta is theoretically feasible.
†Optical coherence tomography (OCT) is able to image the vessel in very high resolution.
‡TEE may identify some of the plaque components in the aorta.

luminal thrombosis, and calcification. The degree of stenosis measures blood flow obstruction. Calculation of the stenosis depends on proper designation of a normal reference segment. One of the major limitations of angiography is that diffuse atherosclerotic disease may narrow the entire lumen of the artery, and as a result underestimate the degree of local stenosis. In addition, because some of the plaques may be displaced outward, the luminal diameter may appear normal despite significant disease.[17]

Intravascular Ultrasound (IVUS)

Ultrasound (US) imaging is based on transmitting and receiving high-frequency sound waves. The time between transmission and reception of the wave is directly related to the distance between the source and reflector.

Catheter-based US is a new approach to the arterial vascular wall imaging. This invasive modality permits direct and real-time imaging of atheroma and provides a cross-sectional, tomographic perspective of the vessel and atherosclerotic disease.[18] Diagnostic applications of IVUS include detection of angiographically unrecognized disease, detection of lesions of uncertain severity (40% to 75% stenosis), and risk stratification of atherosclerotic lesions in interventional practice.

Current-generation catheters (incorporating a transducer) range in diameter from 0.96 to 1.17 mm and provide high-quality images. The spatial resolution is ≈100 to 250 µm (depending on the US probe frequency). On the basis of plaque echogenicity, coronary atheroma can be differentiated into three categories, as follows: (1) highly echoreflective regions with acoustic shadows, often corresponding to calcified tissue; (2) hyperechoic areas representing fibrosis or microcalcifications; or (3) hypoechoic regions corresponding to thrombotic or lipid-rich tissue or a mixture of these elements.[18] IVUS can delineate the thickness and echogenicity of vessel wall structures; however, histopathological information is limited.[18] Spectral information of the radiofrequency signal may facilitate the discrimination of atheroma.[19] Angioscopy (described below) and histological studies generally report low sensitivity to IVUS in detection of thrombus and lipid-rich lesions.[20]

IVUS may be useful in selecting the most appropriate option of transcatheter therapy (rotational atherectomy, stents, etc).[21] For example, lesions with calcification would be expected to be more rigid and, therefore, prone to rupture in response to the mechanical stress of balloon dilation, whereas softer, lipid-rich, noncalcified plaques may stretch but not fracture.[22] Studies aimed at sensitivity and specificity involving large numbers of patients are required to determine the use of IVUS for the detection of atherosclerotic disease.[18]

Methods such as IVUS elastography have been introduced to assess mechanical properties of the vessel wall, which may relate indirectly to the histopathological composition of the atherosclerotic plaque.[23] Intravascular elastography is obtained from cardiac-gated IVUS images coupled with intraluminal pressures during the cardiac cycle. The images provide vessel wall strain information and reflect mechanical properties of the tissue. A preliminary in vitro study demonstrated the successful discrimination of fibrous and lipid-rich plaques (Figure 2) using IVUS elastography.[23] However, the in vivo application of IVUS elastography may be hampered by catheter motion during cardiac contraction.

Angioscopy

Intracoronary angioscopy allows direct visualization of the plaque surface, color of the luminal surface (red, white, or
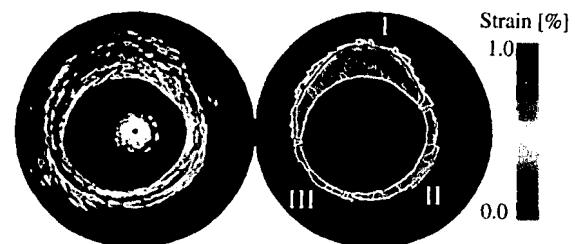

Figure 2. Intravascular US image (left) and elastogram (right) of diseased human femoral artery. Elastogram reveals low strain in plaque (0.24%; I), similar strain in nondiseased vessel wall between 3 and 7 o'clock positions (0.32%; II), and high strain in vessel wall between 7 and 9 o'clock positions (0.96%; III). Region with high strain contains fatty foam cells at lumen-vessel wall boundary and increased macrophage activity. Modified from de Korte et al.[23]

yellow), presence of thrombus, and macroscopic features (tears, ulcerations, and fissures).[24] A recent clinical trial suggested a potential application of this invasive technique. In patients with various coronary syndromes, angiographic findings were directly compared with histomorphology and ex vivo angioscopy of atherectomized material.[25] This study concluded that yellow (lipid-rich) plaques are associated with the development of ACSs. Another study concluded that angioscopic identification of plaque rupture and thrombus was independently associated with adverse outcome in patients with complex lesions after interventional procedures.[26] These features were not identified by either angiography or IVUS. However, like IVUS, this technique is invasive. Angioscopy thus remains a research tool because of the inability to examine small-caliber vessels or cross-stenotic lesions, and the different layers within the arterial wall.

Thermography, Optical Coherence Tomography, Raman Spectroscopy, and Near-Infrared (NIR) Spectroscopy

Several new technologies for invasive atherosclerotic plaque detection may have diagnostic and therapeutic implications.

In vitro[27] and in vivo[28] studies illustrate that detection of heat released by activated inflammatory cells of atherosclerotic plaques may predict plaque disruption and thrombosis. A study using carotid endarterectomy specimens and a needle thermistor demonstrated that atherosclerotic plaques exhibit thermal heterogeneity on their luminal surface.[27] Temperature differences correlated positively with cell (macrophage) density. A catheter-based technique for the temperature measurement of human coronary arteries in vivo has been developed.[28] The system consists of a 3F catheter, with 0.05°C accuracy and a spatial resolution of 500 μm. Using this catheter, thermal heterogeneity was found to be larger in patients with unstable angina compared with those with acute myocardial infarction.[28] Thermal techniques could conceivably be combined with IVUS or optical coherence tomography (see below) to provide both functional and anatomic information.

Optical coherence tomography is analogous to IVUS, but measures the intensity of reflected infrared light rather than acoustic waves.[29] A Michelson interferometer is used as a gate to detect unscattered photons and thus generates high-resolution images. Although penetration is generally 1 to 2 mm, the use of light allows a resolutions of 10 to 30 μm. Initial in vitro imaging (resolution of 16 μm) of human aortic plaques demonstrated a strong correlation with the corresponding histopathology.[29] In vitro optical coherence tomography exhibited superior delineation of structural detail when compared with IVUS.[30] In vivo optical coherence tomography imaging, using a laser as light source, at four frames per second has been obtained in the rabbit esophagus.[31] Potential limitations of optical coherence tomography for in vivo intravascular imaging are the possible reduction of image quality when imaging through blood or large volumes of tissue, relatively slow data acquisition rate, lack of an adequate portable source for in vivo imaging, and multiple scattering.[32] Like IVUS, this technique is invasive, which may restrict its use in patients.

Raman spectroscopy is an optical technique that characterizes the chemical composition of biological tissue. Raman spectra can be obtained by processing the collected light that is scattered by a tissue as it is illuminated with a laser. Raman spectroscopy can be combined with other catheter-based imaging techniques, such as IVUS, to localize and quantify cholesterol and calcium salts in atherosclerotic plaques.[33] Current limitations of Raman spectroscopy are the strong background fluorescence, the absorbance by blood of the laser light, and the relatively long acquisition time. Because this is a 1-dimentional technique (no depth information), it may be more powerful when combined with other imaging techniques.[33]

Infrared spectroscopy also yields information on the chemical composition of tissue. NIR spectroscopy (750 to 2500 nm) has the advantage of deep penetration.[34] Recently, the use of NIR spectroscopy has been explored for the characterization of the composition of atherosclerotic lesions. A study showed a good correlation between NIR spectra and plaque composition by histology for formalin-fixed human atherosclerotic plaques.[35] Another study used a small (2.5-mm diameter) fiberoptic catheter combined with NIR reflectance spectroscopy and detected cholesterol in the rabbit aorta.[36] Similar to Raman spectroscopy, NIR may be combined with other catheter-based imaging techniques.

Noninvasive Imaging

Surface and Transesophageal US

Measurements of carotid and aortic wall thickness as well as qualitative and quantitative analysis of plaque can be determined by surface and transesophageal US. Echogenicity of the plaque reflects its characteristics. Hypoechoic heterogeneous plaque is associated with both intraplaque hemorrhage and lipids, whereas hyperechoic homogeneous plaque is mostly fibrous.[15,18]

The North American Symptomatic Carotid Endarterectomy Trial and the Asymptomatic Carotid Artery Stenosis Study have shown that the degree of stenosis and its hemodynamic consequences play a significant role in producing stroke.[37,38] High-resolution (<0.4 mm axial), real-time B-mode US with Doppler flow imaging has emerged as the modality of choice for examining the carotid arteries.[39]

Using ≥8-MHz transducers, B-mode US can be used for measuring intima-media thickness (IMT) of large- and medium-size peripheral arteries such as the carotid, femoral, or radial. Because of the physical principles of a diagnostic US, the measurement is reliable only at the far arterial wall and does not indicate whether the thickening is due to intima or media infiltration and/or hypertrophy.[40] As with other US methods, this technique is operator-dependent and has low reproducibility.

Several studies have found that carotid and aortic atherosclerosis are markers for coronary atherosclerosis.[13,41,42] Patients with symptomatic CAD have increased IMT compared with asymptomatic controls.[43] Carotid wall thickening was also found in patients with silent ischemia.[44] The relationship between IMT and CAD severity is constant but rather weak.[45] Nevertheless, large prospective studies have demonstrated that IMT may be a useful marker of CAD progression. For

example, the Cardiovascular Health Study found associations between carotid IMT and the incidence of new myocardial infarction or stroke in patients ≥65 years of age.[41] Prevention trials of lipid-lowering treatments using IMT as a surrogate end point have shown that retardation in the progress of IMT correlates with a reduction of clinical end points.[46,47]

Studies also have shown an association between aortic plaque seen on chest x-ray and the subsequent development of clinical CAD.[48] Examinations of the aorta by B-mode US[49] and TEE[50] have been used as predictors of CAD and cardiovascular risk.[14] Using TEE, the French Aortic Plaque in Stroke group[14,15] found a significantly increased risk of all vascular events for patients who had noncalcified aortic plaques >4 mm in thickness. TEE-detected aortic plaque has been correlated with a higher prevalence of CAD and the presence of significant angiographic coronary artery stenosis.[13] In addition, the lack of aortic plaque on TEE has been shown to be predictive of the absence of CAD.[51]

Ultrasonic contrast agents have been introduced to improve image resolution and specificity.[52-54] For example, acoustic liposomes conjugated with monoclonal antibodies can be used for plaque component–targeted imaging. The liposome formulation also has been modified to allow site-specific drug[55] or gene[56] delivery.

Ultrafast Computed Tomography (UFCT)

UFCT allows image acquisition at a faster rate than conventional computed tomography (CT). Fast imaging is essential elimination of cardiac and respiratory motion artifacts. Atherosclerotic calcification is found more frequently in advanced lesions, and may occur in small amounts in early lesions.[57]

Magnetic resonance imaging (MRI), x-ray angiography, and US can identify calcified deposits in blood vessels; however, only electron-beam CT (EBCT)[58] and fast-gated helical or spiral CT[59] can measure the amount or volume of calcium. In EBCT, x-ray radiation passes through the patient and is detected by two 240° detector rings. To measure coronary calcium, 30 to 40 contiguous, 3-mm-thick slices are obtained from the aortic root to the apex of the heart. The scans are usually acquired during one or two separate breath holds. Non-EBCT systems use a continuously rotating x-ray source. Recently, non-EBCT systems have been introduced, using multidetector arrays for short rotation times that improve imaging speed.[60] For example, a 4-slice detector array system provides an 8-fold improved performance over single-slice CT system. Comparison of coronary calcium assessment by EBCT and non-EBCT systems demonstrated good correlation.[59]

Histological and UFCT studies support the association of tissue densities ≥130 Hounsfield units with calcified plaques.[61] However, high-risk plaques often lack calcium.[62] There is an association between coronary calcium and obstructive CAD, and it has been suggested that the amount of coronary calcium is a predictor of risk of coronary events.[63] However, the predictive value of coronary calcification, at least in high-risk subjects, may not be superior to that of standard coronary risk factors.[64] In addition, a high calcium score is sensitive but not a specific marker for coronary

stenosis.[65] The greatest potential for coronary calcium scores appears to be in the detection of advanced coronary atherosclerosis in patients who are apparently at intermediate risk. The new volumetric method for calcium detected the effect of lipid-lowering on coronary calcification.[58] Nevertheless, there is no evidence to support that changes in coronary calcification may correspond to changes in cardiovascular events.[64,66]

UFCT angiography with intravenous injection of a contrast medium is widely used for detection of stenosis in peripheral vessels. With the advent of faster and higher-resolution imaging and soft-tissue delineation with UFCT, assessment of coronary stenosis[60,67] and the detection of noncalcified coronary plaques[68] are being explored.

Nuclear Scintigraphy

Many radiotracers have been developed on the basis of molecules and cells involved in atherogenesis.[69] The potential diagnostic utility of such radiotracers for imaging atherosclerotic lesions has been examined in animal models and in humans.[69] Many proteins labeled with radioiodine, ^{99m}Tc, ^{111}In, or ^{125}In were evaluated.[70] These include lipoproteins (native LDL and oxidized LDL), immunoglobulins against macrophages, smooth muscle cells, and endothelial adhesion molecules.[71,72] These tracers showed significant uptake in experimental atherosclerotic lesions, although the limited clinical trials could not demonstrate utility because of slower clearance of radiotracers from circulation and poor target/background ratios.[73] Radiolabeled peptides[74] and metabolic tracers such as fluorodeoxyglucose, which show faster clearance from circulation and appear to provide higher contrast than radiolabeled proteins, were recently introduced.[70] Similarly, radiolabeled antifibrin antibody fragments and peptides (which bind to glycoprotein IIb/IIIa receptors on activated platelets) clear faster from circulation compared with radiolabeled platelets.[75] A new glycoprotein IIb/IIIa platelet inhibitor, DMP-44, labeled with ^{99m}Tc accurately identifies the platelet-rich thrombus in a canine model.[76] We recently illustrated that in vivo fluorodeoxyglucose positron emission tomography may detect and quantify macrophage content in rabbits with aortic plaques.[77] However, no single radiotracer is ideally suited to image atherosclerosis and to provide the prognostic and clinical indicators necessary for medical and surgical interventions.[69]

Magnetic Resonance Imaging

High-resolution magnetic resonance (MR) has emerged as the potential leading noninvasive in vivo imaging modality for atherosclerotic plaque characterization. MR differentiates plaque components on the basis of biophysical and biochemical parameters such as chemical composition and concentration, water content, physical state, molecular motion, or diffusion. MR provides imaging without ionizing radiation and can be repeated sequentially over time.

High-resolution MR relies on the same principles as other MR techniques. During the examination, the patient is subjected to a high local magnetic field, usually 1.5 T, which aligns the protons in the body. These protons (or spins) are excited by a radiofrequency pulse and subsequently detected by receiver coils. Detected signals are influenced by the

TABLE 2. Plaque Characterization With MR

	Relative MR Signal Intensity*		
	T1W	PDW	T2W
Calcium	Hypointense	Very hypointense	Very hypointense
Lipid	Very hyperintense	Hyperintense	Hypointense
Fibrous	Isointense to slightly hyperintense	Isointense to slightly hyperintense	Isointense to slightly hyperintense
Thrombus†	Variable	Variable	Variable

*Relative to that of immediately adjacent muscle tissue.
†In some cases, surface irregularities; the variable signal intensity may be due to the thrombus age.

relaxation times (T1 and T2), proton density, motion and flow, molecular diffusion, magnetization transfer, changes in susceptibility, etc. Three additional magnetic fields (gradient fields) are applied during MRI; one selects the slice and two encodes spatial information. The timing of the excitation pulses and the successive magnetic field gradients determine the image contrast. The ability to obtain images of the atherosclerotic vessels is dependent on the amount of available signal, contrast, and the lack of noise.

The MR images can be "weighted" to the T1, T2, or proton density values through manipulation of the MR parameters (ie, repetition time and echo time). In a T1-weighted (T1W) image, tissues with low T1 values will be displayed as hyperintense picture elements or pixels (high signal intensity) and, conversely, high T1 values will be displayed as hypointense pixels (low signal intensity). In a T2-weighted (T2W) image, tissues with high T2 values will be portrayed as hyperintense pixels, and those with low T2 values as hypointense pixels. Thus, a T1W and a T2W image for the same anatomy can appear quite different because an MR image is not a photograph, but a computerized map of radio signals emitted by the human body. Finally, a proton density–weighted (PDW) image is an image in which the differences in contrast are proportional to the density of water and fat protons within the tissue. It is also referred to as an intermediate-weighted image because the contrast in the image is a combination of mild T1 and T2 contrast.

Ex Vivo MR Plaque Studies

Early work on applying MR techniques to characterizing plaque focused on lipid assessment with nuclear MR spectroscopy and chemical-shift imaging.[78–80] These techniques suffer from poor signal-to-noise (SNR) ratio, because the concentration of the lipid present in the plaque is very low in comparison with water.[81] Therefore, it has been difficult to extend these methods to an in vivo setting. Current studies are focused on MRI of water protons.

MR Multicontrast Plaque Imaging

After an ex vivo study,[82] Herfkens et al[83] performed the first in vivo patient imaging study of aortic atherosclerosis. Only the anatomic or morphological features such as wall thickening and luminal narrowing were assessed.

Improvements in MR techniques (eg, faster imaging and detection coils), conducive to high resolution and contrast imaging, have permitted the study of the different plaque

components using multicontrast MR, generated by T1, T2, and PDW imaging.[84] Atherosclerotic plaque characterization by MR is based on the signal intensities (Table 2) and morphological appearance of the plaque on T1W, PDW, and T2W images as previously validated.[10,81,85–89]

The plaque fibrous tissues consisting mainly of extracellular matrix elaborated by smooth muscle cells are associated with a short T1. The origin of the T1 shortening (increased signal intensity on T1W images) is specific to protein-water interactions.[90] The plaque lipids consist primarily of unesterified cholesterol and cholesteryl esters and are associated with a short T2.[81] The short T2 (decreased signal intensity of T2W images) of the lipid components is in part due to the micellar structure of lipoproteins, their denaturation by oxidation, or the exchange between cholesteryl esters and water molecules (both from the fatty chain or from the cholesterol ring), with a further interchange between free and bound water.[81] Perivascular fat, mainly composed of triglycerides, has a different appearance on MR than atherosclerotic plaque lipids.[91] The plaque-calcified regions consist primarily of calcium hydroxylapatite and are associated with low signal intensities on the MR images because of their low proton density and because of diffusion-mediated susceptibility effects.[92] The MR appearance and evolution of thrombus or hemorrhage have been investigated in the central nervous system,[93] pelvis,[94] and aorta.[95] These studies showed that the different MR signal intensities of hemorrhage depend on the structure of hemoglobin and its oxidation state.[93] Additional studies in the context of arterial thrombus and atherosclerosis are necessary.

In a recent study, we analyzed 22 human carotid endarterectomy specimens with ex vivo MR and histopathological examination.[96] Cross-sections were matched between the multicontrast MR images and histopathology. The overall sensitivity and specificity for each component were very high. Calcification, fibrous tissue, lipid core, and thrombus were readily identified. Diffusion imaging, which probes the motion of the water molecules, facilitated thrombus detection.[97]

In Vivo MRI Experimental Studies

MR has been used in the study of plaques in several animal models.[98] Skinner et al[99] induced aortic plaque in the rabbit through a combination of atherogenic diet and double-balloon denudation, which showed in vivo aortic plaque progression. In a similar rabbit model, we validated the ability of MRI to

quantify lipid-rich and fibrous components of lesions.[89] Fast-spin echo multicontrast sequences with in-plane resolution of 0.35 mm and slice thickness of 3 mm were obtained. We have asserted that aortic MR atherosclerotic imaging can be used as a tool for documentation of arterial remodeling in the rabbit model.[100] Two separate MRI serial studies[101,102] have shown a significant regression of the aortic plaque in vivo in atherosclerotic rabbits undergoing cholesterol lowering. A significant correlation was found between MR and histopathology for atherosclerotic burden and plaque composition.[102]

Another serial MRI study on the effect of lipid-lowering therapy with 3-hydroxy-3-methylglutaryl–coenzyme A (CoA) reductase inhibitors (statins) and a novel class of agents, acyl-CoA:cholesterol O-acyltransferase (ACAT) inhibitors showed the beneficial effects in a Watanabe rabbit.[103] The combination of statins and ACAT inhibitors induced a significant regression of previously established atherosclerotic lesions.

Using conventional MR systems (ie, 1.5 T), an in-plane spatial resolution ≥300 μm can be achieved with a high SNR and contrast-to-noise ratio for in vivo vessel wall imaging. To study small structures, such as the abdominal aorta of mice (≈<1 mm in luminal diameter), it is necessary to increase the SNR by using high magnetic field scanners equipped with small radiofrequency coils and strong magnetic field gradients.[104] Using a 9.4-T (89-mm-bore system), we studied in vivo atherosclerosis in live animals.[104] The achieved spatial resolution with MR microscopy (MRM) was ≈50 to 97 μm in-plane and 500 μm in slice thickness. Using transgenic apolipoprotein E knockout mice, we showed an excellent agreement between MRM and histological findings for aortic plaque size, shape, and characteristics (Figure 3). We also followed the rapid progression of atherosclerosis in animals with lesions of varying severity.[105] Therefore, high-resolution MRI and MRM may allow convenient and noninvasive quantitative assessment of serial changes in atherosclerosis in different animal models of disease progression and regression.[98]

In Vivo MRI Studies on Human Carotid Artery Plaque

MR has been used for the study of atherosclerotic plaque in the human carotid,[10,106] aortic,[107] peripheral,[108] and coronary[109] arterial disease. In vivo images of advanced lesions in carotid arteries have been obtained from patients referred for endarterectomy.[10] The superficial location and relative absence of motion of carotid arteries present less of a technical challenge for imaging than does the aorta or coronary arteries. Short T2 components were quantified in vivo before surgery and correlated with values obtained in vitro after surgery.[10] Some of the MR studies of carotid arterial plaques include the imaging and characterization of normal and pathological arterial walls,[10] the quantification of plaque size,[106] and the detection of fibrous cap "integrity."[110] Typically the images are acquired with resolution of 0.4×0.4×3 mm³ using a carotid phased-array coil.

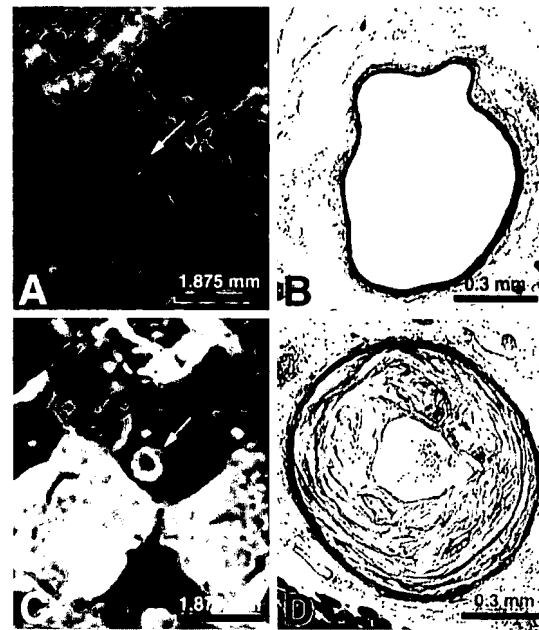Most of the in vivo MR plaque imaging and characterization have been performed using a multicontrast approach with

Figure 3. In vivo MR image of abdominal aorta (arrow) in normal mouse and in apolipoprotein E–knockout mouse showing differences between normal and atherosclerotic arteries. MR images in wild-type mice are shown in panel A (magnified; see scale) and histopathology (B), as shown by the hematoxylin and eosin stain (original magnification ×40). A large atherosclerotic lesion (arrow) that encircles the abdominal aorta of 12-month-old apolipoprotein E–knockout mouse is shown on the MR images in panel C (magnified). These findings correlated with histopathology as shown in panel D. Modified from Fayad et al.[104]

high-resolution black-blood spin echo– and fast spin echo–based MR sequences. The signal from the blood flow is rendered black by the use of preparatory pulses (eg, radiofrequency spatial saturation or inversion recovery pulses) to better visualize the adjacent vessel wall. Hatsukami et al[110] introduced the use of bright blood imaging (ie, 3-dimensional fast time-of-flight imaging) for the visualization of the fibrous cap thickness and morphological integrity. This sequence provides enhancement of the signal from flowing blood and a mixture of T1 and proton density contrast weighting that highlights the fibrous cap.

MR angiography (MRA) and high-resolution black-blood imaging of the vessel wall can be combined (Figure 4). Comparison studies of MRA and contrast angiography have shown good sensitivity and specificity in the aorta and in the carotid, renal, and other peripheral vessels.[111] MRA demonstrates the severity of stenotic lesions and their spatial distribution, whereas the high-resolution black-blood wall characterization technique may show the composition of the plaques and may facilitate the risk stratification and selection of the treatment modality. Improvements in spatial resolution (≥250 μm) have been possible with the design of new phased-array coils[112,113] tailored for carotid imaging[114] and new imaging sequences such as long echo train fast spin echo imaging with "velocity-selective" flow suppression or double-inversion recovery preparatory pulses (black-blood imaging).[107,109]
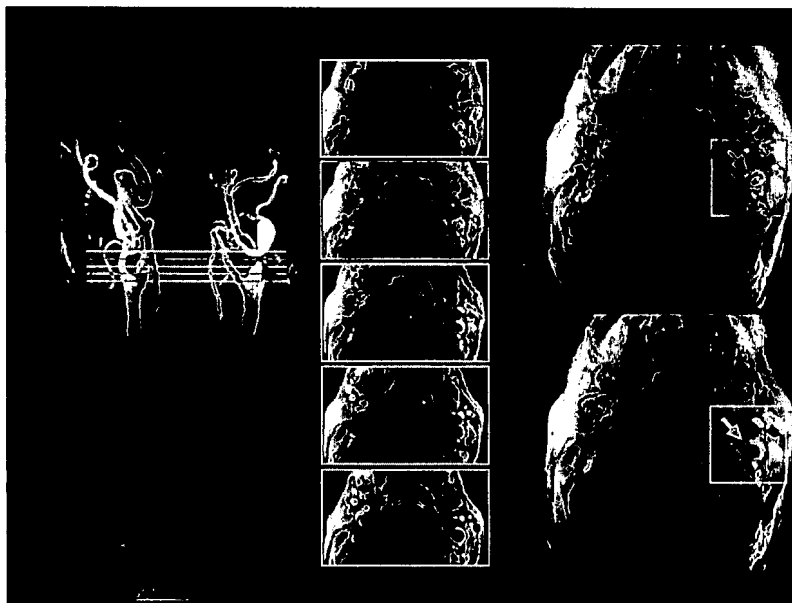
Figure 4. Carotid MR angiogram (left panel) showing severe stenosis in left internal carotid artery (arrow; left panel). MR angiogram was obtained with a contrast-enhanced (gadolinium-diethylenetriaminepentaacetic acid) 3-dimensional fast gradient–echo and carotid–aortic arch phased-array coil. Cross-sectional MR black-blood images of carotid arteries are shown in middle and right panels. Display of MR slice positions are shown in left panel (lines). Magnified views of some carotid plaques are shown in right panel. Arrows indicate carotid plaques.

In Vivo MRI Studies on Human Aortic Plaque

In vivo black-blood MR atherosclerotic plaque characterization of the human aorta has been reported recently.[107,115] The principal challenges associated with MRI of the thoracic aorta are obtaining sufficient sensitivity for submillimeter imaging and exclusion of artifacts caused by respiratory motion and blood flow. Summers et al[115] showed by MRI that the wall thickness of the ascending aorta is increased in patients with homozygous familial hypercholesterolemia. However, conventional T1W spin echo images were obtained and no plaque composition analysis was performed.[115] Fayad et al[107] assessed thoracic aorta plaque composition and size using T1W, T2W, and PDW images. The acquired images had a resolution of $0.8 \times 0.8 \times 5$ mm^3 using a torso phased-array coil. Rapid high-resolution imaging was performed with a fast spin echo sequence in conjunction with velocity-selective flow suppression preparatory pulses. Matched cross-sectional aortic imaging with MR and TEE showed a strong correlation for plaque composition and mean maximum plaque thickness. A patient with a lipid-rich plaque in the descending aorta is shown in Figure 5.

A recent study using MR in asymptomatic subjects from the Framingham Heart Study demonstrated that aortic plaque burden (ie, plaque volume/aortic volume) increased signifi-

cantly with age, and was higher in the abdominal aorta compared with the thoracic aorta.[116] Results ascertained that long-term measures of risk factors and Framingham Heart Study coronary risk score are strongly associated with asymptomatic aortic atherosclerosis as detected by MR.[117]

In Vivo MRI Studies on Coronary Artery Plaque

Preliminary studies in a pig model proclaimed that the difficulties of coronary wall imaging are due to the combination of cardiac and respiratory motion artifacts, nonlinear course, small size, and location of the coronary arteries.[88,118] We extended the black-blood MR methods used in the human carotid artery and aorta for imaging of the coronary arterial lumen and wall.[109] The method was validated in swine coronary lesions induced by balloon angioplasty.[118] The intraobserver and interobserver variability assessment by intraclass correlation for both MRI and histopathology showed good reproducibility, with the intraclass correlation coefficients ranging from 0.96 to 0.99. MRI was also able to visualize intralesion hematoma (sensitivity 82%, specificity 84%).

High-resolution black-blood MR of both normal and atherosclerotic human coronary arteries was performed. The difference in maximum wall thickness between the normal
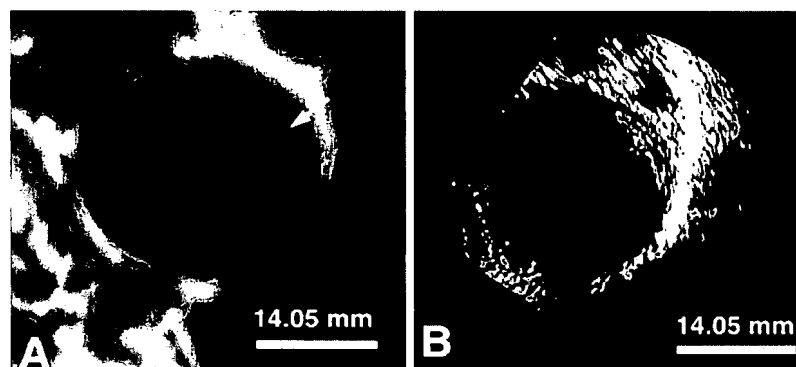

Figure 5. In vivo MR image from a patient with a 4.5-mm-thick plaque in descending thoracic aorta, T2W (A), with corresponding TEE image (B). MR image shows an example of a plaque with a dark area in the center (arrow) identified on the T2W image as a lipid-rich core (A). Lipid-rich core is separated from lumen by a fibrous cap. Plaque characterization was based on information obtained from T1W, PDW, and T2W MR images. Modified from Fayad et al.[107]
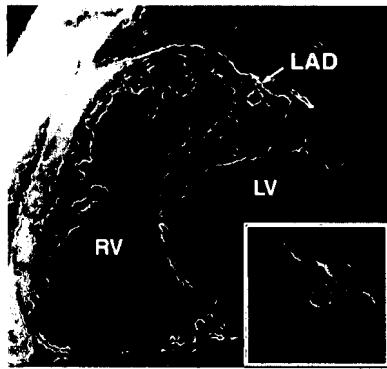
Figure 6. In vivo MRI cross-sectional image of a patient with plaque (arrow) in left anterior descending artery (LAD). Inset represents magnified view of LAD plaque. MR images are 4 mm thick with an in-plane spatial resolution of 750 μm acquired during suspended respiration (<16 seconds) using long-echo train fast spin echo imaging with "velocity-selective" flow suppression. RV indicates right ventricle; LV, left ventricle. Modified from Fayad et al.[109]

subjects and patients ($\geq$40% stenosis) was statistically significant. Figure 6 shows an in vivo MR image of a patient with a plaque in the left anterior descending coronary artery. The coronary MR plaque imaging study by Fayad et al[109] was performed during breath-holding to minimize respiratory motion. To alleviate the need for breath-holding, Botnar et al[119] have combined the black-blood fast spin echo method and a real-time navigator for respiratory gating and real-time slice–position correction.

In Vivo Monitoring of Therapy With MRI

As shown in experimental studies, MR is a powerful tool to investigate serially and noninvasively the progression and regression of atherosclerotic lesions in vivo. We have shown recently that MR can be used to measure the effect of lipid-lowering therapy (statins) in asymptomatic untreated hypercholesterolemic patients with carotid and aortic atherosclerosis.[120] Atherosclerotic plaques were assessed with MR at different time points after initiation of lipid-lowering therapy. Significant regression of atherosclerotic lesions was observed. Despite the early and expected hypolipidemic effect of the statins, a minimum of 12 months was needed to observe changes in the vessel wall. No changes were detected at 6 months. In agreement with previous experimental studies, there was a decrease in the vessel wall area and no change in the lumen area at 12 months.[101,103]

MR of the popliteal artery and its response to balloon angioplasty has been reported by Coulden et al.[108] The extent of plaque could be defined in all patients, such that even in segments of vessel that were angiographically normal, atherosclerotic lesions with cross-sectional areas ranging from 49% to 76% of potential lumen area were identified. After angioplasty, plaque fissuring, and local dissection were easily detected and serial changes in lumen diameter, blood flow, and lesion size were documented. This study illustrated that MR can define the extent of atherosclerotic plaque in the peripheral vasculature and demonstrate the remodeling and restenosis after angioplasty.

Limitations and Potential Improvements of MRI

Thinner slices such as those obtained with 3-dimensional acquisition techniques could further improve artery wall imaging.[121] Tailored coil designs, such as smaller anterior 4-element phased-array coils, may enhance the spatial resolution and may allow the identification of the substructures within coronary atherosclerotic lesions.[113] Additional MR techniques such as water diffusion weighting,[96,97] magnetization transfer weighting,[122] and contrast enhancement[123,124] may provide complementary structural information and allow more detailed plaque characterization. Slowly flowing blood near the vessel walls is another phenomenon that may potentially improve the accuracy of vessel wall imaging with black-blood techniques. Preliminary results in our study and with a similar black blood–MR sequence in the coronary arteries and the brain[109,118] suggest that this effect is minimal. However, new and more robust blood-suppression methods are needed for accurate plaque imaging especially in the carotid artery bifurcation.[125]

Conclusions

Assessment of atherosclerotic plaques by imaging techniques is essential for in vivo identification of vulnerable plaques. Several invasive and noninvasive imaging techniques are available. Most techniques identify luminal diameter or stenosis, wall thickness, and plaque volume, and are ineffective in identifying the high-risk plaques that are vulnerable to rupture and thrombosis. In vivo, high-resolution, multicontrast MRI holds the best promise of noninvasively imaging high-risk plaques. MR allows serial assessment of progression and regression of atherosclerosis. Application of MRI opens new areas for diagnosis, prevention, and treatment (eg, lipid-lowering drug regimens) of atherosclerosis in all arterial locations.

Acknowledgments

References

1. Fuster V, Fayad ZA, Badimon JJ. Acute coronary syndromes: biology. *Lancet.* 1999;353(suppl 2):SII5–SII9.
2. Libby P. Molecular bases of the acute coronary syndromes. *Circulation.* 1995;91:2844–2850.
3. Falk E, Shah PK, Fuster V. Coronary plaque disruption. *Circulation.* 1995;92:657–671.
4. Fuster V. Mechanisms leading to myocardial infarction: insights from studies of vascular biology. *Circulation.* 1994;90:2126–2146.
5. Richardson PD, Davies MJ, Born GV. Influence of plaque configuration and stress distribution on fissuring of coronary atherosclerotic plaques. *Lancet.* 1989;2:941–944.
6. Toschi V, Gallo R, Lettino M, Fallon JT, Gertz SD, Fernandez-Ortiz A, Chesebro JH, Badimon L, Nemerson Y, Fuster V, Badimon JJ. Tissue factor modulates the thrombogenicity of human atherosclerotic plaques. *Circulation.* 1997;95:594–599.
7. Moreno PR, Falk E, Palacios IF, Newell JB, Fuster V, Fallon JT. Macrophage infiltration in acute coronary syndromes: implications for plaque rupture. *Circulation.* 1994;90:775–778.

8. Kaartinen M, Penttila A, Kovanen PT. Accumulation of activated mast cells in the shoulder region of human coronary atheroma, the predilection site of atheromatous rupture. *Circulation.* 1994;90:1669–1678.

9. Glagov S, Zarins C, Giddens DP, Ku DN. Hemodynamics and atherosclerosis: insights and perspectives gained from studies of human arteries. *Arch Pathol Lab Med.* 1988;112:1018–1031.

10. Toussaint JF, LaMuraglia GM, Southern JF, Fuster V, Kantor HL. Magnetic resonance images lipid, fibrous, calcified, hemorrhagic, and thrombotic components of human atherosclerosis in vivo. *Circulation.* 1996;94:932–938.

11. Solberg LA, Strong JP. Risk factors and atherosclerotic lesions: a review of autopsy studies. *Arteriosclerosis.* 1983;3:187–198.

12. Tunick PA, Kronzon I. Atheromas of the thoracic aorta: clinical and therapeutic update. *J Am Coll Cardiol.* 2000;35:545–554.

13. Fazio GP, Redberg RF, Winslow T, Schiller NB. Transesophageal echocardiographically detected atherosclerotic aortic plaque is a marker for coronary artery disease. *J Am Coll Cardiol.* 1993;21:144–150.

14. The French Study of Aortic Plaques in Stroke Group. Atherosclerotic disease of the aortic arch as a risk factor for recurrent ischemic stroke. *N Engl J Med.* 1996;334:1216–1221.

15. Cohen A, Tzourio C, Bertrand B, Chauvel C, Bousser MG, Amarenco P. Aortic plaque morphology and vascular events: a follow-up study in patients with ischemic stroke. FAPS Investigators. French Study of Aortic Plaques in Stroke. *Circulation.* 1997;96:3838–3841.

16. Topol EJ, Nissen SE. Our preoccupation with coronary luminology: the dissociation between clinical and angiographic findings in ischemic heart disease. *Circulation.* 1995;92:2333–2342.

17. Glagov S, Weisenberg E, Zarins CK, Stankunavicius R, Kolettis GJ. Compensatory enlargement of human atherosclerotic coronary arteries. *N Engl J Med.* 1987;316:1371–1375.

18. Nissen SE, Yock P. Intravascular ultrasound: novel pathophysiological insights and current clinical applications. *Circulation.* 2001;103:604–616.

19. Bridal SL, Fornes P, Bruneval P, Berger G. Correlation of ultrasonic attenuation (30 to 50 MHz) and constituents of atherosclerotic plaque. *Ultrasound Med Biol.* 1997;23:691–703.

20. Franzen D, Sechtem U, Hopp HW. Comparison of angioscopic, intravascular ultrasonic, and angiographic detection of thrombus in coronary stenosis. *Am J Cardiol.* 1998;82:1273–1275, A9.

21. Fitzgerald PJ, Yock PG. Mechanisms and outcomes of angioplasty and atherectomy assessed by intravascular ultrasound imaging. *J Clin Ultrasound.* 1993;21:579–588.

22. Lee RT, Grodzinsky AJ, Frank EH, Kamm RD, Schoen FJ. Structure-dependent dynamic mechanical behavior of fibrous caps from human atherosclerotic plaques. *Circulation.* 1991;83:1764–1770.

23. de Korte CL, Pasterkamp G, van der Steen AF, Woutman HA, Bom N. Characterization of plaque components with intravascular ultrasound elastography in human femoral and coronary arteries in vitro. *Circulation.* 2000;102:617–623.

24. Uchida Y, Nakamura F, Tomaru T, Morita T, Oshima T, Sasaki T, Morizuki S, Hirose J. Prediction of acute coronary syndromes by percutaneous coronary angioscopy in patients with stable angina. *Am Heart J.* 1995;130:195–203.

25. Thieme T, Wernecke KD, Meyer R, Brandenstein E, Habedank D, Hinz A, Felix SB, Baumann G, Kleber FX. Angioscopic evaluation of atherosclerotic plaques: validation by histomorphologic analysis and association with stable and unstable coronary syndromes. *J Am Coll Cardiol.* 1996;28:1–6.

26. Feld S, Ganim M, Carell ES, Kjellgren O, Kirkeeide RL, Vaughn WK, Kelly R, McGhie AI, Kramer N, Loyd D, Anderson HV, Schroth G, Smalling RW. Comparison of angioscopy, intravascular ultrasound imaging and quantitative coronary angiography in predicting clinical outcome after coronary intervention in high risk patients. *J Am Coll Cardiol.* 1996;28:97–105.

27. Casscells W, Hathorn B, David M, Krabach T, Vaughn WK, McAllister HA, Bearman G, Willerson JT. Thermal detection of cellular infiltrates in living atherosclerotic plaques: possible implications for plaque rupture and thrombosis. *Lancet.* 1996;347:1447–1451.

28. Stefanadis C, Diamantopoulos L, Vlachopoulos C, Tsiamis E, Dernellis J, Toutouzas K, Stefanadi E, Toutouzas P. Thermal heterogeneity within human atherosclerotic coronary arteries detected in vivo: a new method of detection by application of a special thermography catheter. *Circulation.* 1999;99:1965–1971.

29. Brezinski ME, Tearney GJ, Bouma BE, Izatt JA, Hee MR, Swanson EA, Southern JF, Fujimoto JG. Optical coherence tomography for optical

biopsy: properties and demonstration of vascular pathology. *Circulation.* 1996;93:1206–1213.

30. Patwari P, Weissman NJ, Boppart SA, Jesser C, Stamper D, Fujimoto JG, Brezinski ME. Assessment of coronary plaque with optical coherence tomography and high-frequency ultrasound. *Am J Cardiol.* 2000;85:641–644.

31. Tearney GJ, Brezinski ME, Bouma BE, Boppart SA, Pitris C, Southern JF, Fujimoto JG. In vivo endoscopic optical biopsy with optical coherence tomography. *Science.* 1997;276:2037–2039.

32. Fujimoto JG, Boppart SA, Tearney GJ, Bouma BE, Pitris C, Brezinski ME. High resolution in vivo intra-arterial imaging with optical coherence tomography. *Heart.* 1999;82:128–133.

33. Romer TJ, Brennan JF 3rd, Puppels GJ, Zwinderman AH, van Duinen SG, van der Laarse A, van der Steen AF, Bom NA, Bruschke AV. Intravascular ultrasound combined with Raman spectroscopy to localize and quantify cholesterol and calcium salts in atherosclerotic coronary arteries. *Arterioscler Thromb Vasc Biol.* 2000;20:478–483.

34. Zhu Q, Conant E, Chance B. Optical imaging as an adjunct to sonograph in differentiating benign from malignant breast lesions. *J Biomed Opt.* 2000;5:229–236.

35. Moreno PR, Lodder RA, O'Connor WN, Muller JE. Characterization of composition and vulnerability of atherosclerotic plaques by near-infrared spectroscopy. *Circulation.* 1998;98(suppl I):I-146. Abstract.

36. Charash WE, Lodder RA, Moreno PR, Purushothaman RK, Swain JA, O'Connor WN, Muller JE. Detection of simulated vulnerable plaque using a novel infrared spectroscopy catheter. *J Am Coll Cardiol.* 2000;35:38A. Abstract.

37. Barnett HJ, Taylor DW, Eliasziw M, Fox AJ, Ferguson GG, Haynes RB, Rankin RN, Clagett GP, Hachinski VC, Sackett DL, Thorpe KE, Meldrum HE. Benefit of carotid endarterectomy in patients with symptomatic moderate or severe stenosis. North American Symptomatic Carotid Endarterectomy Trial Collaborators. *N Engl J Med.* 1998;339:1415–1425.

38. Executive Committee for the Asymptomatic Carotid Atherosclerosis Study. Endarterectomy for asymptomatic carotid stenosis. *JAMA.* 1995;273:1421–1428.

39. Weinberger J, Ramos L, Ambrose JA, Fuster V. Morphologic and dynamic changes of atherosclerotic plaque at the carotid artery bifurcation: sequential imaging by real time B-mode ultrasonography. *J Am Coll Cardiol.* 1988;12:1515–1521.

40. Pignoli P, Tremoli E, Poli A, Oreste P, Paoletti R. Intimal plus medial thickness of the arterial wall: a direct measurement with ultrasound imaging. *Circulation.* 1986;74:1399–1406.

41. O'Leary DH, Polak JF, Kronmal RA, Manolio TA, Burke GL, Wolfson SK Jr. Carotid-artery intima and media thickness as a risk factor for myocardial infarction and stroke in older adults. Cardiovascular Health Study Collaborative Research Group. *N Engl J Med.* 1999;340:14–22.

42. Khoury Z, Schwartz R, Gottlieb S, Chenzbraun A, Stern S, Keren A. Relation of coronary artery disease to atherosclerotic disease in the aorta, carotid, and femoral arteries evaluated by ultrasound. *Am J Cardiol.* 1997;80:1429–1433.

43. Burke GL, Evans GW, Riley WA, Sharrett AR, Howard G, Barnes RW, Rosamond W, Crow RS, Rautaharju PM, Heiss G. Arterial wall thickness is associated with prevalent cardiovascular disease in middle-aged adults. The Atherosclerosis Risk in Communities (ARIC) Study. *Stroke.* 1995;26:386–391.

44. Nagai Y, Metter EJ, Earley CJ, Kemper MK, Becker LC, Lakatta EG, Fleg JL. Increased carotid artery intimal-medial thickness in asymptomatic older subjects with exercise-induced myocardial ischemia. *Circulation.* 1998;98:1504–1509.

45. Crouse JR 3rd, Craven TE, Hagaman AP, Bond MG. Association of coronary disease with segment-specific intimal-medial thickening of the extracranial carotid artery. *Circulation.* 1995;92:1141–1147.

46. Salonen R, Nyyssonen K, Porkkala E, Rummukainen J, Belder R, Park JS, Salonen JT. Kuopio Atherosclerosis Prevention Study (KAPS): a population-based primary preventive trial of the effect of LDL lowering on atherosclerotic progression in carotid and femoral arteries. *Circulation.* 1995;92:1758–1764.

47. de Groot E, Jukema JW, Montauban van Swijndregt AD, Zwinderman AH, Ackerstaff RG, van der Steen AF, Bom N, Lie KI, Bruschke AV. B-mode ultrasound assessment of pravastatin treatment effect on carotid and femoral artery walls and its correlations with coronary arteriographic findings: a report of the Regression Growth Evaluation Statin Study (REGRESS). *J Am Coll Cardiol.* 1998;31:1561–1567.

48. Witteman JC, Kannel WB, Wolf PA, Grobbee DE, Hofman A, D'Agostino RB, Cobb JC. Aortic calcified plaques and cardiovascular disease (the Framingham Study). *Am J Cardiol.* 1990;66:1060–1064.

49. Weinberger J, Azhar S, Danisi F, Hayes R, Goldman M. A new noninvasive technique for imaging atherosclerotic plaque in the aortic arch of stroke patients by transcutaneous real-time B-mode ultrasonography: an initial report. *Stroke.* 1998;29:673–676.

50. Tunick PA, Krinsky GA, Lee VS, Kronzon I. Diagnostic imaging of thoracic aortic atherosclerosis. *AJR Am J Roentgenol.* 2000;174: 1119–1125.

51. Parthenakis F, Skalidis E, Simantirakis E, Kounali D, Vardas P, Nihoyannopoulos P. Absence of atherosclerotic lesions in the thoracic aorta indicates absence of significant coronary artery disease. *Am J Cardiol.* 1996;77:1118–1121.

52. Lanza GM, Wallace KD, Scott MJ, Cacheris WP, Abendschein DR, Christy DH, Sharkey AM, Miller JG, Gaffney PJ, Wickline SA. A novel site-targeted ultrasonic contrast agent with broad biomedical application. *Circulation.* 1996;94:3334–3340.

53. Demos SM, Alkan-Onyuksel H, Kane BJ, Ramani K, Nagaraj A, Greene R, Klegerman M, McPherson DD. In vivo targeting of acoustically reflective liposomes for intravascular and transvascular ultrasonic enhancement. *J Am Coll Cardiol.* 1999;33:867–875.

54. Lindner JR, Song J, Xu F, Klibanov AL, Singbartl K, Ley K, Kaul S. Noninvasive ultrasound imaging of inflammation using microbubbles targeted to activated leukocytes. *Circulation.* 2000;102:2745–2750.

55. Tiukinhoy SD, Huang S, Khan AA, MacDonald RC, McPherson DD. Novel acoustic drug-encapsulated liposomes for site-specific delivery. *J Am Coll Cardiol.* 2001;37:256A. Abstract.

56. Tiukinhoy SD, Mahowald ME, Shively VP, Nagaraj A, Kane BJ, Klegerman ME, MacDonald RC, McPherson DD, Matsumura JS. Development of echogenic, plasmid-incorporated, tissue-targeted cationic liposomes that can be used for directed gene delivery. *Invest Radiol.* 2000;35:732–738.

57. Wexler L, Brundage B, Crouse J, Detrano R, Fuster V, Maddahi J, Rumberger J, Stanford W, White R, Taubert K. Coronary artery calcification: pathophysiology, epidemiology, imaging methods, and clinical implications. A statement for health professionals from the American Heart Association Writing Group. *Circulation.* 1996;94:1175–1192.

58. Callister TQ, Raggi P, Cooil B, Lippolis NJ, Russo DJ. Effect of HMG-CoA reductase inhibitors on coronary artery disease as assessed by electron-beam computed tomography. *N Engl J Med.* 1998;339: 1972–1978.

59. Becker CR, Kleffel T, Crispin A, Knez A, Young J, Schoepf UJ, Haberl R, Reiser MF. Coronary artery calcium measurement: agreement of multirow detector and electron beam CT. *AJR Am J Roentgenol.* 2001; 176:1295–1298.

60. Ohnesorge B, Flohr T, Becker C, Kopp AF, Schoepf UJ, Baum U, Knez A, Klingenbeck-Regn K, Reiser MF. Cardiac imaging by means of electrocardiographically gated multisection spiral CT: initial experience. *Radiology.* 2000;217:564–571.

61. Rumberger JA, Simons DB, Fitzpatrick LA, Sheedy PF, Schwartz RS. Coronary artery calcium area by electron-beam computed tomography and coronary atherosclerotic plaque area: a histopathologic correlative study. *Circulation.* 1995;92:2157–2162.

62. Moreno PR, Raman Purushothaman K, O'Connor WN, Fuster V, Muller JE. Lack of association between calcification and vulnerability in human atherosclerotic plaques. *J Am Coll Cardiol.* 2000;35:303A. Abstract.

63. Raggi P, Callister TQ, Cooil B, He ZX, Lippolis NJ, Russo DJ, Zelinger A, Mahmarian JJ. Identification of patients at increased risk of first unheralded acute myocardial infarction by electron-beam computed tomography. *Circulation.* 2000;101:850–855.

64. O'Rourke RA, Brundage BH, Froelicher VF, Greenland P, Grundy SM, Hachamovitch R, Pohost GM, Shaw LJ, Weintraub WS, Winters WL Jr, Forrester JS, Douglas PS, Faxon DP, Fisher JD, Gregoratos G, Hochman JS, Hutter AM Jr, Kaul S, Wolk MJ. American College of Cardiology/ American Heart Association Expert Consensus document on electron-beam computed tomography for the diagnosis and prognosis of coronary artery disease. *Circulation.* 2000;102:126–140.

65. Bielak LF, Kaufmann RB, Moll PP, McCollough CH, Schwartz RS, Sheedy PF 2nd. Small lesions in the heart identified at electron beam CT: calcification or noise? *Radiology.* 1994;192:631–636.

66. Greenland P, Abrams J, Aurigemma GP, Bond MG, Clark LT, Criqui MH, Crouse JR 3rd, Friedman L, Fuster V, Herrington DM, Kuller LH, Ridker PM, Roberts WC, Stanford W, Stone N, Swan HJ, Taubert KA, Wexler L. Prevention Conference V. Beyond secondary prevention:

identifying the high-risk patient for primary prevention: noninvasive tests of atherosclerotic burden: Writing Group III. *Circulation.* 2000; 101:e16–e22.

67. Achenbach S, Moshage W, Ropers D, Nossen J, Daniel WG. Value of electron-beam computed tomography for the noninvasive detection of high-grade coronary-artery stenoses and occlusions. *N Engl J Med.* 1998;339:1964–1971.

68. Becker CR, Knez A, Ohnesorge B, Schoepf UJ, Reiser MF. Imaging of noncalcified coronary plaques using helical CT with retrospective ECG gating. *AJR Am J Roentgenol.* 2000;175:423–424.

69. Vallabhajosula S. Radioisotopic imaging of atheroma. In: Fuster V, ed. *The Vulnerable Atherosclerotic Plaque: Understanding, Identification, and Modification.* Armonk, NY: Futura Publishing; 1999:213–229.

70. Vallabhajosula S, Fuster V. Atherosclerosis: imaging techniques and the evolving role of nuclear medicine. *J Nucl Med.* 1997;38:1788–1796.

71. Vallabhajosula S, Paidi M, Badimon JJ, Le NA, Goldsmith SJ, Fuster V, Ginsberg HN. Radiotracers for low density lipoprotein biodistribution studies in vivo: technetium-99 m low density lipoprotein versus radioiodinated low density lipoprotein preparations. *J Nucl Med.* 1988;29: 1237–1245.

72. Iuliano L, Mauriello A, Sbarigia E, Spagnoli LG, Violi F. Radiolabeled native low-density lipoprotein injected into patients with carotid stenosis accumulates in macrophages of atherosclerotic plaque: effect of vitamin E supplementation. *Circulation.* 2000;101:1249–1254.

73. Loscalzo J, Rocco TP. Imaging arterial thrombi: an elusive goal. *Circulation.* 1992;85:382–385.

74. Hardoff R, Braegelmann F, Zanzonico P, Herrold EM, Lees RS, Lees AM, Dean RT, Lister-James J, Borer JS. External imaging of atherosclerosis in rabbits using an ^{123}I-labeled synthetic peptide fragment. *J Clin Pharmacol.* 1993;33:1039–1047.

75. Blum JE, Handmaker H. Plenary session: Friday imaging symposium: role of small-peptide radiopharmaceuticals in the evaluation of deep venous thrombosis. *Radiographics.* 2000;1999:20:1187–1193.

76. Mitchel J, Waters D, Lai T, White M, Alberghini T, Salloum A, Knibbs D, Li D, Heller GV. Identification of coronary thrombus with a IIb/IIIa platelet inhibitor radiopharmaceutical, technetium-99 m DMP-444: a canine model. *Circulation.* 2000;101:1643–1646.

77. Helft G, Worthley SG, Zhang ZY, Tang C, Rodriguez O, Wei T, Fallon JT, Fayad ZA, Mahac J, Buchsbaum M, Fuster V, Badimon JJ. Noninvasive in vivo imaging of atherosclerotic lesions using fluorine-18 deoxyglucose (18-FDG) PET correlates with macrophage content in a rabbit model. *Circulation.* 1999;100(suppl I):I-311. Abstract.

78. Pearlman JD, Zajicek J, Merickel MB, Carman CS, Ayers CR, Brookeman JR, Brown MF. High-resolution ^{1}H NMR spectral signature from human atheroma. *Magn Reson Med.* 1988;7:262–279.

79. Mohiaddin RH, Firmin DN, Underwood SR, Abdulla AK, Klipstein RH, Rees RS, Longmore DB. Chemical shift magnetic resonance imaging of human atheroma. *Br Heart J.* 1989;62:81–89.

80. Toussaint JF, Southern JF, Fuster V, Kantor HL. ^{13}C-NMR spectroscopy of human atherosclerotic lesions: relation between fatty acid saturation, cholesteryl ester content, and luminal obstruction. *Arterioscler Thromb.* 1994;14:1951–1957.

81. Toussaint JF, Southern JF, Fuster V, Kantor HL. T2-weighted contrast for NMR characterization of human atherosclerosis. *Arterioscler Thromb Vasc Biol.* 1995;15:1533–1542.

82. Kaufman L, Crooks LE, Sheldon PE, Rowan W, Miller T. Evaluation of NMR imaging for detection and quantification of obstructions in vessels. *Invest Radiol.* 1982;17:554–560.

83. Herfkens RJ, Higgins CB, Hricak H, Lipton MJ, Crooks LE, Sheldon PE, Kaufman L. Nuclear magnetic resonance imaging of atherosclerotic disease. *Radiology.* 1983;148:161–166.

84. Fayad ZA, Fuster V. Characterization of atherosclerotic plaques by magnetic resonance imaging. *Ann N Y Acad Sci.* 2000;902:173–186.

85. Merickel MB, Carman CS, Brookeman JR, Mugler JP, Brown MF, Ayers CR. Identification and 3-D quantification of atherosclerosis using magnetic resonance imaging. *Comput Biol Med.* 1988;18:89–102.

86. Martin AJ, Gotlieb AI, Henkelman RM. High-resolution MR imaging of human arteries. *J Magn Reson Imaging.* 1995;5:93–100.

87. von Ingersleben G, Schmiedl UP, Hatsukami TS, Nelson JA, Subramaniam DS, Ferguson MS, Yuan C. Characterization of atherosclerotic plaques at the carotid bifurcation: correlation of high-resolution MR imaging with histologic analysis: preliminary study. *Radiographics.* 1997;17:1417–1423.

88. Worthley SG, Helft G, Fuster V, Fayad ZA, Fallon JT, Osende JI, Roque M, Shinnar M, Zaman AG, Rodriguez OJ, Verhallen P, Badimon JJ.

High resolution ex vivo magnetic resonance imaging of in situ coronary and aortic atherosclerotic plaque in a porcine model. *Atherosclerosis.* 2000;150:321–329.

89. Helft G, Worthley SG, Fuster V, Zaman AG, Schechter C, Osende J, Rodriguez OJ, Fayad ZA, Fallon JT, Badimon JJ. Atherosclerotic aortic component quantification by noninvasive magnetic resonance: an in vivo study in rabbits. *J Am Coll Cardiol.* 2001;37:1149–1154.

90. Edzes HT, Samulski ET. Cross relaxation and spin diffusion in the proton NMR or hydrated collagen. *Nature.* 1977;265:521–523.

91. Rapp JH, Connor WE, Lin DS, Inahara T, Porter JM. Lipids of human atherosclerotic plaques and xanthomas: clues to the mechanism of plaque progression. *J Lipid Res.* 1983;24:1329–1335.

92. Kucharczyk W, Henkelman RM. Visibility of calcium on MR and CT: can MR show calcium that CT cannot? *AJNR* Am J Neuroradiol. 1994; 15:1145–1148.

93. Bradley WG Jr. MR appearance of hemorrhage in the brain. *Radiology.* 1993;189:15–26.

94. Yamashita Y, Hatanaka Y, Torashima M, Takahashi M. Magnetic resonance characteristics of intrapelvic haematomas. *Br J Radiol.* 1995;68: 979–985.

95. Murray JG, Manisali M, Flamm SD, VanDyke CW, Lieber ML, Lytle BW, White RD. Intramural hematoma of the thoracic aorta: MR image findings and their prognostic implications. *Radiology.* 1997;204: 349–355.

96. Shinnar M, Fallon JT, Wehrli S, Levin M, Dalmacy D, Fayad ZA, Badimon JJ, Harrington M, Harrington E, Fuster V. The diagnostic accuracy of ex vivo magnetic resonance imaging for human atherosclerotic plaque characterization. *Arterioscler Thromb Vasc Biol.* 1999; 19:2756–2761.

97. Toussaint JF, Southern JF, Fuster V, Kantor HL. Water diffusion properties of human atherosclerosis and thrombosis measured by pulse field gradient nuclear magnetic resonance. *Arterioscler Thromb Vasc Biol.* 1997;17:542–546.

98. Pohost GM, Fuisz AR. From the microscope to the clinic: MR assessment of atherosclerotic plaque. *Circulation.* 1998;98:1477–1478.

99. Skinner MP, Yuan C, Mitsumori L, Hayes CE, Raines EW, Nelson JA, Ross R. Serial magnetic resonance imaging of experimental atherosclerosis detects lesion fine structure, progression and complications in vivo. *Nat Med.* 1995;1:69–73.

100. Worthley SG, Helft G, Fuster V, Zaman AG, Fayad ZA, Fallon JT, Badimon JJ. Serial in vivo MRI documents arterial remodeling in experimental atherosclerosis. *Circulation.* 2000;101:586–589.

101. McConnell MV, Aikawa M, Maier SE, Ganz P, Libby P, Lee RT. MRI of rabbit atherosclerosis in response to dietary cholesterol lowering. *Arterioscler Thromb Vasc Biol.* 1999;19:1956–1959.

102. Worthley SG, Helft G, Fuster V, Fayad ZA, Zaman AG, Fallon JT, Badimon JJ. Serial noninvasive in vivo MRI monitors progression and regression of individual atherosclerotic lesions in a rabbit model. *J Am Coll Cardiol.* 2000;35:432A. Abstract.

103. Worthley SG, Helft G, Osende JI, Corti R, Fayad ZA, Fallon JT, Zaman AG, Fuster V, Badimon JJ. Serial evaluation of atherosclerosis with in vivo MRI: study of atorvastatin and avasimibe in WHHL rabbits. *Circulation.* 2000;102(suppl II):II-809. Abstract.

104. Fayad ZA, Fallon JT, Shinnar M, Wehrli S, Dansky HM, Poon M, Badimon JJ, Charlton SA, Fisher EA, Breslow JL, Fuster V. Noninvasive in vivo high-resolution magnetic resonance imaging of atherosclerotic lesions in genetically engineered mice. *Circulation.* 1998;98: 1541–1547.

105. Aguinaldo JGS, Choudhury RP, Rong JX, Yodice C, Fallon JT, Fisher EA, Fayad ZA. Severity of atherosclerotic lesions in ApoE$^{-/-}$ mice assessed by non-invasive in vivo high resolution magnetic resonance microscopy. *Circulation.* 2000;102(suppl II):II-459. Abstract.

106. Yuan C, Beach KW, Smith LH Jr, Hatsukami TS. Measurement of atherosclerotic carotid plaque size in vivo using high resolution magnetic resonance imaging. *Circulation.* 1998;98:2666–2671.

107. Fayad ZA, Nahar T, Fallon JT, Goldman M, Aguinaldo JG, Badimon JJ, Shinnar M, Chesebro JH, Fuster V. In vivo MR evaluation of athero-

sclerotic plaques in the human thoracic aorta: a comparison with TEE. *Circulation.* 2000;101:2503–2509.

108. Coulden RA, Moss H, Graves MJ, Lomas DJ, Appleton DS, Weissberg PL. High resolution magnetic resonance imaging of atherosclerosis and the response to balloon angioplasty. *Heart.* 2000;83:188–191.

109. Fayad ZA, Fuster V, Fallon JT, Jayasundera T, Worthley SG, Helft G, Aguinaldo JG, Badimon JJ, Sharma SK. Noninvasive in vivo human coronary artery lumen and wall imaging using black-blood magnetic resonance imaging. *Circulation.* 2000;102:506–510.

110. Hatsukami TS, Ross R, Polissar NL, Yuan C. Visualization of fibrous cap thickness and rupture in human atherosclerotic carotid plaque in vivo with high-resolution magnetic resonance imaging. *Circulation.* 2000;102:959–964.

111. Yucel EK, Anderson CM, Edelman RR, Grist TM, Baum RA, Manning WJ, Culebras A, Pearce W. AHA scientific statement: magnetic resonance angiography: update on applications for extracranial arteries. *Circulation.* 1999;100:2284–2301.

112. Fayad ZA, Connick TJ, Axel L. An improved quadrature or phased-array coil for MR cardiac imaging. *Magn Reson Med.* 1995;34: 186–193.

113. Fayad ZA, Hardy CJ, Giaquinto R, Kini A, Sharma S. Improved high resolution MRI of human coronary lumen and plaque with a new cardiac coil. *Circulation.* 2000;102(suppl II):II-399. Abstract.

114. Hayes CE, Mathis CM, Yuan C. Surface coil phased arrays for high-resolution imaging of the carotid arteries. *J Magn Reson Imaging.* 1996;6:109–112.

115. Summers RM, Andrasko-Bourgeois J, Feuerstein IM, Hill SC, Jones EC, Busse MK, Wise B, Bove KE, Rishforth BA, Tucker E, Spray TL, Hoeg JM. Evaluation of the aortic root by MRI: insights from patients with homozygous familial hypercholesterolemia. *Circulation.* 1998;98: 509–518.

116. Jaffer FA, O'Donnell CJ, Kissinger KV, Chan SK, Botnar RM, Edelman RR, Manning WJ. MRI assessment of aortic atherosclerosis in an asymptomatic population: the Framingham Heart Study. *Circulation.* 2000;102(suppl II):II-458. Abstract.

117. O'Donnell CJ, Larson MG, Jaffer FA, Kissinger KV, Levy D, Manning WJ. Aortic atherosclerosis detected by MRI is associated with contemporaneous and longitudinal risk factors: the Framingham Heart Study (FHS). *Circulation.* 2000;102(suppl II):II-836. Abstract.

118. Worthley SG, Helft G, Fuster V, Fayad ZA, Rodriguez OJ, Zaman AG, Fallon JT, Badimon JJ. Noninvasive in vivo magnetic resonance imaging of experimental coronary artery lesions in a porcine model. *Circulation.* 2000;101:2956–2961.

119. Botnar RM, Stuber M, Kissinger KV, Kim WY, Spuentrup E, Manning WJ. Noninvasive coronary vessel wall and plaque imaging with magnetic resonance imaging. *Circulation.* 2000;102:2582–2587.

120. Corti R, Fayad ZA, Fuster V, Worthley SG, Helft G, Chesebro J, Mercuri M, Badimon JJ. Effects of lipid-lowering by simvastatin on human atherosclerotic lesions: a longitudinal study by high-resolution, noninvasive magnetic resonance imaging. *Circulation.* 2001;104:249–252.

121. Luk-Pat GT, Gold GE, Olcott EW, Hu BS, Nishimura DG. High-resolution three-dimensional in vivo imaging of atherosclerotic plaque. *Magn Reson Med.* 1999;42:762–771.

122. Pachot-Clouard M, Vaufrey F, Darrasse L, Toussainti JF. Magnetization transfer characteristics in atherosclerotic plaque components assessed by adapted binomial preparation pulses. *MAGMA.* 1998;7:9–15.

123. Lin W, Abendschein DR, Haacke EM. Contrast-enhanced magnetic resonance angiography of carotid arterial wall in pigs. *J Magn Reson Imaging.* 1997;7:183–190.

124. Yu X, Song SK, Chen J, Scott MJ, Fuhrhop RJ, Hall CS, Gaffney PJ, Wickline SA, Lanza GM. High-resolution MRI characterization of human thrombus using a novel fibrin-targeted paramagnetic nanoparticle contrast agent. *Magn Reson Med.* 2000;44:867–872.

125. Steinman DA, Rutt BK. On the nature and reduction of plaque-mimicking flow artifacts in black blood MRI of the carotid bifurcation. *Magn Reson Med.* 1998;39:635–641.

Origin of atherosclerosis in childhood and adolescence[1-4]

Henry C McGill Jr, C Alex McMahan, Edward E Herderick, Gray T Malcom, Richard E Tracy, and Jack P Strong for the Pathobiological Determinants of Atherosclerosis in Youth (PDAY) Research Group

ABSTRACT   Atherosclerosis begins in childhood as deposits of cholesterol and its esters, referred to as fatty streaks, in the intima of large muscular arteries. In some persons and at certain arterial sites, more lipid accumulates and is covered by a fibromuscular cap to form a fibrous plaque. Further changes in fibrous plaques render them vulnerable to rupture, an event that precipitates occlusive thrombosis and clinically manifest disease (sudden cardiac death, myocardial infarction, stroke, or peripheral arterial disease). In adults, elevated non-HDL-cholesterol concentrations, low HDL-cholesterol concentrations, hypertension, smoking, diabetes, and obesity are associated with advanced atherosclerotic lesions and increased risk of clinically manifest atherosclerotic disease. Control of these risk factors is the major strategy for preventing atherosclerotic disease. To determine whether these risk factors also are associated with early atherosclerosis in young persons, we examined arteries and tissue from ≈3000 autopsied persons aged 15–34 y who died of accidental injury, homicide, or suicide. The extent of both fatty streaks and raised lesions (fibrous plaques and other advanced lesions) in the right coronary artery and in the abdominal aorta was associated positively with non-HDL-cholesterol concentration, hypertension, impaired glucose tolerance, and obesity and associated negatively with HDL-cholesterol concentration. Atherosclerosis of the abdominal aorta also was associated positively with smoking. These observations indicate that long-range prevention of atherosclerosis and its sequelae by control of the risk factors for adult coronary artery disease should begin in adolescence and young adulthood.   *Am J Clin Nutr* 2000;72(suppl):1307S–15S.

KEY WORDS   Coronary arteries, aorta, atherosclerosis, risk factors, fatty streaks, adolescents, young adults

INTRODUCTION

The natural history of atherosclerosis, as described nearly 50 y ago (1), is depicted in **Figure 1** (2). This description of origin and progression is inferred predominantly from observations of the arteries of persons autopsied at various ages. It is based on the assumption that any type of lesion occurring in one age group (for example, fatty streaks in adolescents) may be transformed into another type of lesion occurring at the same anatomic site in an older age group (for example, fibrous plaques in young adults and middle-aged persons). There has been little or no doubt for many years that the raised lesions of atherosclerosis (a collective term

for fibrous plaques and the associated complications) determine the risk of clinically manifest coronary artery disease (CAD), both for populations and for individuals. CAD events become frequent in a population when the average extent of coronary artery raised lesions in middle-aged persons approaches ≈30% of the coronary intimal surface (3); individuals with CAD have on average ≈60% of the coronary intimal surface involved with raised lesions (4–6). Recent studies by angiography, ultrasonography, and histochemistry show that the qualities of raised lesions also predict risk of an occlusive event (7).

Lowering serum lipid concentrations by diet and drugs reduces both first events of CAD (primary prevention) (8) and recurrent events (secondary prevention) (9) among adults. However, no trials have intervened in childhood, adolescence, or young adulthood and subsequently followed the subjects into middle age, and such a trial is not likely to be feasible. The age at which preventive regimens should begin depends on the extrapolation of results in adults to younger persons, on the significance of the juvenile fatty streak, and on the conditions affecting the transformation of fatty streaks into raised lesions.
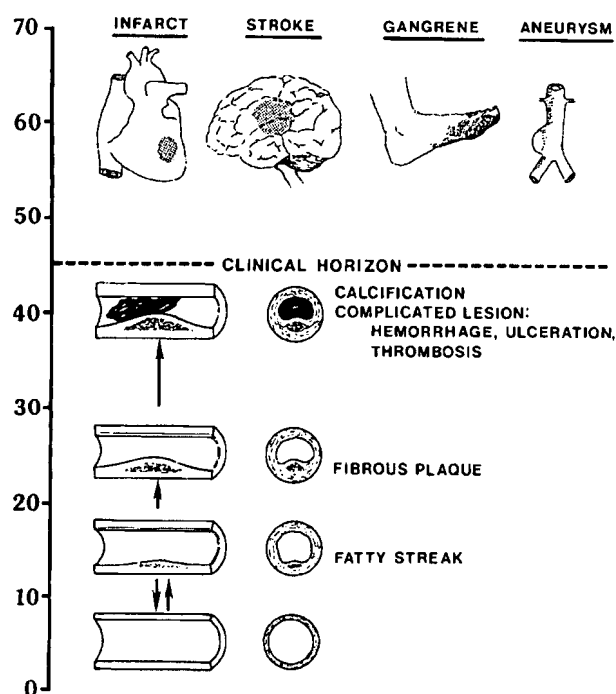
NATURAL HISTORY OF ATHEROSCLEROSIS

FIGURE 1. The development of the fatty streak in childhood is depicted as a reversible process. In adolescence, some fatty streaks accumulate more lipid and begin to develop a fibromuscular cap, forming the lesion termed a fibrous plaque. In subsequent years, fibrous plaques enlarge and undergo calcification, hemorrhage, ulceration or rupture, and thrombosis. Thrombotic occlusion precipitates clinical disease, depending on which artery is affected. Reproduced from reference 2.

In this article, we review the evidence that the fatty streak is the initial lesion of atherosclerosis and is the precursor of clinically important raised lesions, and relate this evidence to emerging knowledge of the molecular and cellular biology of atherosclerosis. We describe evidence regarding the associations of adult CAD risk factors with atherosclerosis in young persons and discuss the implications of these observations for the long-range prevention of CAD.

ORIGIN AND FATE OF THE FATTY STREAK

Aortic fatty streaks

Almost every North American child over the age of 3 y has some degree of aortic fatty streaks (10). Extensive aortic fatty streaks were present in children from post–World War I eastern Europe (11). Aortic fatty streaks were probably present in our hominid ancestors before they emerged as a separate species because fatty streaks occur frequently in both Old and New World nonhuman primates living in their natural habitat (12, 13) and in other mammalian species (14). Aortic fatty streaks differ only slightly in extent among children and adolescents of all populations, regardless of the frequency or severity of advanced atherosclerosis and CAD in adults in those populations (15). Women have more extensive aortic fatty streaks than do men in

all populations (15), yet women develop an equal extent of aortic raised lesions (3). The thoracic aorta has about the same extent of fatty streaks as does the abdominal aorta, but raised lesions develop appreciably only in the abdominal aorta (3). The ecologic, epidemiologic, and topographic analyses that showed little or no relation between aortic fatty streaks and the clinically important lesions of atherosclerosis are largely responsible for the skepticism about the significance of the fatty streak (16–18).

Coronary artery fatty streaks

The relation of fatty streaks to more advanced lesions is different in the coronary arteries than in the aorta. Fatty streaks begin to appear in the coronary arteries 5–10 y later than in the aorta (15, 19). Comparisons of the localization of lesions in the coronary arteries show a close correspondence between the localization of fatty streaks in young persons and that of raised lesions in older persons (20). In nonblack populations, the extent of coronary artery fatty streaks in young persons predicts the extent of raised lesions in older persons (15). However, although women have about the same extent of or more coronary artery fatty streaks than do men, they have only half the extent of raised lesions at older ages (15).

Transitional lesions

The classification of atherosclerotic lesions in the coronary arteries as fatty streaks or fibrous plaques may not tell the whole story. The coronary arteries of white male children, adolescents, and young adults (who are at highest risk of advanced atherosclerosis and CAD) have more intimal cellular infiltration and connective tissue than do the coronary arteries of women or blacks. By the third decade, these differences are more pronounced and white male coronary arteries also show more vascularization (21). These observations were confirmed in a larger number of subjects from populations with a wide range of susceptibility to advanced atherosclerosis (22).

Chemical, physicochemical, histologic, and electron microscopic studies of fatty steaks and raised lesions of both the coronary arteries and the aorta (23–28) showed that both fatty streaks and raised lesions (as defined by gross criteria) contain free and esterified cholesterol, isotropic and anisotropic crystals, extracellular and intracellular lipid, collagen, and macrophages, and differ only in the proportions of each component. These observations suggest that there is a continuous spectrum of lesions ranging from those composed predominantly of lipid-filled macrophages (foam cells) in a relatively normal intima (the fatty streak) to those containing predominantly extracellular lipid and cholesterol ester crystals with a collagenous and muscular cap (the fibrous plaque). Between these 2 extremes of the fatty streak and the fibrous plaque, transitional stages of atherosclerosis exist that are not identifiable by gross examination alone.

These transitional stages were related to age by histologic examination of a standard site in the left coronary arteries of >500 persons from birth to 29 y of age (29). About one-third of children under 9 y of age had simple intimal fatty streaks composed exclusively of macrophage foam cells. By the age of puberty, more than one-half of the children had larger accumulations of macrophage foam cells, extracellular lipid, and lipid in smooth muscle cells. A small percentage of these children had large accumulations of extracellular lipid. By the late 20s, about one-third of the young adults had well-developed raised lesions with large extracellular lipid cores and thick fibromuscular caps.

These results correspond with the observation 36 y earlier of advanced coronary artery lesions in young (average age: 22 y) soldiers killed in the Korean War (30). Thus, there seems little doubt that in the coronary arteries the juvenile fatty streak—an apparently innocuous cluster of macrophage foam cells in the arterial intima—can, in some individuals, progress to advanced atherosclerotic lesions within a few decades.

The fatty streak as a byproduct of macrophage function

The origin of the ubiquitous juvenile fatty streak has long been an enigma, but now we have a plausible molecular and cellular mechanism for its origin and its transformation into a fibrous plaque. The discovery of oxidized LDL (31) and its uptake by the macrophage receptor for acetylated LDL (32) led to the identification of a family of macrophage receptors, commonly known as scavenger receptors (33–35), that bind a wide range of ligands (36) and probably are also involved in host defense mechanisms. One scavenger receptor that has a high affinity for oxidized LDL also recognizes apoptotic cells and facilitates their phagocytosis (37, 38). The common denominator of oxidized LDL and apoptotic cells is probably a modified phospholipid (39, 40).

These observations suggest that macrophages are stationed in all tissues, including the arterial wall. Each macrophage possesses a battery of versatile receptors that enable it to participate in host defenses and to remove apoptotic cell debris. Some of these receptors also have an affinity for the LDL that is oxidatively modified during or after passage through the endothelium. Any one of several conditions can accelerate the uptake of oxidized LDL: higher concentrations of LDL susceptible to oxidation, more rapid oxidation of LDL, less antioxidants, genetic variations in receptor structure and function (41), impairment of the macrophage's ability to discharge the phagocytosed sterols (42), or secretion of cytokines by macrophages loaded with cholesterol (43). A combination of a few of the factors favoring LDL oxidation and macrophage lipid accumulation and retention, even with a normal plasma LDL concentration, might explain the initial cluster of macrophage foam cells. If the process is accelerated by an elevated plasma LDL concentration, and overloaded foam cells die to form a pool of extracellular lipid, the transitional lesion forms. Macrophages stimulate adjacent smooth muscle cells to accumulate lipid (44). Inflammatory cytokines are generated, attract more macrophages, and autocatalyze the chronic inflammatory process. Thus, plausible molecular and cellular mechanisms can now explain the origin of the fatty streak as a physiologic process that can transform the fatty streak into a pathologic lesion under certain conditions. The risk factors for adult CAD augment the process of transforming the fatty streak into a lesion that causes arterial occlusion.

CORONARY ARTERY DISEASE RISK FACTORS AND ATHEROSCLEROSIS IN YOUTH

Association of risk factors for CAD with atherosclerosis

The longitudinal epidemiologic studies of the 1950s left little doubt that certain individual characteristics, which came to be known as risk factors, predict the probability that an individual will subsequently develop a clinical manifestation of atherosclerosis. Early attempts to relate these risk factors to atherosclerotic lesions yielded negative results (45–48), and these reports are frequently cited by skeptics of the hypothesis that serum cholesterol

is an important intervening variable in the etiology of atherosclerosis (16). However, positive results began to emerge when better methods of quantifying atherosclerosis were developed, when antemortem risk factor measurements became available, and when investigators began to examine subjects dying as a result of accidents and other external causes rather than elderly persons dying of chronic diseases (49–60). The cumulative evidence is now overwhelming that the major risk factors for clinically manifest CAD (elevated serum cholesterol, hypertension, smoking, and diabetes) are strongly associated with atherosclerosis in the aorta and coronary arteries of adults older than ≈ 35 y of age. A few studies have extended the associations to 25 y of age (61, 62).

Risk factors and atherosclerosis in youth

In the 1980s, several epidemiologic studies measured serum total and lipoprotein cholesterol, blood pressure, adiposity, and other variables identified as risk factors for adult CAD in children and adolescents (63, 64). These studies showed that, although the average values were lower than those in adults, there were wide ranges of values for these variables beginning during the preschool period. These findings suggested that the predisposition to accelerated atherosclerosis might begin early in life and that control of these variables might be useful in long-range primary prevention.

Except for the rare cases of homozygous familial hypercholesterolemia in which accelerated atherosclerosis is common (65), and except for the studies of 25–44-y-old men cited above (61, 62), little evidence existed regarding the relation of the adult CAD risk factors to atherosclerosis in children, adolescents, or young adults under the age of 35 y. This issue is important in deciding at what age hygienic measures (eg, diet, physical activity, and weight control) should be advocated to control the risk factors and thereby retard the progression of atherosclerosis in youth and defer the onset of CAD years later.

In the Bogalusa Heart Study, atherosclerotic lesions were measured in arteries from 66 persons aged 6–30 y whose risk factors had been measured during life and who were autopsied after death due to accidents, homicide, or suicide (66). LDL-cholesterol concentrations were positively associated with the percentage of surface involved by fatty streaks in the coronary arteries and aorta. The number of subjects was not sufficient to detect associations with raised lesions nor to examine associations within age, sex, and race subgroups.

The Pathobiological Determinants of Atherosclerosis in Youth Study

In 1985 a group of investigators organized the Pathobiological Determinants of Atherosclerosis in Youth (PDAY) Study to obtain more extensive information about the relation of risk factors to atherosclerotic lesions in youth (67). These investigators collected arteries, blood, and selected tissues from ≈ 3000 persons aged 15–34 y who had died within 72 h of accidental injury, homicide, or suicide, and were autopsied within 48 h of death in a medical examiner's laboratory. Seven collaborating centers collected this material following a standardized procedure and submitted specimens and information to central laboratories for analysis.

PDAY collection teams removed the aorta and coronary arteries from each body. They split the aorta in half longitudinally, fixed one half for gross examination, and preserved fixed and frozen samples from the other half for histochemical and chemical analyses. They opened the right coronary artery longitudinally and
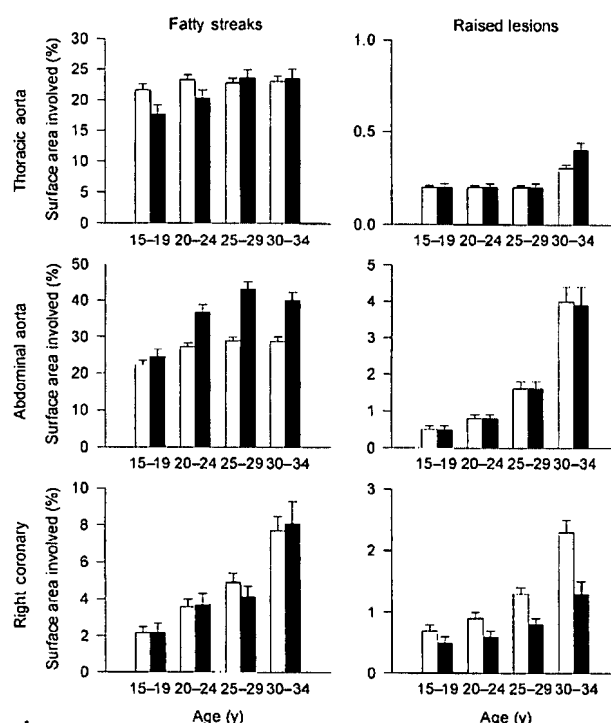
FIGURE 2. The mean (+SE) extent of fatty streaks and raised lesions by 5-y age groups of men (□) and women (■) in the thoracic aorta, abdominal aorta, and right coronary artery. The values are adjusted for race, non-HDL-cholesterol concentration, HDL-cholesterol concentration, and smoking. Drawn from data reported in reference 74.

fixed it in the flattened state for gross examination, fixed the left anterior descending coronary artery by pressure perfusion for histologic study, and froze the circumflex coronary artery for chemical analyses.

A central laboratory measured total and HDL cholesterol in postmortem serum and derived the non-HDL-cholesterol concentration by subtraction. The laboratory also measured thiocyanate in postmortem serum as an indicator of smoking status and measured glycosylated hemoglobin in red blood cells as a measure of blood glucose and incipient diabetes mellitus. Mean arterial blood pressure was estimated by an algorithm that used the thickness of the intima of small renal arteries. Adiposity was evaluated as the body mass index (BMI; in kg/m²) computed from the weight and height of the body measured at autopsy.

The fixed aortas and right coronary arteries were stained with Sudan IV (Sigma-Aldrich, St Louis) to display fatty streaks. A team of pathologists in a central laboratory estimated the percentage of intimal surface of the left half of the aorta and the right coronary artery that was involved with fatty streaks and with raised lesions, a category that included fibrous plaques and plaques with calcification or ulceration. In this age group the raised lesions were predominantly uncomplicated fibrous plaques. Photographs of the stained arteries were digitized in another central laboratory and converted to standardized formats. Computerized algorithms produced composite images of specified groups that showed the prevalence of fatty streaks and raised lesions at each pixel location over the entire arterial surface (68, 69).

Percentage of surface involvement was also computed for specified regions of each artery.

The collection phase of the project, which began in June 1987, was completed in August 1994. A total of 2876 subjects met the study criteria. Of these, serum for the measurement of lipoprotein cholesterol and thiocyanate was available for 1506 subjects and red blood cells for measurement of glycosylated hemoglobin were available for 2544 subjects. Kidney samples for assessment of hypertension were available for 2833 cases. About one-half of the subjects were white and the other one-half were black; about three-quarters were men and one-quarter were women. About one-third of the subjects died of accidents, one-half of homicide, and one-tenth of suicide. In preliminary analyses, the associations of risk factors with atherosclerosis were similar across all cause-of-death categories and these were pooled for the final analyses.

The major results describing the progression of atherosclerosis with age and the associations of serum lipids, smoking, hypertension, glycosylated hemoglobin, adiposity, and polymorphisms in candidate genes have been reported (70–77) and further analyses of the data are under way. In this review, we focus on effects of the risk factor variables most closely related to nutrition: serum lipoprotein cholesterol concentrations, glycosylated hemoglobin, and adiposity.

Risk factors among PDAY subjects

Non-HDL- and HDL-cholesterol concentrations were remarkably similar to those reported between 1980 and 1993 in surveys of living populations (74). The major limitations in use of these values are errors introduced by hemodilution as a result of the infusion of fluids or hemoconcentration due to hemorrhage after injury and before death. We excluded cases with serum cholesterol concentrations <2.59 mmol/L (100 mg/dL) to eliminate severely diluted sera. Errors due to hemodilution or hemoconcentration are likely to degrade associations but are not likely to produce spurious associations.

About one-half of the subjects aged >20 y were smokers as indicated by a serum thiocyanate concentration ≥90 μmol/L (74), a prevalence higher than in most surveys based on self-reported smoking habits. This higher prevalence was probably due to the association of smoking with accidents and suicides and use of an objective marker for smoking.

About 40% of the subjects had a BMI >25 and 10% had a BMI >30 (72). These results are consistent with surveys of adiposity in US adolescents and young adults (78). About 2% of the cases had glycosylated hemoglobin concentrations ≥0.08 (72). The prevalence of hypertension was similar to that seen in living populations (75).

Progression of atherosclerosis with age

Shown in **Figure 2** is the average extent of fatty streaks and raised lesions of the thoracic aorta, the abdominal aorta, and the right coronary artery by sex and 5-y age groups. The values are adjusted for race, non-HDL- and HDL-cholesterol concentrations, and smoking. By 15–19 y of age, fatty streaks occupied ≈25% of the aortic intima in both the thoracic and abdominal aortas. In subsequent age groups, fatty streaks remained constant in the thoracic aorta, but increased to occupy ≈40% of the abdominal aorta by the age of 30–34 y. By the age of 30–34 y, raised lesions occupied <0.5% of the thoracic aorta, but occupied ≈5% of the abdominal aortic surface. In the abdominal
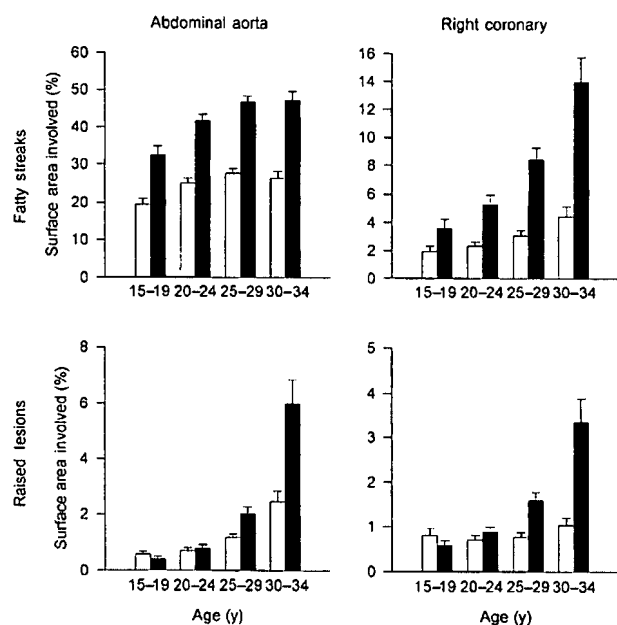
FIGURE 3. The mean (+SE) extent of fatty streaks and raised lesions in the abdominal aorta and right coronary artery by 5-y age groups in persons with a favorable lipoprotein profile [□; non-HDL cholesterol <2.89 mmol/L (108 mg/dL), HDL cholesterol >1.55 mmol/L (60 mg/dL)] compared with an unfavorable lipoprotein profile [■; non-HDL cholesterol >3.88 mmol/L (150 mg/dL), HDL cholesterol <1.11 mmol/L (43 mg/dL)]. Values are adjusted for race, sex, and smoking. Drawn from data reported in reference 74.

aorta, fatty streaks were more extensive in women than in men, but the extent of raised lesions did not differ significantly between men and women.

In the right coronary artery, fatty streaks increased in extent from ≈2% of the intimal surface at the age of 15–19 y to ≈8% at the age of 30–34 y and were equal in men and women. Raised lesions increased from ≈0.5% at the age of 15–19 y to >2% at the age of 30–34 y in men, but women had about one-half the extent of raised lesions at all ages. These results are consistent with results from many previous studies (3, 10, 15, 19) showing that the thoracic aorta is highly susceptible to fatty streaks, but not to raised lesions; that the abdominal aortas of women have more extensive fatty streaks than the abdominal aortas of men but an equal extent of raised lesions; and that the coronary arteries of women and men have an equal extent of fatty streaks, but that women have less extensive raised lesions.

Association of serum lipoprotein cholesterol concentrations with atherosclerosis

Non-HDL-cholesterol concentrations were positively associated with both fatty streaks and raised lesions in both the aorta and the right coronary artery; the opposite was true of HDL-cholesterol concentrations. Compared in **Figure 3** are fatty streaks and raised lesions in persons with favorable lipoprotein profiles (lowest third of non-HDL-cholesterol concentration, highest third of HDL-cholesterol concentration) and in those with unfavorable lipoprotein profiles (highest third of non-HDL cholesterol, lowest third of HDL cholesterol) (74). The

values are adjusted for race, sex, and smoking. The unfavorable profile was associated with more extensive fatty streaks in both the abdominal aorta and the right coronary artery in all age groups. In the right coronary artery of 30–34-y-olds, the difference was nearly 3-fold. The lipoprotein profile began to affect raised lesions in the 20–24-y age group, and the difference in raised lesions was nearly 3-fold by 30–34 y. The unfavorable lipoprotein profile as defined here (combination of high non-HDL and low HDL cholesterol) is not rare: ≈10% of the PDAY cases fell into this category.

Association of BMI with atherosclerosis

The BMI was associated with more extensive fatty streaks and raised lesions in the right coronary arteries of men but not of women (**Figure 4**) (72).

Association of glycosylated hemoglobin with atherosclerosis

An elevated glycosylated hemoglobin concentration (≥0.08), which corresponds to an average blood glucose concentration of ≥8.3 mmol/L (150 mg/dL) for the previous 2 or 3 mo, was associated with increased fatty streaks and raised lesions of the right coronary artery (**Figure 5**) and with raised lesions of the abdominal aorta (72).

Association of smoking with atherosclerosis

In the abdominal aorta, smoking was associated with more extensive fatty streaks in the 15–24-y age group and with 3-fold more extensive raised lesions in the aorta in the 25–34-y age group (74). Smoking was also associated with a greater population of macrophage foam cells in atherosclerotic lesions (79).

Association of hypertension with atherosclerosis

Hypertension (mean arterial pressure ≥110 mm Hg) was associated with more extensive raised lesions in the right coronary artery and abdominal aorta, but did not affect fatty streaks (75).
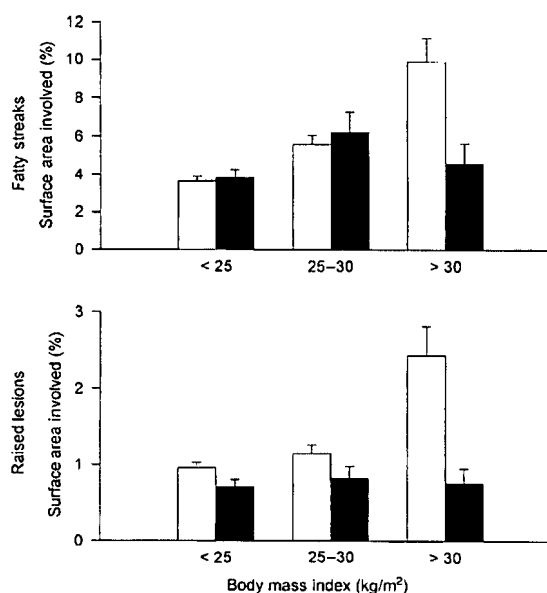

FIGURE 4. The mean (+SE) extent of fatty streaks and raised lesions in the right coronary artery by BMI in men (□) and (■). Values are adjusted for race and age. Drawn from data reported in reference 73.
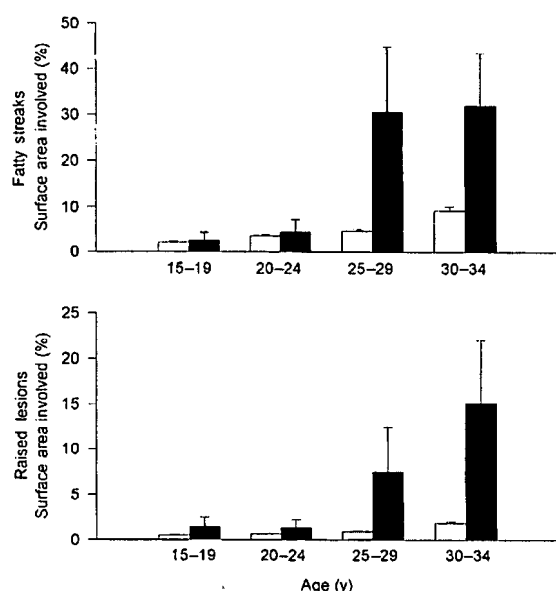
FIGURE 5. The mean (+SE) extent of fatty streaks and raised lesions in the right coronary artery by age and normal glycosylated hemoglobin concentration ($\square$; <0.08) compared with elevated glycosylated hemoglobin concentration ($\blacksquare$; ≥0.08). Values are adjusted for race and sex. Drawn from data reported in reference 73.

The extent of raised lesions followed that of fatty streaks by ≈5 y and the topographic distributions of fatty streaks and raised lesions were similar in all age groups. These results are consistent with those derived from a different population (20) and suggest that local factors in the artery wall affect fatty streaks and raised lesions similarly.

SUMMARY AND IMPLICATIONS FOR THE PREVENTION OF CORONARY ARTERY DISEASE

Fatty streaks as the initial lesions of atherosclerosis

Morphologic observations show a continuous progression from uncomplicated juvenile fatty streaks to raised lesions. The associations of risk factors with fatty streaks and raised lesions are similar and the topographic distributions of fatty streaks and raised lesions are similar in the coronary arteries and the abdominal aorta. The juvenile fatty streak, defined grossly, varies widely in characteristics. Under certain conditions and at certain anatomic sites, it is converted into a fibrous plaque and eventually undergoes other changes that directly cause arterial occlusion. Although harmless if it remains a fatty streak, the fatty streak nevertheless appears to be the initial lesion of atherosclerosis.

Mechanisms of transformation to raised lesions

The associations of CAD risk factors with fatty streaks and raised lesions in young adults are consistent with the cellular and molecular mechanisms derived from emerging knowledge of oxidized LDL, macrophages, and scavenger receptors. An elevated LDL concentration is the most common determinant of progression. HDL has antioxidant properties (80) and provides reverse cholesterol transport. Smoking has many effects, including increasing oxidative stress (81). Estrogen also has many effects, including antioxidant and antiinflammatory properties (82, 83). Hyperglycemia increases the formation of advanced
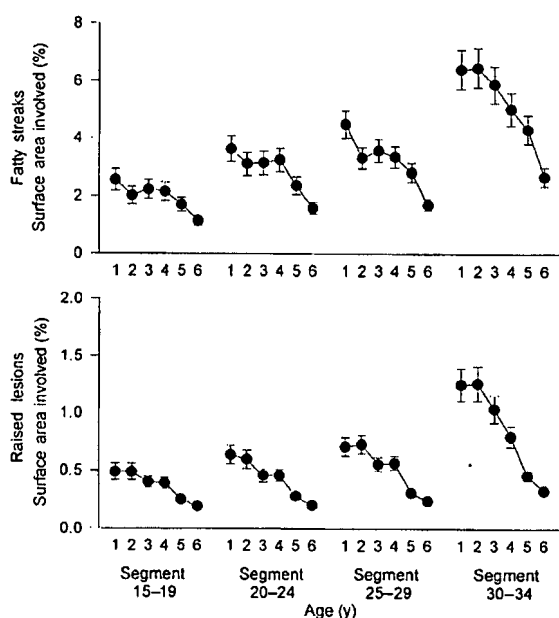
Topography of coronary fatty streaks and raised lesions

The topographic association of fatty streaks with raised lesions in the right coronary arteries of PDAY specimens is shown in **Figures 6** and **7**. In Figure 6, composite computerized images of right coronary artery intima stained with Sudan IV (fatty streaks) by 5-y age groups of white males are shown in the left panel and raised lesions are shown in the right panel.

Age 15–19 y

Age 20–24 y

Age 25–29 y

Age 30–34 y

00-02   02-04   04-06   06-08   08-10   10+

FIGURE 6. Composite digitized images of the right coronary artery of white males by 5-y age groups to depict the prevalence of fatty streaks stained with Sudan IV (Sigma-Aldrich, St Louis) (left panel) and the prevalence of raised lesions (right panel). n = 193 (15–19 y), 231 (20–24 y), 276 (25–29 y), and 234 (30–34 y). Color scale at bottom indicates prevalence.

FIGURE 7. The mean (+SE) extent of fatty streaks and raised lesions in 1-cm segments of right coronary artery by 5-y age groups. Values were adjusted for race and sex and were generated by computerized digital image analysis.

glycosylation end products, which are ingested by scavenger receptors and further damage macrophages (84).

Mechanisms by which obesity augments raised lesions in men but not in women are not yet obvious. Despite many hypotheses involving the angiotensin system, it is not clear how hypertension accelerates the formation of raised lesions but not fatty streaks. It is still necessary to consider local anatomic and hemodynamic factors to account for the localization of fatty streaks, and for the tendency of fatty streaks in some locations to progress and in other sites to regress or remain static.

Implications for the prevention of CAD

We now have evidence that serum lipoprotein concentrations, smoking, obesity, and hyperglycemia are closely associated with fatty streaks in the second decade of life. The same risk factors, along with hypertension, are associated with raised lesions in the third decade of life. These results indicate that the long-range prevention of CAD should begin in childhood with control of the risk factors for CAD to limit the extent of juvenile fatty streaks and, more critically, to prevent or retard their progression to raised lesions.

NOTE ADDED IN PROOF

Subsequent to the submission of the manuscript, several articles that supplemented or modified statements in this article were published by the PDAY Research Group.

Transitional lesion

We state that "transitional stages of atherosclerosis... are not identifiable by gross examination alone." Wissler et al (85) compared the microscopic characteristics of several gross lesions in PDAY cases with microscopic counterparts and developed crite-

ria for the identification of transitional lesions, known as fatty plaques or raised fatty streaks. These criteria were applied to ≈3000 aortas and coronary arteries, and the areas previously designated fatty streaks were divided into flat fatty streaks and raised fatty streaks. There were significant associations of raised fatty streaks with the risk factors for adult CAD (eg, non-HDL cholesterol- and HDL-cholesterol concentrations, hypertension, smoking, obesity, and impaired glucose tolerance), and these associations became evident in the late teenage years, earlier than the associations with grossly detected raised lesions (86). These results are consistent with the hypothesized progression of atherosclerosis from fatty streaks to fibrous plaques under the influence of the risk factors for adult CAD.

The microscopic qualities of atherosclerotic lesions at a standard site in the left anterior descending coronary artery were evaluated in 760 PDAY cases by using the American Heart Association (AHA) grading method (87) and computerized morphometry (88). Advanced (AHA grade 4–5) lesions were more frequent in men than in women and were positively associated with non-HDL-cholesterol concentrations, obesity, hypertension, and impaired glucose tolerance. AHA grade 2–3 lesions were associated with low HDL-cholesterol concentrations and smoking. Approximately 19% of 30–34-y-old men and 8% of 30–34-y-old women had stenosis ≥40%, and stenosis was associated with high non-HDL-cholesterol concentrations and obesity. The effects became evident in the 15–19-y age group. These results show that the risk factors affect the microscopic qualities related to the progression and the gross extent of atherosclerosis in youth.

Regional variations in the progression of atherosclerosis

PDAY investigators extended the analyses of computerized images of the right coronary artery and aorta shown in Figures 6 and 7 to >2000 cases (89). The results confirmed quantitatively the statements in this article about the topographic localization of aortic and coronary artery fatty streaks and their relationship to raised lesions that develop in the same areas in subsequent years. Estimates of the risk factor effects are ≈25% stronger in the vulnerable arterial segments than are estimates for the entire arterial intimal surface. The results also showed that there are some variations between arterial segments in their susceptibility to different risk factors, eg, smoking selectively augments atherosclerosis in the dorsolateral region of the distal third of the abdominal aorta.

REFERENCES

1. Duff GL, McMillan GC. Pathology of atherosclerosis. Am J Med 1951;1:92–108.
2. McGill HC Jr, Geer JC, Strong JP. Natural history of human atherosclerotic lesions. In: Sandler M, Bourne GH, eds. Atherosclerosis and its origin. New York: Academic Press, 1963:39–65.
3. Tejada C, Strong JP, Montenegro MR, Restrepo C, Solberg LA. Distribution of coronary and aortic atherosclerosis by geographic location, race, and sex. Lab Invest 1968;18:509–26.
4. Strong JP, Solberg LA, Restrepo C. Atherosclerosis in persons with coronary heart disease. Lab Invest 1968;18:527–37.
5. Deupree RH, Fields, RI, McMahan CA, Strong JP. Atherosclerotic lesions and coronary heart disease. Key relationships in necropsied cases. Lab Invest 1973;28:252–62.
6. Newman WP, Strong JP, Johnson WD, Oalmann MC, Tracy RE, Rock WA. Community pathology of atherosclerosis and coronary heart disease in New Orleans. Lab Invest 1981;44:496–501.

7. Libby P. Molecular bases of the acute coronary syndromes. Circulation 1995;91:2844–50.
8. West of Scotland Coronary Prevention Group. West of Scotland Coronary Prevention Study: identification of high-risk groups and comparison with other cardiovascular intervention trials. Lancet 1996;348:1339–42.
9. Scandinavian Simvastatin Survival Study Group. Randomised trial of cholesterol lowering in 4444 patients with coronary heart disease: the Scandinavian Simvastatin Survival Study (4S). Lancet 1994;344:1383–9.
10. Holman RL, McGill HC Jr, Strong JP, Geer JC. The natural history of atherosclerosis. The early aortic lesions as seen in New Orleans in the middle of the 20th century. Am J Pathol 1958;2:209–35.
11. Zinserling WD. Untersuchungen über Atherosklerose. 1. Über die Aortaverfettung bei Kindern. (Investigations of atherosclerosis. 1. Aortic fatty streaks in children.) Virchows Arch Pathol Anat Physiol Klin Med 1925;255:677–705 (in German).
12. McGill HC Jr, Strong JP, Holman RL, Werthessen NT. Arterial lesions in the Kenya baboon. Circ Res 1960;8:670–9.
13. Middleton CC, Rosal J, Clarkson TB, Newman WP, McGill HC Jr. Arterial lesions in squirrel monkeys. Arch Pathol 1967;83:352–8.
14. Getty R. The gross and microscopic occurrence and distribution of spontaneous atherosclerosis in the arteries of swine. In: Roberts JC, Strause R, eds. Comparative atherosclerosis. New York: Harper and Row, 1965:11–20.
15. McGill HC Jr. Fatty streaks in the coronary arteries and aorta. Lab Invest 1968;18:560–4.
16. Stehbens WE. The epidemiological relationship of hypercholesterolemia, hypertension, diabetes mellitus and obesity to coronary heart disease and atherogenesis. J Clin Epidemiol 1990;43:733–41.
17. Olson RE. The dietary recommendations of the American Academy of Pediatrics. Am J Clin Nutr 1995;61:271–3.
18. Newman TB, Garber AM, Holtzman NA, Hulley SB. Problems with the report of the Expert Panel on Blood Cholesterol Levels in Children and Adolescents. Arch Pediatr Adolesc Med 1995;149:241–7.
19. Strong JP, McGill HC Jr. The natural history of coronary atherosclerosis. Am J Pathol 1962;40:37–49.
20. Montenegro MR, Eggen DA. Topography of atherosclerosis in the coronary arteries. Lab Invest 1968;18:586–93.
21. Robertson WB, Geer JC, Strong JP, McGill HC Jr. The fate of the fatty streak. Exp Mol Pathol 1963;2(suppl):28–39.
22. Geer JC, McGill HC Jr, Robertson WB, Strong JP. Histologic characteristics of coronary artery fatty streaks. Lab Invest 1968;18:105–10.
23. Hata Y, Hower J, Insull W. Cholesteryl ester-rich inclusions from human aortic fatty streak and fibrous plaque lesions in atherosclerosis. Am J Pathol 1974;75:423–56.
24. Katz SS, Shipley GG, Small DM. Physical chemistry of the lipids of human atherosclerotic lesions. Demonstration of a lesion intermediate between fatty streaks and advanced plaques. J Clin Invest 1976;58:200–11.
25. Bocan TMA, Guyton JR. Human aortic fibrolipid lesions. Am J Pathol 1985;120:192–206.
26. Bocan TMA, Schifani TA, Guyton JR. Ultrastructure of the human aortic fibrolipid lesion. Am J Pathol 1986;123:413–34.
27. Guyton JR, Klemp KF. Transitional features in human atherosclerosis. Intimal thickening, cholesterol clefts, and cell loss in human aortic fatty streaks. Am J Pathol 1993;143:1444–57.
28. Guyton JR, Klemp KF. Development of the atherosclerotic core region. Chemical and ultrastructural analysis of microdissected atherosclerotic lesions from human aorta. Arterioscler Thromb 1994;14:1305–14.
29. Stary HC. Evolution and progression of atherosclerotic lesions in coronary arteries of children and young adults. Arteriosclerosis 1989;9(suppl):19–32.
30. Enos WF, Holmes RH, Beyer J. Coronary disease among United States soldiers killed in action in Korea. JAMA 1953;152:1090–3.
31. Henriksen T, Mahoney EM, Steinberg D. Enhanced macrophage degradation of low density lipoprotein previously incubated with cultured endothelial cells: recognition by receptors for acetylated low density lipoproteins. Proc Natl Acad Sci U S A 1981;78:6499–503.
32. Steinberg D, Lewis A. Conner Memorial Lecture: oxidative modification of LDL and atherogenesis. Circulation 1997;95:1062–71.
33. Ottnad E, Parthasarathy S, Sambrano GR, et al. A macrophage receptor for oxidized low density lipoprotein distinct from the receptor for acetyl low density lipoprotein: partial purification and role in recognition of oxidatively damaged cells. Proc Natl Acad Sci U S A 1995;92:1391–5.
34. Ramprasad MP, Fischer W, Witztum JL, Sambrano GR, Quehenberger O, Steinberg D. The 94- to 97-kDa mouse macrophage membrane protein that recognizes oxidized low density lipoprotein and phosphatidylserine-rich liposomes is identical to macrosialin, the mouse homologue of human CD68. Proc Natl Acad Sci U S A 1995;92:9580–4.
35. Lougheed M, Lum CM, Ling W, Suzuki H, Kodama T, Steinbrecher U. High affinity saturable uptake of oxidized low density lipoprotein by macrophages from mice lacking the scavenger receptor class A type I/II. J Biol Chem 1997;272:12938–44.
36. Pearson AM. Scavenger receptors in innate immunity. Curr Opin Immunol 1996;8:20–8.
37. Sambrano GR, Steinberg D. Recognition of oxidatively damaged and apoptotic cells by an oxidized low density lipoprotein receptor on mouse peritoneal macrophages: role of membrane phosphatidylserine. Proc Natl Acad Sci U S A 1995;92:1396–400.
38. Savill J. Recognition and phagocytosis of cells undergoing apoptosis. Br Med Bull 1997;53:491–8.
39. Sakai M, Miyazaki A, Hakamata H, et al. The scavenger receptor serves as a route for internalization of lysophosphatidylcholine in oxidized low density lipoprotein-induced macrophage proliferation. J Biol Chem 1996;271:27346–52.
40. Terpstra V, Bird DA, Steinberg D. Evidence that the lipid moiety of oxidized low density lipoprotein plays a role in its interaction with macrophage receptors. Proc Natl Acad Sci U S A 1998;95:1806–11.
41. Giry C, Giroux LM, Roy M, Davignon J, Minnich A. Characterization of inherited scavenger receptor overexpression and abnormal macrophage phenotype in a normolipidemic subject with planar xanthomas. J Lipid Res 1996;37:1422–35.
42. Gelissen IC, Brown AJ, Mander EL, Kritharides L, Dean RT, Jessup W. Sterol efflux is impaired from macrophage foam cells selectively enriched with 7-ketocholesterol. J Biol Chem 1996;271:17852–60.
43. Wang N, Tabas I, Winchester R, Ravalli S, Rabbani LE, Tall A. Interleukin 8 is induced by cholesterol loading of macrophages and expressed by macrophage foam cells in human atheroma. J Biol Chem 1996;271:8837–42.
44. Vijayagopal P, Glancy DL. Macrophages stimulate cholesteryl ester accumulation in cocultured smooth muscle cells incubated with lipoprotein-proteoglycan complex. Arterioscler Thromb Vasc Biol 1996;16:1112–21.
45. Landé KE, Sperry WM. Human atherosclerosis in relation to the cholesterol content of the blood serum. Arch Pathol 1936;22:301–12.
46. Patterson JC, Cornish BR, Armstrong EC. The serum lipids in human atherosclerosis. An interim report. Circulation 1956;13:224–34.
47. Patterson JC, Dyer L, Armstrong EC. Serum cholesterol levels in human atherosclerosis. Can Med Assoc J 1960;82:6–11.
48. Mathur KS, Patney NL, Kumar V, Sharma RD. Serum cholesterol and atherosclerosis in man. Circulation 1961;23:847–52.
49. Spain DM, Bradess VA, Greenblatt IJ. Postmortem studies on coronary atherosclerosis, serum beta lipoproteins and somatotypes. Am J Med Sci 1955;228:294–301.
50. Schwartz CJ, Stenhouse NS, Taylor AE, White TA. Coronary disease severity at necropsy. Br Heart J 1965;27:731–9.
51. Strong JP, Richards ML. Cigarette smoking and atherosclerosis in autopsied men. Atherosclerosis 1976;23:451–76.

52. Rhoads GG, Blackwelder WC, Stemmermann GN, Hayashi T, Kagan A. Coronary risk factors and autopsy findings in Japanese-American men. Lab Invest 1978;38:304–11.

53. Holme I, Enger SC, Helgeland A, et al. Risk factors and raised atherosclerotic lesions in coronary and cerebral arteries. Statistical analysis from the Oslo Study. Arteriosclerosis 1981;1:250–6.

54. Sorlie PD, Garcia-Palmieri MR, Castillo-Staab MI, Costas R Jr, Oalmann MC, Havlik R. The relation of antemortem factors to atherosclerosis at autopsy. The Puerto Rico Heart Health Program. Am J Pathol 1981;103:345–52.

55. Solberg LA, Strong JP. Risk factors and atherosclerotic lesions: a review of autopsy studies. Arteriosclerosis 1983;3:187–98.

56. Okumiya N, Tanaka K, Ueda K, Omae T. Coronary atherosclerosis and antecedent risk factors: pathologic and epidemiologic study in Hisayama, Japan. Am J Cardiol 1985;56:62–6.

57. Holme I, Solberg LA, Weissfeld L, et al. Coronary risk factors and their pathway of action through coronary raised lesions, coronary stenoses and coronary death. Multivariate statistical analysis of an autopsy series: the Oslo Study. Am J Cardiol 1985;55:40–7.

58. Solberg LA, Strong JP, Holme I, et al. Stenoses in the coronary arteries: relation to atherosclerotic lesions, coronary heart disease, and risk factors. The Oslo Study. Lab Invest 1985;53:648–55.

59. Reed DM, MacLean CJ, Hayashi T. Predictors of atherosclerosis in the Honolulu heart program. Biologic, dietary, and lifestyle characteristics. Am J Epidemiol 1987;126:214–25.

60. Reed DM, Strong JP, Resch J, Hayashi T. Serum lipids and lipoproteins as predictors of atherosclerosis: an autopsy study. Arteriosclerosis 1989;9:560–4.

61. Oalmann MC, Malcom GT, Toca VT, Guzm MA, Strong JP. Community pathology of atherosclerosis and coronary heart disease: post mortem serum cholesterol and extent of coronary atherosclerosis. Am J Epidemiol 1981;113:396–403.

62. Strong JP, Oalmann MC, Newman WP III, et al. Coronary heart disease in young black and white males in New Orleans: Community Pathology Study. Am Heart J 1984;108:747–59.

63. Lauer RM, Connor WE, Leaverton PE, Reiter MA, Clarke WR. Coronary heart disease risk factors in school children: the Muscatine Study. J Pediatr 1975;86:697–706.

64. Berenson GS, McMahan CA, Voors AW, et al, eds. Cardiovascular risk factors in children: the early natural history of atherosclerosis and essential hypertension. New York: Oxford University Press, 1980.

65. Sprecher DL, Schaefer EJ, Kent KM, et al. Cardiovascular features of homozygous familial hypercholesterolemia: analysis of 16 patients. Am J Cardiol 1984;54:20–30.

66. Berenson GS, Wattigney WA, Tracy RE, et al. Atherosclerosis of the aorta and coronary arteries and cardiovascular risk factors in persons aged 6 to 30 years and studied at necropsy (The Bogalusa Heart Study). Am J Cardiol 1992;70:851–8.

67. Wissler RW. USA multicenter study of the pathobiology of atherosclerosis in youth. Ann N Y Acad Sci 1991;623:26–39.

68. Cornhill JF, Barrett WA, Herderick EE, Mahley RW, Fry DL. Topographic study of sudanophilic lesions in cholesterol-fed minipigs by image analysis. Arteriosclerosis 1985;5:415–26.

69. Cornhill JF, Herderick EE, Stary HC. Topography of human aortic sudanophilic lesions. Monogr Atheroscler 1990;15:13–9.

70. Pathobiological Determinants of Atherosclerosis in Youth (PDAY) Research Group. Relationship of atherosclerosis in young men to serum lipoprotein cholesterol concentrations and smoking: a preliminary report from the Pathobiological Determinants of Atherosclerosis in Youth (PDAY) Research Group. JAMA 1990;264:3018–24.

71. Pathobiological Determinants of Atherosclerosis in Youth (PDAY) Research Group. Natural history of aortic and coronary atherosclerotic lesions in youth. Findings from the PDAY Study. Arterioscler Thromb 1993;13:1291–8.

72. McGill HC Jr, McMahan CA, Malcom GT, Oalmann MC, Strong JP, Pathobiological Determinants of Atherosclerosis in Youth (PDAY) Research Group. Relation of glycohemoglobin and adiposity to atherosclerosis in youth. Arterioscler Thromb Vasc Biol 1995;15:431–40.

73. McGill HC Jr, Strong JP, Tracy RE, McMahan CA, Oalmann MC, Pathobiological Determinants of Atherosclerosis in Youth (PDAY) Research Group. Relation of a postmortem renal index of hypertension to atherosclerosis in youth. Arterioscler Thromb Vasc Biol 1995; 15:2222–8.

74. McGill HC Jr, McMahan CA, Malcom GT, Oalmann MC, Strong JP, PDAY Research Group. Effects of serum lipoproteins and smoking on atherosclerosis in young men and women. Arterioscler Thromb Vasc Biol 1997;17:95–106.

75. McGill HC Jr, McMahan CA, Tracy RE, et al. Relation of a postmortem renal index of hypertension to atherosclerosis and coronary artery size in young men and women. Arterioscler Thromb Vasc Biol 1998;18:1108–18.

76. Hixson JE, Pathobiological Determinants of Atherosclerosis in Youth (PDAY) Research Group. Apolipoprotein E polymorphisms affect atherosclerosis in young males. Arterioscler Thromb 1991;11: 1237–244.

77. Hixson JE, McMahan A, McGill HC Jr, Strong JP, Pathobiological Determinants of Atherosclerosis in Youth (PDAY) Research Group. Apo B insertion/deletion polymorphisms are associated with atherosclerosis in young black but not young white males. Arterioscler Thromb 1992;12:1023–9.

78. Kuczmarski RJ, Flegal KM, Campbell SM, Johnson CL. Increasing prevalence of overweight among US adults. The National Health and Nutrition Examination Surveys, 1960–1991. JAMA 1994;272: 205–11.

79. Botti TP, Amin H, Hiltscher L, Wissler RW, PDAY Research Group. A comparison of the quantitation of macrophage foam cell populations and the extent of apolipoprotein E deposition in developing atherosclerotic lesions in young people: high and low serum thiocyanate groups as an indication of smoking. Atherosclerosis 1996;124:191–202.

80. Graham A, Hassall DG, Rafique S, Own JS. Evidence for a paraoxonase-independent inhibition of low-density lipoprotein oxidation by high-density lipoprotein. Atherosclerosis 1997;135:193–204.

81. Marangon K, Herbeth B, Lecomte E, et al. Diet, antioxidant status, and smoking habits in French men. Am J Clin Nutr 1998;67:231–9.

82. Shwaery GT, Vita JA, Keaney JF Jr. Antioxidant protection of LDL by physiological concentrations of 17β-estradiol. Circulation 1997;95:1378–85.

83. Koh KK, Bui MN, Mincemoyer R, Cannon RO III. Effects of hormone therapy on inflammatory cell adhesion molecules in postmenopausal healthy women. Am J Cardiol 1997;80:1505–7.

84. Horiuchi S, Higashi T, Ikeda K, et al. Advanced glycation end products and their recognition by macrophage and macrophage-derived cells. Diabetes 1996;45(suppl):S73–6.

85. Wissler RW, Hiltscher L, Oinuma T, for the PDAY Research Group. The lesions of atherosclerosis in the young. From fatty streaks to intermediate lesions. In: Fuster V, Ross R, Topol EJ, eds. Atherosclerosis and coronary artery disease. Vol 1. Philadelphia: Lippincott-Raven Publishers, 1996:475–89.

86. McGill H Jr, McMahan C, Zieske A, et al. Associations of coronary heart disease risk factors with the intermediate lesion of atherosclerosis in youth. Arterioscler Thromb Vasc Biol 2000;20: 1998–2004.

87. Stary HC. The histological classification of atherosclerotic lesions in human coronary arteries. In: Fuster V, Ross RR, Topol EJ, eds. Atherosclerosis and coronary artery disease. Philadelphia: Lippincott-Raven Publishers, 1996:463–74.

88. McGill HC Jr, McMahan CA, Zieske AW, et al. Association of coronary heart disease risk factors with microscopic qualities of coronary atherosclerosis in youth. Circulation 2000;102: 374–9.

89. McGill HC Jr, McMahan CA, Herderick EE, et al. Effects of coronary heart disease risk factors on atherosclerosis of selected regions of the aorta and right coronary artery. Arterioscler Thromb Vasc Biol 2000;20:836–45.

THERAPEUTIC ANTAGONISTS AND CONFORMATIONAL REGULATION OF INTEGRIN FUNCTION

Motomu Shimaoka and Timothy A. Springer

Integrins are a structurally elaborate family of adhesion molecules that transmit signals bi-directionally across the plasma membrane by undergoing large-scale structural rearrangements. By regulating cell–cell and cell–matrix contacts, integrins participate in a wide range of biological processes, including development, tissue repair, angiogenesis, inflammation and haemostasis. From a therapeutic standpoint, integrins are probably the most important class of cell-adhesion receptors. Recent progress in the development of integrin antagonists has resulted in their clinical application and has shed new light on integrin biology. On the basis of their mechanism of action, small-molecule integrin antagonists fall into three different classes. Each of these classes affect the equilibria that relate integrin conformational states, but in different ways.

Members of the integrin family of adhesion molecules are non-covalently-associated α/β heterodimers that mediate cell–cell, cell–extracellular matrix and cell–pathogen interactions by binding to distinct, but often overlapping, combinations of ligands (BOX 1). Eighteen different integrin α-subunits and eight different β-subunits are present in vertebrates, which form at least twenty-four α/β heterodimers, perhaps making integrins the most structurally and functionally diverse family of cell-adhesion molecules[1,2] (FIG. 1). Half of integrin α-subunits contain inserted (I) domains, which are the principal ligand-binding domains when present[3,4]. The complexity, and structural and functional diversity of integrins allows this family of adhesion molecules to play a pivotal role in broad contexts of biology, including inflammation, innate and antigen-specific immunity, haemostasis, wound healing, tissue morphogenesis, and regulation of cell growth and differentiation[1,2]. Conversely, dysregulation of integrins is involved in the pathogenesis of many disease states, from autoimmunity to thrombotic vascular diseases to cancer metastasis[5]. Therefore, extensive efforts have been directed towards the discovery and development of integrin antagonists for clinical applications. Significant advances have been made in targeting

αIIbβ3 on platelets for inhibiting thrombosis[6], αvβ3 and αvβ5 for blocking tumour metastasis, angiogenesis and bone resorption[7], and β2 integrins and α4 integrins on leukocytes for treating autoimmune diseases and other inflammatory disorders[8,9].

Small-molecule integrin inhibitors not only interfere with ligand binding, but also stabilize particular integrin conformations, which has provided insights into integrin structural rearrangements. In this review, we focus not only on antagonists of integrins as promising therapeutics, but also on what the drug discovery literature can teach us about the conformational regulation of integrin structure and function, and what structural and mutational studies on integrins teach us about the mechanism of action of antagonists. The reader is referred elsewhere for reviews of the extremely large variety of small molecules and antibodies that have been developed as integrin antagonists, and results in animal model studies and human clinical trials[5–17].

Overview of integrin structure

Integrin heterodimers and integrin domains. Integrins are large glycoproteins with multiple domains. Integrin ligand-binding function is tightly linked to molecular conformation. On activation, dramatic

The Center for Blood Research, Department of Anesthesia and Pathology, Harvard Medical School, 200 Longwood, Boston, Massachussets 02115, USA. Correspondence to T. A. S. e-mail: springeroffice@ cbr.med.harvard.edu doi:10.1038/nrd1174

Box 1 | **Integrin ligands**

Integrins bind extracellular matrix ligands as well as cell-surface receptors. Fibrinogen — a dimeric soluble plasma protein that plays important roles in blood clotting, wound healing and inflammation[106,107] — is also one of the most important extracellular matrix ligands for integrins including αIIbβ3, αvβ3, αMβ2 and αXβ2. Fibrinogen is proteolytically converted by thrombin to fibrin that self-assembles into an insoluble clot with a network-like structure. Binding to and crosslinking of αIIbβ3 on platelets by fibrinogen is required for platelet aggregation, which is crucial in thrombus formation. Fibrinogen also binds to αMβ2 and αXβ2, and is involved in inflammation by facilitating leukocyte adhesion to fibrinogen-deposited tissue and implants.

On the other hand, intercellular adhesion molecules (ICAMs) are immunoglobulin superfamily members that are among the most important cell-surface ligands for integrins including αLβ2, αMβ2, αXβ2 and αDβ2 (REF. 92). ICAM-1 is expressed on endothelial cells as well as on leukocytes. ICAM-1 is upregulated on endothelial cells by inflammatory stimuli such as tumour-necrosis factor-α. By interacting with β2 integrins, ICAM-1 plays a pivotal role in leukocyte migration into the tissue from the blood stream. ICAM-1 on antigen-presenting cells functions as a co-stimulatory molecule to T-cell receptors by signalling through leukocyte function-associated antigen-1 on T cells and taking part in immunological synapse formation[90].

rearrangements occur in the overall spatial relationships of integrin domains[4]. Understanding the structural basis of integrin activation in detail is essential for understanding the mechanism of antagonism by therapeutics, as well as for the design of second-generation antagonists with novel mechanisms of action.

Integrins comprise two non-covalently-associated type I transmembrane glycoprotein α- and β-subunits.

Each subunit contains a large extracellular domain, a single transmembrane domain and, except for integrin β4, a short cytoplasmic tail (FIG. 2). The integrin α-subunit ectodomain of >940 residues contains four domains (five in I-domain-containing integrins) and the β-subunit of ~640 residues contains eight domains (FIG. 2). The crystal structure of extracellular parts of αvβ3 integrin that lacks an I domain revealed the structure in a bent conformation of eight domains, and a portion of the ninth, out of the twelve domains predicted to be present (FIG. 2b)[18]. The structures of INTEGRIN-EGF DOMAINS 2 and 3 of the β2 subunit were determined by nuclear magnetic resonance, and these complemented a part of the missing portions of the αvβ3 structure[19]. The N-terminal portions of the α- and β-subunits fold into the globular headpiece, which is connected through α- and β-tailpiece domains to the membrane[18,20–22]. Dramatic rearrangements occur in the orientation of these domains during integrin activation (FIG. 3a–c)[23]. In this review, we focus on the β-propeller, I-like and I domains, because these are the ligand-binding domains and the domains to which known antagonists bind (FIGS 3c and 4). However, it should be emphasized that in the bent conformation, extensive interfaces — totalling >4,000 Å^2 of solvent-accessible surface — are buried between the headpiece and tailpiece, and between the α-tailpiece and β-tailpiece. These interfaces stabilize the bent conformation, and are important in regulating the equilibrium between the bent and extended integrin conformations (FIG. 3a–c)[23,24].

INTEGRIN-EGF DOMAIN
A module in cysteine-rich repeats in the integrin β-subunit stalk region adopts a nosecone-shaped variant of the epidermal growth factor (EGF) fold, termed an integrin-EGF (I-EGF) domain.
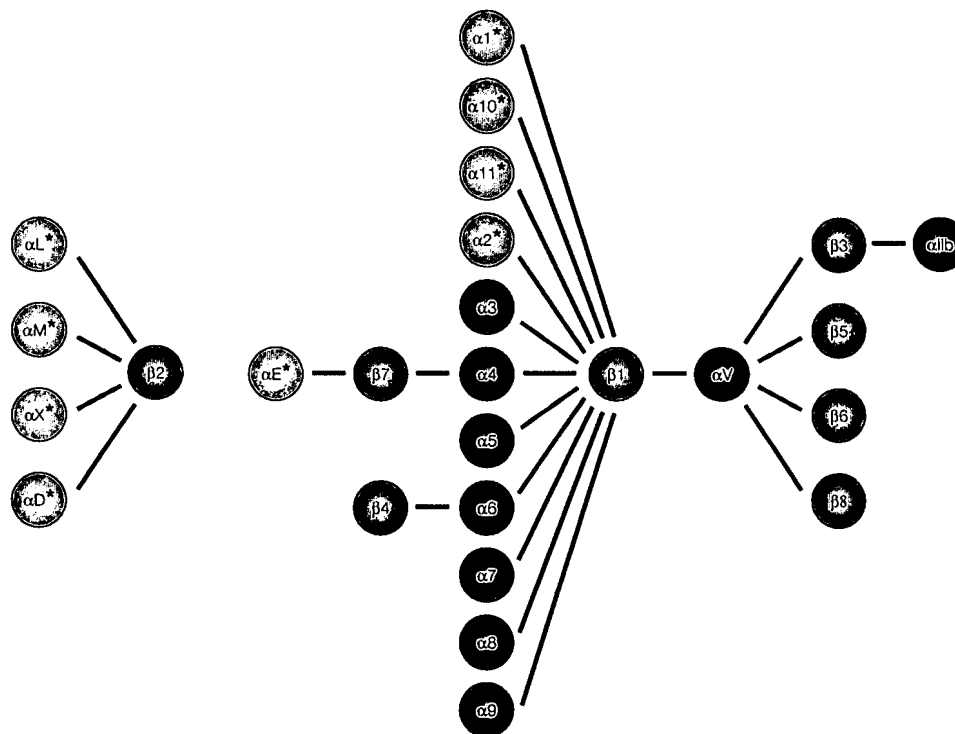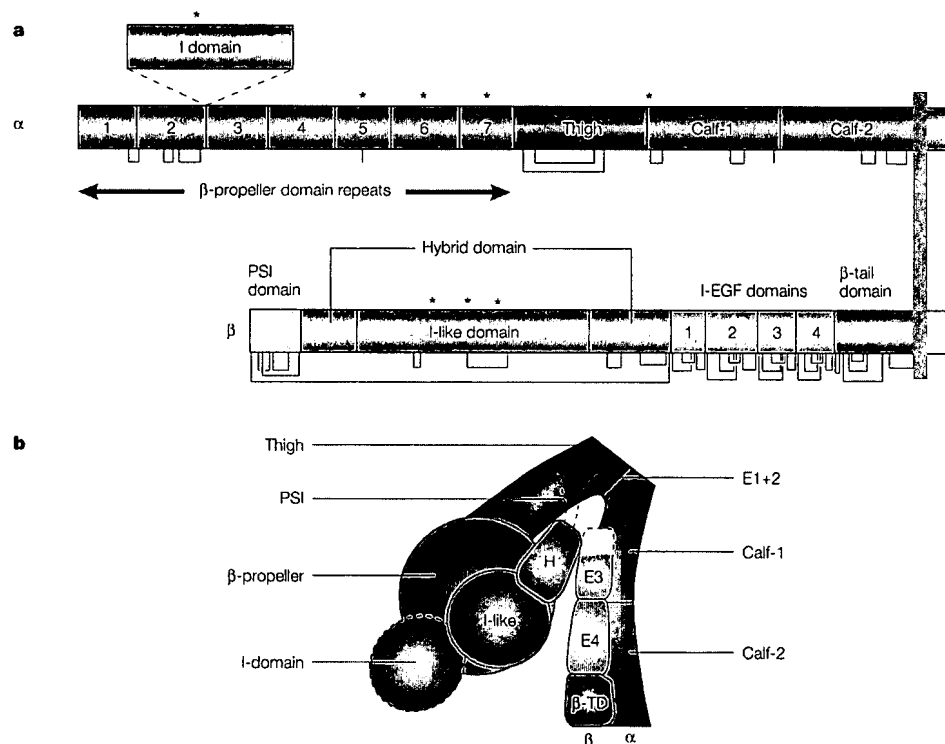
Figure 1 | **Integrin heterodimer composition.** Integrin α- and β-subunits form 24 heterodimers that recognize distinct but overlapping ligands. Half of the α-subunits contain I domains (asterisked).

Figure 2 | **Integrin architecture. a** | Organization of domains within the primary structure. Some α-subunits contain an I domain inserted in the position denoted by the broken lines. Cysteines and disulphide bonds are shown as lines below the stick figures. Red and blue asterisks denote Ca^{2+}- and Mg^{2+}-binding sites, respectively. **b** | Arrangement of domains within the three-dimensional crystal structure of αvβ3 (REF. 18), with an I domain added. Each domain is colour-coded as in **a**. β-TD, β-tail domain; I-EGF, integrin-epidermal growth factor domain; PSI, plexin/semaphorin/integrin.

vWF-type A domains: I domain and I-like domain. All integrin β-subunits and half of integrin α-subunits contain von Willebrand factor (vWF)-type A domains of ~200 amino acids in length, also referred to as the I domain in the α-subunit and the I-like domain in the β-subunit, respectively (FIGS 1 and 2)[3,4]. Each domain adopts an α/β Rossmann fold with a metal-ion-dependent adhesion site (MIDAS) on the 'top' of the domain, whereas its C- and N-terminal connections are on the distal 'bottom' face[4,18,25,26] (FIGS 5 and 6). Divalent cations are universally required for integrins to bind ligands and the metal at the MIDAS directly coordinates to a glutamic acid (Glu) or aspartic acid (Asp) residue in the ligand. This metal-dependent interaction through the MIDAS has a central role in ligand recognition by the I and I-like domains.

I domain. The I domain, which is inserted between blades 2 and 3 of the β-propeller domain of the α-subunit (FIG. 2a)[27], is a major ligand-binding domain and recognizes ligand directly when it is present[28,29]. The ability of the I domain to bind ligand is controlled by conformational changes; the affinity of the I domain for its ligand is enhanced by downward axial displacement of its C-terminal helix, which is conformationally linked

to alterations of the MIDAS loops and Mg^{2+} coordination[30–32] (FIG. 5). In the case of αLβ2, compared with the default, low-affinity conformation, downward displacements by one and two turns of the helix lead to intermediate- and high-affinity conformations with ~500- and 10,000-fold increased affinity, respectively[32].

Conversely, binding of ligand to the MIDAS of the I domain induces conformational change by stabilizing the high-affinity conformation. These changes include rearrangements in metal coordination in the MIDAS and backbone movements in the loops surrounding the MIDAS, which are linked to a downward axial displacement of the C-terminal helix (FIG. 4)[25,32,33].

I-like domain. The β-subunit I-like domain, which is inserted in the hybrid domain of the β-subunit (FIGS 2a, 3b and 3c), directly binds ligand in integrins that lack I domains in the α-subunit (FIGS 3c and 7). By contrast, when the I domain is present, the I-like domain functions indirectly by regulating the I domain (FIG. 4). Compared to the I domain, the I-like domain contains two long loops, including one which is important for determining ligand specificity, and is referred to as the specificity-determining loop (SDL)[34]. On either side of the MIDAS, the I-like domain contains

a Bent form with closed headpiece   **b** Extended form with closed headpiece   **c** Extended form with open headpiece bound by cRGD
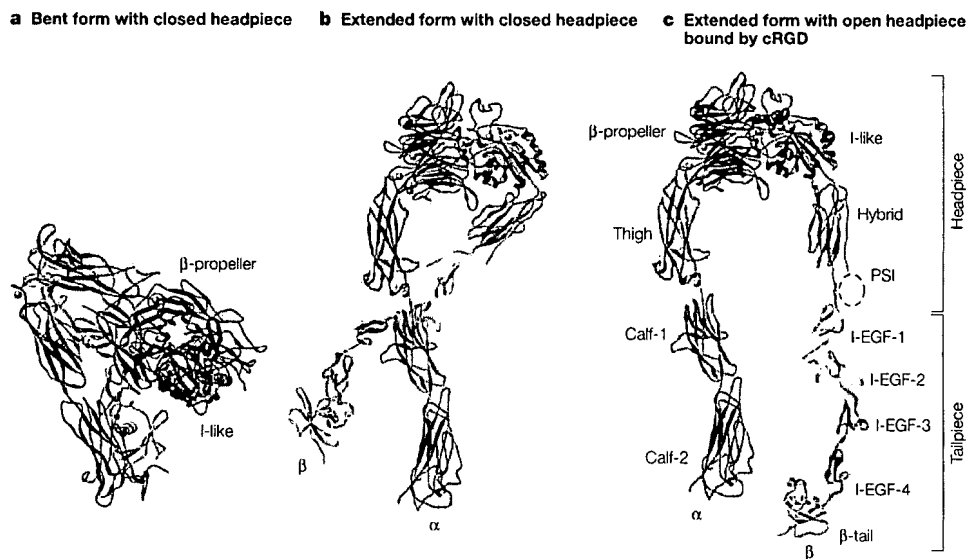
Figure 3 | **Domain organization and global conformational changes of the extracellular portion of integrins.** Three distinctive conformations are illustrated for integrin αvβ3, which lacks an I domain. The conformations are based on crystal[18,35], nuclear magnetic resonance[19] and electron microscopy[23] structures. Ribbon representations were prepared as described[108]. **a** | Bent conformation (low affinity). **b** | Extended conformation with closed headpiece (intermediate affinity). **c** | Extended conformation with open headpiece (high affinity) bound by cyclic Arg-Gly-Asp (cRGD) peptide (shown as a space-filling representation with black balls). Ca^{2+} and Mg^{2+} ions are gold and silver spheres, respectively. I-EGF, integrin-epidermal growth factor domain; PSI, plexin/semaphorin/integrin.

two adjacent metal coordination sites, the adjacent to MIDAS (ADMIDAS) site and the ligand-associated metal binding site (LIMBS) (FIG. 7)[18,35].

The function of the I-like domain seems to be regulated by conformational changes similar to those observed in the I domain, in which a downward movement of the C-terminal α-helix allosterically alters the geometry of the MIDAS and increases the affinity for ligand[4,36]. Outward swing of the hybrid domain relative to the I-like domain (FIGS 3b and c) is thought to be coupled to the downward shift of the C-terminal α-helix of the I-like domain[23,24].

β-propeller domain. The N-terminal region of the integrin α-subunit contains seven repeats of ~60 amino acids, which fold into a seven-bladed β-propeller domain[18,27] (FIG. 2). A β-propeller domain with the same topology is found in the trimeric G-protein β-subunit. The β-propeller domain directly participates in ligand recognition in those integrins that lack α I domains[3].

Structure of the headpiece in integrins that lack I domains. The structure of αvβ3 reveals that the I-like domain makes extensive contact with the β-propeller domain, with the 'top' ligand-binding faces of each domain oriented at ~90° to one another (FIG. 3c)[18]. Loops in blades 2, 3 and 4 of the β-propeller domain are prominent in the ligand-binding site. The structure of αvβ3 in complex with a cyclic peptide containing an Arg-Gly-Asp (RGD) sequence demonstrated binding to both the α- and β-subunits at the β-propeller/I-like

domain interface (FIG. 3c). The Asp carboxylic acid side chain coordinates directly to the metal of the β-subunit I-like domain MIDAS, whereas the Arg side chain binds to the α-subunit β-propeller domain[35]. Mapping by mutagenesis of residues important in binding to fibrinogen, the biological ligand of αIIbβ3, demonstrated a much larger interaction surface, centered on blades 2 to 4 of the α-subunit β-propeller domain and the SDL loop of the β-subunit I-like domain (FIG. 7)[37,38].

Intriguing structural homology exists between the integrin β-propeller domain and the trimeric G-protein β-subunit, and between integrin I and I-like domains and G-protein α-subunits[18,27]. Dissociation of these domains on activation occurs in G-proteins; however, in integrin activation there is little rigid body movement of the β-propeller domain relative to the I-like domain[39]. Instead, ligand-binding affinity seems to be regulated primarily by conformational changes in loops of the I-like domain and β-propeller domain.

Structure of the headpiece in integrins that contain I domains. In integrins that contain I domains, the I domain binds ligand, whereas the β-propeller and I-like domains have a regulatory role (FIG. 4)[40,41]. The bottom of the I domain is connected at its N and C termini to blades 2 and 3 of the β-propeller, respectively. A linker of ~15 residues C-terminal to the I domain is located near the β-propeller/I-like domain interface, which corresponds to the ligand-binding face in integrins that lack I domains. It has been proposed that the I-like domain, when activated, interacts with a portion of this linker,

and thereby relays activation to the I domain[4,36,42]. The polypeptide linker between the C terminus of the I domain and β-sheet 3 of the β-propeller domain, including αL residue Glu-310, is important in I domain activation[31]. I domain activation is induced by a downward pull on the C-terminal α-helix or linker[4,43]. It is proposed that the universally conserved residue Glu-310 in the I domain linker is an 'intrinsic ligand,' and that binding of the activated β2 I-like domain to this intrinsic ligand pulls the C-terminal α-helix of the I domain downward, and activates high affinity for ligand (FIG. 4)[4,36,42].

Structural basis of signal transmission. Intracellular signalling pathways that are activated by other receptors (for example, receptors coupled to G-proteins or tyrosine kinases) impinge on integrin cytoplasmic domains and enhance the activity of the extracellular headpiece for ligand binding[44-46]. Recently, the basis for bi-directional signal transmission across the membrane by integrins has been explained. The integrin α- and β-cytoplasmic tails associate with each other and constrain the integrin in its inactive form. Dissociation of the α/β cytoplasmic tails by signals within the cell leads to the activation of the extracellular parts of the integrin[21,23,47-49]. In the latent, low-affinity state, the integrin assumes a bent conformation (FIG. 3a)[19,23]. Separation of the α- and β-subunit cytoplasmic domains is linked to separation of the transmembrane domains and the membrane-proximal segments of the α- and β-extracellular domains, which destabilizes the interface between the headpiece and tailpiece, and induces a switchblade-like opening to an extended conformation (FIG. 3b). This re-orientates the ligand-binding face and exposes activation epitopes in the tailpiece. In the extended conformation, two different conformations of the headpiece, termed closed (FIG. 3b) and open (FIG. 3c), are seen[23]. In the bent conformation, only the closed conformation of the headpiece is present[18]. Therefore, extension facilitates adoption of the open conformation of the headpiece, which corresponds to the ligand-bound and high-affinity conformation[23]. In the open headpiece conformation, there is a marked change in orientation between the I-like domain and hybrid domain (FIG. 3b and 3c), and this is postulated to be linked through movement of the C-terminal I-like domain α7 helix to conformational changes at the I-like domain MIDAS, similar to the conformational changes seen in I domains[23]. Linked changes in β-propeller loops may also occur. Notably, many antibody epitopes that are buried in the bent conformation become exposed in the extended conformation. As described below, ligand-mimetic integrin antagonists also induce the high-affinity, extended conformation. This has important clinical implications, especially for αIIbβ3 antagonists.

In solution, and apparently on the cell surface as well, integrins are not fixed in a particular conformation, but equilibrate between them[23] (FIG. 3a-c). Whether or not the equilibrium favours the bent, low-affinity conformation or the extended, high-affinity conformation is affected by the presence of activating
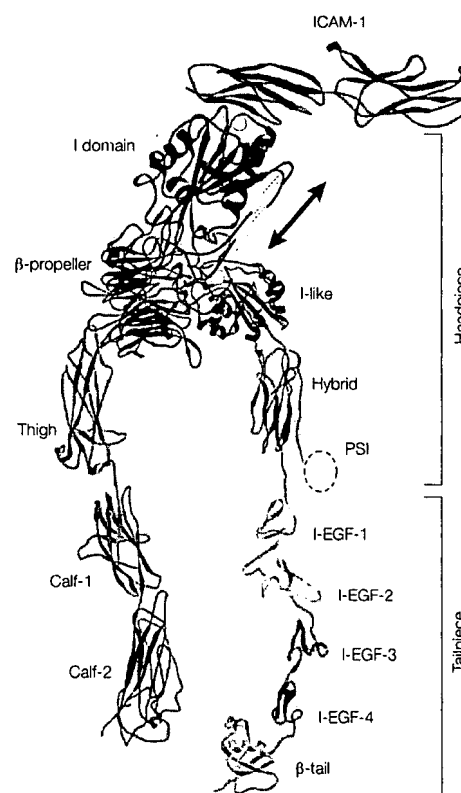

Figure 4 | **Model of integrin αLβ2, which contains an I domain, bound to ICAM-1.** Domains, except for the I domain and intercellular adhesion molecule-1 (ICAM-1), are the same as those of αvβ3 in FIG. 3c. The αL I domain and its complex with the N-terminal 2 domains of ICAM-1 are cartoons based on crystal structures[32]; the C-terminal I domain α-helix is represented by a cylinder in its low-affinity (blue) and high-affinity (orange) conformation. The I domain is joined at the point of its insertion in the β-propeller domain but its orientation is arbitrary; the I domain and ICAM-1 are shown at slightly larger scale for emphasis. Mg²⁺ ions at the metal-ion-dependent adhesion site of the I and the I-like domains are gold spheres. Ca²⁺ ions and a metal at the β2 ligand-associated metal binding site are not shown. I-EGF, integrin-epidermal growth factor domain; PSI, plexin/semaphorin/integrin.

intracellular factors and the concentration of extracellular ligands. Activation by signals within the cell (inside–out signalling) induces straightening and stabilizes the extended form. Binding of extracellular ligands also stabilizes the extended conformation and therefore enhances the separation of integrin tails, which transmits signals to the cytoplasm (outside–in signalling). Therefore, transition from the bent to the extended conformation is a bi-directional, allosteric mechanism for relaying conformational signals between the integrin headpiece and the cytoplasmic domains. All biological integrin ligands are multivalent, and can therefore also induce integrin clustering, which seems to be required, in addition to conformational change, for outside–in signalling.
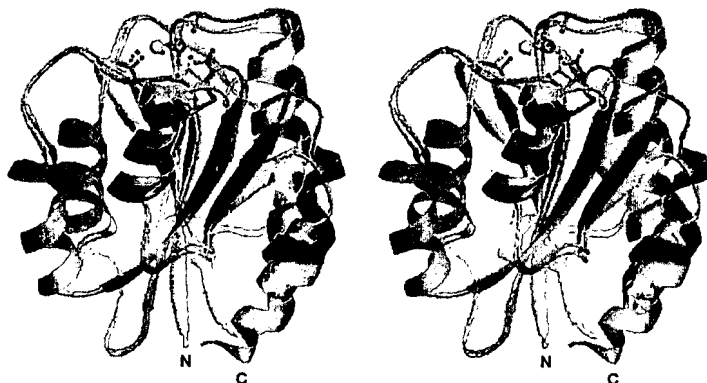
Figure 5 | **Stereo view of alternative conformations of the αM I domain.** The regions with significant conformational changes are shown in blue (closed, low affinity) and yellow (open, high affinity). Regions with similar backbones are in gray. Mg^{2+} ions and side chains of metal-coordinating residues at the metal-ion-dependent adhesion site are in blue (closed, low affinity) and yellow (open, high affinity) with red oxygen atoms. Ribbon diagrams are prepared as described[4].

Integrins lacking I domains: αIIbβ3

αIIbβ3 biology. αIIbβ3, which is the receptor for fibrinogen/fibrin, is expressed exclusively on platelets and their precursors, and mediates platelet aggregation and thrombus formation. On resting platelets, αIIbβ3 is inactive, but when platelets are exposed to agonists such as thrombin, ADP and platelet-activating factor, αIIbβ3 undergoes changes to the extended, active conformation that binds fibrinogen, and additional αIIbβ3 receptors are mobilized to the cell surface from an α-granule storage pool[10]. Platelet aggregation is a prerequisite for thrombus formation, which first diminishes and then stops blood supply to organs, and subsequently results in tissue ischaemia. Integrin αIIbβ3 has a key role in the pathogenesis of thrombotic cardiovascular diseases, such as ischaemic heart disease and stroke. The development of integrin antagonists was pioneered with αIIbβ3, for which there are three distinct clinically approved therapeutics and an extremely large medicinal chemistry literature[5,6,10].

Structural features of biological ligands. In addition to fibrinogen, αIIbβ3 binds to plasma and matrix proteins, such as vWF, fibronectin, thrombospondin and vitronectin. These ligands all share an RGD or RGD-like motif that is central in their receptor binding site. A subset of integrins that lack I domains, including αIIbβ3, αvβ3, and α5β1, recognize the RGD motif. Plasma fibrinogen is a disulphide-linked dimer, with each monomer containing disulphide-linked α-, β-, and γ-subunits. The monomers dimerize at their N-terminal ends. The crucial recognition motif for αIIbβ3 is an RGD-like Lys-Gln-Ala-Gly-Asp-Val (KQAGDV) motif near the C-terminal end of the γ-subunit, although two RGD sites in the α-subunit may also be recognized[3].

A family of integrin ligands containing RGD or KGD motifs found in snake venom are named disintegrins for their ability to inhibit platelet aggregation by interacting with αIIbβ3. In contrast to fibrinogen,

which binds only active αIIbβ3, the disintegrin echistatin can bind potently to both active and inactive forms of the integrin[50].

Antagonist action and effects on conformation. Using the RGD motif and disintegrins as leads, αIIbβ3 antagonists have been developed that are cyclic peptides containing the RGD or KGD sequence, peptidomimetics, or small molecules that imitate the integrin-binding properties of the RGD peptide in terms of overall geometry and the presence of a basic moiety and free carboxyl group[6] (FIG. 8a). The antagonists function as ligand-mimetic competitive inhibitors. A crystal structure of a cyclic RGD peptide bound to the closely related αvβ3 integrin demonstrates that the Arg guanidinium moiety forms salt bridges to Asp residues in β-propeller loops, and the Asp carboxyl group ligates the metal ion in the I-like domain MIDAS, whereas the Gly makes few interactions and essentially serves as a spacer[35]. These observations are in excellent agreement with structure–activity relationships observed for small-molecule antagonists[6,51]. Furthermore, the contacts of the cyclic RGD peptide with αvβ3 (FIG. 3c) correspond to the centre of the binding site for fibrinogen in αIIbβ3 defined by mutagenesis (FIG. 7).

Antagonist-induced active conformation. Binding of natural ligands to integrins induces exposure of neoepitopes referred to as ligand-induced binding site (LIBS) epitopes[20,52–55]. The exposure of LIBS epitopes is a consequence of conformational changes, and is usually induced by activation as well as binding of ligands. Some, if not all, small-molecule antagonists of αIIbβ3 induce LIBS epitopes just as natural ligands do, indicating that the antagonists induce the active conformation (FIG. 9a–c)[56–58].

Two-step binding kinetics also demonstrate that a conformational rearrangement occurs on ligand binding. Two-step kinetics have been demonstrated for both the binding of purified fibrinogen to purified integrin αIIbβ3 (REFS 59,60), and the binding of fluorescent RGD peptidomimetics to αIIbβ3 on intact platelets[61]. In a fast reaction, a low-affinity complex is first formed. In a reaction with slower kinetics, the low-affinity complex is converted to a higher-affinity complex. The $t_{1/2}$ for conversion by peptidomimetics is 11–16 seconds (REF. 61). These findings are consistent with observations that cyclic RGD peptides bind to the bent, low-affinity conformation of αvβ3 (REF. 35) (FIG. 3a), and induce conversion to the extended conformation with open headpiece[23] (FIG. 3c).

Most ligand-mimetic antagonists induce LIBS epitopes that are topographically widely distributed over the αIIb and β3 subunits, whereas some, such as lamifiban (Ro44-9883) and tirofiban (MK383), induce only a subset of LIBS[58,62]. Some antagonists, including tirofiban and lamifiban, bind to the active form of αIIbβ3 with markedly higher affinity than to the inactive form, similarly to the natural ligand fibrinogen. Others, such as L-736622, bind to active and inactive forms with equal affinity, similarly to the disintegrin echistatin[50].

In addition to the induction of the active conformation, high-affinity small-molecule antagonists of αIIbβ3 tighten association between the α- and β-subunits. When αIIbβ3 is incubated in SDS at room temperature, the non-covalently-associated subunits separate and migrate as α- and β-monomers in SDS-PAGE. However, when pre-treated with high-affinity small-molecule antagonists or echistatin, αIIbβ3 migrates as an α/β complex in SDS-PAGE[63-65]. Formation of the SDS-stable α/β complex requires cations, possibly because of the metal requirement for antagonist binding to the I-like domain MIDAS. A fragment of αIIbβ3 containing only headpiece domains is also stabilized as a dimer in SDS-PAGE by a high-affinity antagonist[19]. This shows that it is the α-subunit β-propeller interface with the β-subunit I-like domain that is stabilized by the compounds, which is consistent with compound binding across this interface.

All clinically approved αIIbβ3 antagonists elicit THROMBOCYTOPAENIA in a small subgroup of up to 2% of patients[6,10,66]. The exposure of neoepitopes by ligand-mimetic antagonists is an obvious concern, although the antibody antagonist abciximab, which does not induce neoepitopes, also elicits thrombocytopaenia. Recently, drug-dependent antibodies against αIIbβ3 have been associated with the incidence of thrombocytopaenia in trials of the oral αIIbβ3 antagonist roxifiban[10,66]. Interestingly, the antibodies show specificity for the αIIbβ3–antagonist complex; that is, a lack of, or limited, crossreactivity with αIIbβ3 complexed with chemically distinct antagonists. Furthermore, drug-dependent antibodies were found to pre-exist in the general population at a frequency of 1%[66].

Agonistic effects of antagonists. The functional consequences of the antagonist-induced active conformation have been hotly debated[6,67,68]. Agonistic effects of antagonists have been demonstrated with RGD peptides and small-molecule antagonists that are known to induce LIBS[56,57]. Purified αIIbβ3, pre-incubated with RGD peptide, followed by removal of bound peptide, is activated for binding to soluble fibrinogen, whereas the continued presence of RGD peptide inhibits fibrinogen binding. When platelets are incubated with RGD or small-molecule antagonists, then fixed, and washed to remove the antagonists, fibrinogen binding is activated. So, antagonists not only expose LIBS epitopes but also induce the high-affinity ligand-binding conformation. By contrast, on intact, unfixed platelets, the antagonist-induced active conformation is reversible and does not persist after the antagonist is washed out[56,68]. The reversibility of the antagonist-induced active conformation in intact platelets has important implications for the development of therapeutics, because without it drug clearance would be expected to result in enhanced platelet aggregation. Membrane and/or cytoplasmic interactions have been proposed to explain the reversal in the antagonist-induced active conformation that is seen in intact platelets but not in purified αIIbβ3 (REF. 57).

Figure 6 | **Ribbon diagram of the αL I domain in complex with an α I allosteric antagonist**[95]. The I domain adopts a Rossmann fold in which the central β-strands (green) are surrounded by seven α-helices (blue). A Mg^{2+} ion (yellow) is located at the metal-ion-dependent adhesion site (MIDAS) on the 'top' of the domain, whereas the C and the N termini, which connect to the β-propeller domain, are on the bottom. The α I allosteric antagonist (shown by a space-filling representation with silver carbon atoms and red oxygen atoms) binds in the hydrophobic pocket underneath the C-terminal α-helix and stabilizes the I domain in the closed conformation. The side chains within the antagonist-binding pocket are shown with gold bonds and carbon atoms, red oxygen atoms, and blue nitrogen atoms. The residues crucial for binding to ICAM-1 and ICAM-2 are shown with purple side chains and yellow sulphur, red oxygen, and blue nitrogen atoms. Note that these residues are located around the MIDAS, distal from the antagonist binding site.

A striking feature of integrins is their ability to transmit signals bi-directionally across membranes, and so the induction of an active conformation by antagonists raises the question of whether they could trigger outside–in signalling in a manner similar to natural ligands. However, antagonists fail to trigger Ca^{2+} signalling in resting platelets, although after pre-activation by thrombin, antagonists could elicit Ca^{2+} signalling indirectly via thromboxane A_2 production[58]. Antagonists did not induce degranulation as measured by P-selectin expression in resting platelets[69]. In contrast to biological ligands, αIIbβ3 antagonists are monovalent, and this seems to explain their lack of efficacy in initiating outside–in signalling in spite of potent induction of LIBS. Indeed, RGD peptides immobilized on beads, but not in solution, elicit Ca^{2+} signalling through αvβ3 integrin[70].

Integrins lacking I domains: αvβ3

αvβ3 biology. The integrin αvβ3 recognizes a wide range of extracellular matrix ligands, including vitronectin, fibrinogen, fibronectin, thrombospondin,
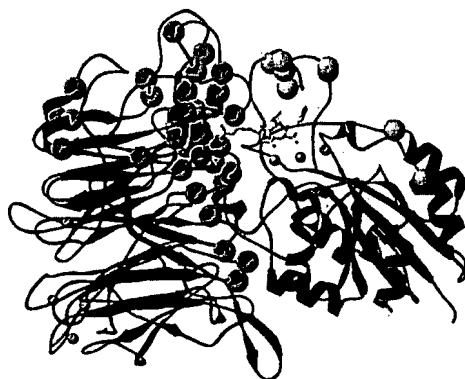
REVIEWS

Figure 7 | αIIbβ3 headpiece and critical residues for ligand binding. The αIIb β-propeller domain is modelled on that of αvβ3. The β-propeller (blue) and the I-like domain (red) are shown as ribbon representations. Critical residues for binding of αIIbβ3 to fibrinogen were identified by mutagenesis and defined as described[37,38] and are shown as Cα-spheres of similar colour to the ribbon backbone. Ca^{2+} ions at the β-propeller and the adjacent to metal-ion-dependent adhesion site of the I-like domain are orange. Mg^{2+} ions at the metal-ion-dependent adhesion site and ligand-associated metal binding site are black and silver, respectively. A cyclic Arg-Gly-Asp (RGD) peptide is shown with yellow bonds and red oxygen atoms and blue nitrogen atoms.

vWF and osteopontin. Cells including smooth muscle cells, endothelial cells, monocytes and platelets express αvβ3. Increased expression of αvβ3 is observed on the vasculature in tumours and on several invasive malignant cells, indicating a role in tumour angiogenesis and metastasis[71]. Inhibition of angiogenesis and tumour cell growth by αvβ3 and αvβ5 antagonists has been seen in vivo[7,71], but, surprisingly, genetic ablation of these receptors does not block angiogenesis and can even enhance it[72]. Among other mononuclear phagocytes, αvβ3 is expressed on osteoclasts, where it has an important function in interacting with the bone matrix and in bone resorption. Antagonists of αvβ3 block bone resorption in vitro and in vivo, making αvβ3 an important target in diseases such as osteoporosis[73].

Antagonist action and effects on conformation. Antagonists of αvβ3 (FIG. 8a) are RGD mimetics that were developed to be selective for αvβ3 as compared with αIIbβ3, and compared with integrins containing the αv subunit associated with other integrin β-subunits (αvβ1, αvβ5, αvβ6 and αvβ8; FIG. 1). The specificity of cyclic-RGD-containing peptides for αvβ3 over αIIbβ3 was achieved by chemically favouring a type I β-turn over a type II β-turn[74]. This alteration of the β-turn changes the orientation of the Arg residue that binds to the α-subunit relative to the Asp residue that binds to the β-subunit, thereby affecting α-subunit specificity. Similarly, non-peptidic antagonists that are selective for αIIbβ3 can be converted to selectivity for αvβ3 by chemically altering the structure and orientation of the basic moiety that mimics the Arg guanidinium group[51]. In agreement with this finding, the salt bridges that αv

and αIIb β-propeller domains form with the Arg guanidinium group must differ. In the αvβ3–cyclic RGD crystal structure, Asp residues in the loops connecting β-propeller blades 2 and 3, and connecting blades 3 and 4, donate salt bridges[35]. In each of these loops in αIIb, an Asp is not present in the same position, but an Asp residue is present one residue further towards the C terminus in the same loop.

As described above, αvβ3 antagonists bind to the bent, low-affinity conformation of αvβ3 (REF. 35) and induce conversion to the extended, high-affinity conformation[23] and exposure of LIBS epitopes[75,76]. High-affinity αvβ3 antagonists stabilize association of the αv and β3 subunits in SDS[65]. An interesting agonist activity of a cyclic RGD antagonist has been observed[77]. At concentrations near the K_D of the antagonist, it stimulated binding of purified αvβ3 to multiple ligands, whereas at higher concentrations it inhibited binding; however, a similar agonistic effect on native cell-surface αvβ3 has not been reported.

Integrins lacking I domains: α4β1

α4β1 biology. The integrin α4β1 is expressed on lymphocytes and monocytes, as well as on some connective tissue cells. There is a transient requirement for α4 in placentation and early heart development; however, in adult animals α4 is much more important in immune function[78]. α4β1 also functions in interactions between bone marrow stromal cells and haematopoietic progenitor cells, particularly B-cell progenitors. α4β1 is important in physiological lymphocyte trafficking, as well as in leukocyte migration during inflammation, and is implicated in the pathogenesis of autoimmune and allergic diseases[9,79]. Furthermore, a monoclonal antibody to α4 has shown therapeutic benefit in controlled trials in multiple sclerosis and Crohn's disease patients[80,81]. α4β1 binds to the immunoglobulin superfamily (IgSF) molecule vascular cell adhesion molecule-1 (VCAM-1) on vascular endothelial cells, and mediates both rolling and firm adhesion in shear flow[2,82]. α4β1 also binds to fibronectin in the extracellular matrix.

Structural features of biological ligands. In contrast to other integrins, including αIIbβ3, αvβ3, and α5β1, which bind to the RGD motif in the tenth fibronectin type 3 (FN3) module of fibronectin, α4β1 binds to a distinct site. α4β1 binds to an LDV motif in fibronectin which is present in an alternatively spliced region following the fourteenth FN3 module. This region is termed connecting segment 1 (CS-1), and is non-homologous to the fibronectin type 1, type 2 and type 3 modules.

VCAM-1 contains six tandem IgSF domains. α4β1 recognizes both domains 1 and 2. The most crucial site for recognition is an Asp residue in an IDS motif that protrudes from domain 1 near the interface with domain 2. The three-dimensional structure of domains 1 and 2 of VCAM-1 shows that the short loop bearing the IDS sequence is highly ordered[83], in contrast to the flexible, long loop bearing the RGD sequence in FN3 module 10 of fibronectin[84]; a structure for the CS-1 segment of fibronectin is not yet available.
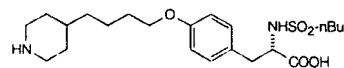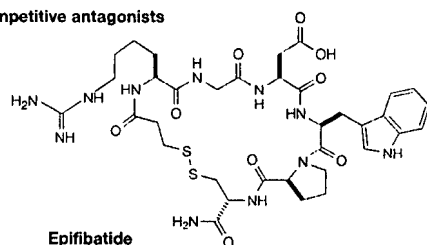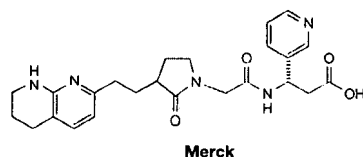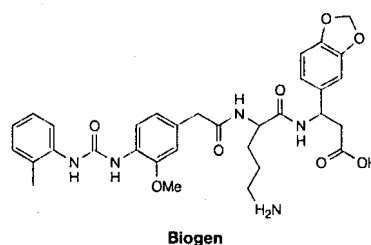
a α/β I-like competitive antagonists

αIIbβ3

Epifibatide

Tirofiban

αvβ3

Merck

SmithKline-Beecham (SB-265123)

α4β1

Roche

Biogen

b α I allosteric antagonists

BIRT0377
Boehringer-Ingelheim

LFA703
Novartis

A-286982
ICOS/Abbott/Biogen

c α/β I-like allosteric β2 antagonists and comparison to α/β I-like competitive α4 antagonists

α4β1

αLβ2 ± αMβ2

Compound 3
Genentech

Compound 4
Genentech

XVA143
Roche

Compound 1
Genentech

Tanabe

Figure 8 | **Chemical structures of small-molecule integrin antagonists. a** | α/β I-like competitive antagonists. Two clinically approved small-molecule antagonists of αIIbβ3 (REF. 6), two representative αvβ3 antagonists[109,110], and two representative α4β1 antagonists[14] are shown. **b** | α I allosteric antagonists. BIRT0377 (REF. 96), LFA703 (REF. 111), and A-286982 (REF. 97) are shown. **c** | α/β I-like allosteric β2 antagonists compared with α/β I-like competitive α4 antagonists. The antagonists are all poly-substituted (S)-2-benzoylaminopropionic acids. Compounds 1, 3, 4 (REFS 102,103), XVA143 (REFS 98,101), and a Tanabe α4β1 antagonist[14] are shown. The integrins antagonized by these compounds, which both contain I domains (αLβ2 and αMβ2) and lack I domains (α4β1) are indicated.

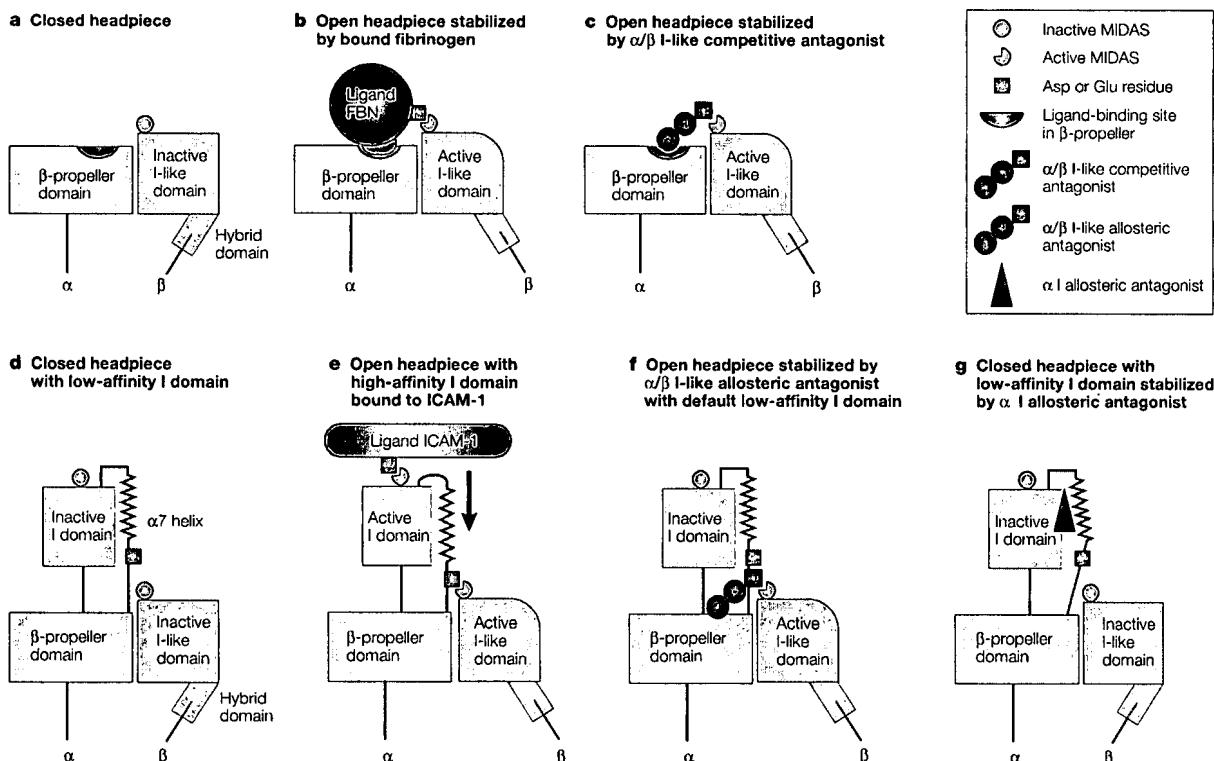**a** Closed headpiece

b Open headpiece stabilized by bound fibrinogen

c Open headpiece stabilized by α/β I-like competitive antagonist

d Closed headpiece with low-affinity I domain

e Open headpiece with high-affinity I domain bound to ICAM-1

f Open headpiece stabilized by α/β I-like allosteric antagonist with default low-affinity I domain

g Closed headpiece with low-affinity I domain stabilized by α I allosteric antagonist

Figure 9 | **Mechanisms of inhibition and impact on integrin conformation of small-molecule antagonists.** Cartoons illustrate conformational changes in the headpiece of a representative integrin that lacks an I domain, αIIbβ3 (a–c), and a representative integrin that contains an I domain, αLβ2 (d–g). For clarity, only headpiece domains are shown, and domains in legs are simplified as lines. The outward-oriented (obtuse angled) hybrid domain correlates with exposure of activation-dependent epitopes in the legs and adoption of the extended conformation. FBN, fibrinogen; ICAM-1, intercellular adhesion molecule-1; MIDAS, metal-ion-dependent adhesion site.

Antagonist action and effects on conformation. Starting from cyclic peptides or random screening, a wide variety of small-molecule α4β1 antagonists have been developed, all of which contain a crucial carboxyl group that mimics the Asp of the LDV or IDS sequences[14,15,17] (FIG. 8a). Chemical crosslinking demonstrated binding of one of these antagonists to the MIDAS loops of the β1 I-like domain, which confirms binding to the same site as biological ligands[85]. Mutagenesis has demonstrated the importance of the β1 I-like domain MIDAS and nearby α4 β-propeller loops in the binding of fibronectin and VCAM-1 (REF. 86). An LDV peptide that blocks α4β1-mediated adhesion induces LIBS epitopes[54,87]. Therefore, ligand mimetics seem to stabilize α4β1 integrin in an active conformation. Multiple affinity states of α4β1 are revealed by binding of a fluorescent LDV peptide derivative[88].

Integrins containing I domains: β2 integrins

Biology of β2 integrins. The β2 integrins (αLβ2 or lymphocyte function-associated protein-1; αMβ2 or Mac-1; αXβ2 or p150,95; and αDβ2) (FIG. 1) are expressed exclusively on leukocytes. αLβ2 and αMβ2 are crucial in leukocyte migration into sites of inflammation, and, in the case of αLβ2, into lymphoid tissues

(BOX 2) (REFS 2,89). αLβ2 is required for a wide variety of cell–cell interactions, including T cells with antigen-presenting cells, B cells with T cells, and natural killer cells with target cells, and acts as a co-stimulatory molecule in essentially all T-cell responses, which correlates with its participation in the formation of the IMMUNO-LOGICAL SYNAPSE[90]. As shown by mutation of the β2 integrin subunit in leukocyte adhesion deficiency I, β2 integrins are essential for host defence against microorganisms. Furthermore, β2 integrins are important in the pathogenesis of leukocyte-mediated tissue injuries in inflammation and autoimmunity[13]. Of the leukocyte integrins, only αLβ2 is expressed on most lymphocytes, whereas αMβ2 predominates on neutrophils (αLβ2 and αXβ2 are also present). Diseases in which neutrophils are important, such as cerebral and myocardial infarction and shock, have usually been targeted with antagonists of all β2 integrins or of αMβ2. By contrast, diseases in which lymphocytes are important, such as psoriasis, rheumatoid arthritis, and organ transplant rejection, have usually been targeted with antagonists specific for αLβ2 (REFS 5,12,13,91). Phase III clinical trials in psoriasis with a monoclonal antibody against the αL I domain have been successfully concluded[11].

IMMUNOLOGICAL SYNAPSE
T-cell recognition of an antigen presenting cell (APC), which is the initial and crucial process in the antigen-specific immune response, takes place at the nanometer-scale gap of the interface between the T cell and APC. This interface is a specialized cell–cell junction, at which crucial signals to initiate and maintain the immune response are transduced from APC to T cell or vice versa. The interface is called an immunological synapse after the neuronal synapse, a segregated gap through which information is transmitted in chemical form (neurotransmitter) from one neuron to another.

Structural features of ligands for β2 integrins. αLβ2 binds exclusively to IgSF cell-surface molecules termed intercellular adhesion molecules (ICAMs), whereas αMβ2 binds to ICAM-1, fibrinogen, complement component iC3b and many other protein ligands. The major endothelial ligand for both αLβ2 and αMβ2 is ICAM-1, which comprises five tandem Ig-like domains[92]. The binding sites for αLβ2 and αMβ2 are located in domain 1 and domain 3 of ICAM-1, respectively. An acidic residue, Glu-34, in domain 1 of ICAM-1 directly ligates the metal at the MIDAS motif of the αL I domain, as recently shown by X-ray crystallography[32] (FIG. 4). In contrast to the crucial Asp in VCAM-1, which is in a protruding loop, the crucial Glu of ICAM-1 is present in a β-sheet in a relatively flat surface[83]. A different acidic residue in domain 3 is implicated in recognition by the αM I domain[93].

Antagonist action and effects on conformation

Direct inhibition of ligand binding to the I domain. As the top face of the I domain around the MIDAS directly binds ligands, binding of inhibitors to the same site on the I domain is a straightforward way to block function competitively. Indeed, many inhibitory antibodies map to the I domain[28,94]. Although most inhibitory I domain antibodies directly block ligand binding, some that bind more distal to the MIDAS inhibit ligand binding indirectly, similarly to the α I allosteric antagonists discussed below[41].

Allosteric I domain inhibitors. As discussed above, the affinity of the I domain is allosterically regulated by conformational change. Downward axial displacement of the C-terminal helix is linked to structural rearrangements at the ligand-binding site, the MIDAS (FIG. 5 and 9d,e). One class of small-molecule inhibitors, termed α I allosteric antagonists (FIG. 8b), bind underneath the C-terminal α-helix of the αL I domain (FIG. 6) (REFS 95–97). The antagonists bind to and stabilize the closed conformation of the I domain, inhibit conversion to the high-affinity, open conformation, and thereby allosterically inhibit ligand binding to the distal MIDAS site (FIG. 9g). The mode of action of the antagonists is confirmed by a

mutant αL I domain that is locked in the open, high-affinity conformation with an engineered disulphide bond that stabilizes the position of the C-terminal α-helix (the high-affinity I domain)[30,40,41]. αLβ2 containing the locked open, high-affinity I domain is resistant to inhibition by α I allosteric antagonists[41].

Binding of α I allosteric antagonists to the pocket under the C-terminal α-helix of the I domain affects not only the conformation of the I domain regionally, but also the conformation of the αLβ2 heterodimer globally. Some α I allosteric antagonists perturb the binding of antibodies against the I-like domain[98]. Furthermore, the antagonists reduce exposure by the activating agent Mn^{2+} of activation-dependent epitopes in the β2 I-like domain, as well as in the α- and β-subunit legs[99,100]. Downward movement of the I domain C-terminal helix seems to be a prerequisite for binding of the intrinsic ligand Glu-310 in the αL I domain linker to the MIDAS of the β2 I-like domain (FIG. 9). In the absence of this interaction, activation of the I-like domain is inhibited, as shown by suppression of exposure by Mn^{2+} of an epitope in the I-like domain. Suppression of epitope exposure in the α- and β-legs shows that the α I allosteric antagonists shift the conformational equilibrium toward the bent conformation. Therefore, the conformation of the I domain is linked, apparently through the I-like domain, to the conformation of the leg domains. These results highlight the extensiveness of conformational linkages within integrins.

α/β I-like allosteric antagonists. The I-like domain of the β2 subunit of αLβ2 is a regulatory domain[41]. A class of αLβ2 and αMβ2 small-molecule antagonists patented by Roche and Genentech[101,102] (FIG. 8c) has recently been found to perturb the interface between the I domain and the I-like domain[98,100]. These inhibitors are polysubstituted (S)-2-benzoylaminopropionic acids, in common with some inhibitors of α4β1, which lacks an I domain (FIG. 8). Indeed, compound 1, which was used as a lead to develop αLβ2 and αMβ2 antagonists at both Genentech and Roche, was initially discovered during random screening as an α4β1 antagonist at Roche, and inhibits

---

Box 2 | **Multi-step model of leukocyte migration**

Infiltration and accumulation of leukocytes in the extravascular space is a hallmark of inflammation. Leukocyte–endothelial cell interaction, which involves multiple processes mediated by adhesion molecules and chemokines, is crucial in guiding leukocytes from the blood stream to the site of inflammation[2]. The initial step is rolling, which is mediated by selectins and their carbohydrate ligands and, additionally, α4 integrins. The rapid k_{on} and k_{off} of selectin–carbohydrate ligand interaction allows flowing leukocytes to tether and roll along endothelial cells under shear flow. Rolling slows down flowing leukocytes and places them in proximity to endothelial cells where chemokines are transported and expressed. Rolling facilitates encounter of leukocytes that express chemokine receptors to the corresponding chemokines presented on the apical surface of the endothelial cells. The second step is activation of G-protein-coupled receptors on leukocytes by the chemokine, which triggers signals that activate integrins. In turn, the ligand-binding activity of integrins is rapidly enhanced by inside–out signalling. Binding of integrins to ligands on endothelium such as intercellular adhesion molecule-1 mediate firm adhesion and arrest of the leukocyte on the endothelium. These three steps take place in sequence but not in parallel. So, inhibition of any one of the three steps results in essentially complete blockade of leukocyte migration. Although the β2 integrins, αMβ2 and αLβ2, are most generally utilized in neutrophil and lymphocyte migration, respectively, α4 integrins such as α4β1 and α4β7 also participate in leukocyte migration, and play a pivotal role in certain tissues. The α4β1 and α4β7 integrins mediate rolling adhesion prior to activation, and firm adhesion after activation.

αLβ2 and α4β1 with similar micromolar potency. This novel class of αLβ2 antagonists cannot inhibit the binding of isolated wild-type or mutant intermediate-affinity or high-affinity I domains to ICAM-1, whereas purified ICAM-1 does inhibit these binding interactions[100]. Therefore, the Genentech compounds do not mimic ICAM-1, as previously suggested[103]. Furthermore, these inhibitors bind to αLβ2, even when the α I domain is deleted, but do not bind when the I-like domain MIDAS is mutated[100]. They can demonstrate α-subunit selectivity, indicating that a portion of the α-subunit near the I-like domain — probably the β-propeller domain — might be involved in binding. Therefore, they are designated as α/β I-like allosteric antagonists.

As described above, the α I domain seems to be activated when the β I-like domain binds to a conserved Glu residue in the linker following the I domain; that is, the intrinsic ligand. The findings indicate that α/β I-like allosteric antagonists bind to the MIDAS of the β2 I-like domain as mimics of the intrinsic ligand, competitively inhibit binding of the intrinsic ligand in the I domain linker to the I-like domain, and consequently leave the I domain in the low-energy, inactive, closed conformation (FIG. 9f). At the same time, the α/β I-like allosteric antagonists stabilize the I-like domain in its active configuration by mimicking intrinsic ligand binding, as shown by induction of activation epitopes in the β2 I-like domain and αL and β2 legs[100]. So, as a consequence of I-like domain activation, the α/β allosteric antagonists stabilize the extended integrin conformation. It is interesting that the antagonists inhibit I domain activation, whereas they stabilize the rest of the integrin in the active conformation.

Most α I allosteric antagonists are highly selective for αLβ2. When α/β I-like allosteric antagonists have been tested against integrins in addition to αLβ2, cross-reactivity against αMβ2 and αXβ2 has been observed with selectivity usually close to 1 (no selectivity) and always less than 100-fold[98,100]. However, IC_{50} values differ among antagonists. It has been possible to build α-subunit selectivity into αvβ3 and αIIbβ3 antagonists as discussed above. The α/β I-like allosteric antagonists of β2 integrins seem to bind to an analogous site at the I-like domain interface with the β-propeller, and it should be possible to chemically build in selectivity for αLβ2 and αMβ2.

Like α/β I-like allosteric antagonists, antibodies to the β2 I-like domain block ligand binding indirectly[41]. However, in contrast to the α/β I-like allosteric antagonists that stabilize the I-like domain in the active conformation, inhibitory I-like domain monoclonal antibodies stabilize the I-like domain in the inactive conformation and inhibit induction of activation epitopes (A. Salas et al., personal communication).

So far, all potent small-molecule antagonists of I-domain-containing integrins are allosteric inhibitors, whereas antagonists of integrins that lack I domains are ligand-mimetic, competitive inhibitors. It will be interesting to see whether potent, competitive small-molecule antagonists of I-domain-containing integrins can be discovered.

Other integrins

The integrins reviewed above are sufficient to illustrate the three different classes of integrin antagonists to date: α/β I-like competitive antagonists, α/β I-like allosteric antagonists, and α I allosteric antagonists. These integrins were chosen because they illustrate particularly well the mutually beneficial relationship between integrin drug discovery and our understanding of integrin structure and function. Nonetheless, it should be emphasized that there are other integrins that are important therapeutic targets. Among these are α4β7 and α1β1, which will be covered very briefly.

α4β7 overlaps to some extent with α4β1 in specificity, but also recognizes mucosal addressin cell adhesion molecule-1 (MAdCAM-1), and is important in trafficking of lymphocytes to mucosal tissues[2,82]. Studies in animal models with an antibody specific to α4β7 validate it as a target in ulcerative colitis and Crohn's disease[104]. Both selective α4β7 and dual-acting α4β1 and α4β7 small-molecule antagonists have been developed. The efficacy of an antibody to α4, which inhibits both α4β1 and α4β7, in Crohn's disease and multiple sclerosis clinical trials[80,81] indicates that dual-acting α4β1 and α4β7 small-molecule antagonists[14,17] might have an attractive clinical profile.

α1β1, in addition to α2β1, α10β1 and α11β1, contains an I domain that binds to collagen[1,78] (FIG. 1). α1β1 is expressed on chronically activated, but not on resting, T lymphocytes, and an antibody against α1β1, and to a lesser extent α2β1, shows efficacy in a wide variety of animal models of autoimmune disease[105]. Apparently, α1β1 is important in T-cell migration or co-stimulation after these cells enter inflammatory sites. It should be possible to develop α/β I-like allosteric antagonists that block activation of the α1 I domain, in a manner analogous to those that block β2 integrins. Indeed, the chemical relationship described above between α4β1 α/β I-like competitive antagonists and αLβ2 α/β I-like allosteric antagonists suggests that α4β1 competitive antagonists would be good starting points for the development of α1β1 α/β I-like allosteric antagonists.

Concluding perspectives

Integrin antagonists are already well established as therapeutics for cardiovascular disease, and other applications including inflammatory disease seem extremely promising. Work with small-molecule antagonists has enhanced our understanding of the multiple structural linkages between integrin domains that enable bi-directional communication between the ligand-binding site and the cytoplasmic domains, and which regulate transitions between the bent, low-affinity conformation and the extended, high-affinity conformation. Conversely, structural studies on integrins, and mutational studies that stabilize particular conformations of integrins, have yielded important insights into the binding sites for antagonists and their mechanisms of action. The finding that both competitive antagonists and allosteric antagonists affect integrin conformation has important clinical implications. Most antagonists stabilize the extended,

high-affinity integrin conformation, in which neoepitopes are exposed. However, one class of antagonists of the integrin I domain stabilizes the bent, low-affinity conformation. It should be possible to develop a new class of antagonists of integrins lacking I domains that selectively bind to and stabilize the bent conformation; for example, compounds that would bind to and stabilize the extensive inter-domain interfaces that are present in the bent, but not in the extended, integrin conformations[23]. Further structural work on integrins and their complexes should accelerate the development of current and novel classes of integrin antagonists.

1. Hynes, R. O. Integrins: versatility, modulation, and signaling in cell adhesion. *Cell* 69, 11–25 (1992).
2. Springer, T. A. Traffic signals for lymphocyte recirculation and leukocyte emigration: the multi-step paradigm. *Cell* 76, 301–314 (1994).
3. Humphries, M. J. Integrin structure. *Biochem. Soc. Trans.* 28, 311–339 (2000).
4. Shimaoka, M., Takagi, J. & Springer, T. A. Conformational regulation of integrin structure and function. *Annu. Rev. Biophys. Biomol. Struct.* 31, 485–516 (2002).
   Comprehensively reviews conformational changes of integrins with emphasis on the conformational regulation of ligand binding by I domains.
5. Curley, G. P., Blum, H. & Humphries, M. J. Integrin antagonists. *Cell. Mol. Life Sci.* 56, 427–441 (1999).
6. Scarborough, R. M. & Gretler, D. D. Platelet glycoprotein IIb-IIIa antagonists as prototypical integrin blockers: novel parenteral and potential oral antithrombotic agents. *J. Med. Chem.* 43, 3453–3473 (2000).
7. Varner, J. A. & Cheresh, D. A. Tumor angiogenesis and the role of vascular cell integrin αvβ3. *Important Adv. Oncol.* 69–87 (1996).
8. Giblin, P. A. & Kelly, T. A. Antagonists of β2 integrin-mediated cell adhesion. *Annu. Rep. Med. Chem.* 36, 181–190 (2001).
9. Yusuf-Makagiansar, H., Anderson, M. E., Yakovleva, T. V., Murray, J. S. & Siahaan, T. J. Inhibition of LFA-1/ICAM-1 and VLA-4/VCAM-1 as a therapeutic approach to inflammation and autoimmune diseases. *Med. Res. Rev.* 22, 146–167 (2002).
10. Bennett, J. S. Novel platelet inhibitors. *Annu. Rev. Med.* 52, 161–184 (2001).
11. Cather, J. C. & Menter, A. Modulating T cell responses for the treatment of psoriasis: a focus on efalizumab. *Expert Opin. Biol. Ther.* 3, 361–370 (2003).
12. Harlan, J. M. & Winn, R. K. Leukocyte–endothelial interactions: clinical trials of anti-adhesion therapy. *Crit. Care Med.* 30, S214–S219 (2002).
13. Harlan, J. M., Winn, R. K., Vedder, N. B., Doerschuk, C. M. & Rice, C. L. in *Adhesion: Its Role in Inflammatory Disease* (eds Harlan, J. R. & Liu, D.) 117–150 (W. H. Freeman, New York, 1992).
14. Jackson, D. Y. α4 integrin antagonists. *Curr. Pharm. Des.* 8, 1229–1253 (2002).
15. Lin, K. C. & Castro, A. C. Very late antigen 4 (VLA4) antagonists as anti-inflammatory agents. *Curr. Opin. Chem. Biol.* 2, 453–457 (1998).
16. Liu, G. Inhibitors of LFA-1/ICAM-1 interaction: from monoclonal antibodies to small molecules. *Drugs Future* 26, 767–778 (2001).
17. Tilley, J. W., Chen, L., Sidduri, A. & Fotouhi, N. The discovery of VLA-4 antagonists. *Curr. Med. Chem. Rev.* (in the press).
18. Xiong, J.-P. et al. Crystal structure of the extracellular segment of integrin αVβ3. *Science* 294, 339–345 (2001).
   The landmark determination of the crystal structure of αvβ3, which demonstrated an unexpected V-shape, or the bent conformation.
19. Beglova, N., Blacklow, S. C., Takagi, J. & Springer, T. A. Cysteine-rich module structure reveals a fulcrum for integrin rearrangement upon activation. *Nature Struct. Biol.* 9, 282–287 (2002).
   NMR structure determination of integrin EGF-like domains where activating and activation-dependent epitopes map. Superposition of the integrin EGF-like domains onto the structure of the bent conformation showed these epitopes buried in the bent conformation, strongly indicating that it represents the low-affinity conformation.
20. Du, X. et al. Long range propagation of conformational changes in integrin αIIbβ3. *J. Biol. Chem.* 268, 23087–23092 (1993).
21. Takagi, J., Erickson, H. P. & Springer, T. A. C-terminal opening mimics 'inside-out' activation of integrin α5β1. *Nature Struct. Biol.* 8, 412–416 (2001).
22. Weisel, J. W., Nagaswami, C., Vilaire, G. & Bennett, J. S. Examination of the platelet membrane glycoprotein IIb-IIIa complex and its interaction with fibrinogen and other ligands by electron microscopy. *J. Biol. Chem.* 267, 16637–16643 (1992).
23. Takagi, J., Petre, B. M., Walz, T. & Springer, T. A. Global conformational rearrangements in integrin extracellular domains in outside-in and inside-out signaling. *Cell* 110, 599–611 (2002).
   EM image reconstruction, hydrodynamic and ligand-binding studies on αvβ3 revealed that low-affinity bent conformation is converted by activation to the high-affinity extended conformation, which is further stabilized by ligand binding.
24. Luo, B.-H., Springer, T. A. & Takagi, J. Stabilizing the open conformation of the integrin headpiece with a glycan wedge increases affinity for ligand. *Proc. Natl Acad. Sci. USA* 100, 2403–2408 (2003).
25. Lee, J.-O., Rieu, P., Arnaout, M. A. & Liddington, R. Crystal structure of the A domain from the α subunit of integrin CR3 (CD11b/CD18). *Cell* 80, 631–638 (1995).
26. Huang, C., Zang, Q., Takagi, J. & Springer, T. A. Structural and functional studies with antibodies to the integrin β2 subunit: a model for the I-like domain. *J. Biol. Chem.* 275, 21514–21524 (2000).
27. Springer, T. A. Folding of the N-terminal, ligand-binding region of integrin α-subunits into a β-propeller domain. *Proc. Natl Acad. Sci. USA* 94, 65–72 (1997).
28. Diamond, M. S., Garcia-Aguilar, J., Bickford, J. K., Corbi, A. L. & Springer, T. A. The I domain is a major recognition site on the leukocyte integrin Mac-1 (CD11b/CD18) for four distinct adhesion ligands. *J. Cell Biol.* 120, 1031–1043 (1993).
29. Michishita, M., Videm, V. & Arnaout, M. A. A novel divalent cation-binding site in the A domain of the β2 integrin CR3 (CD11b/CD18) is essential for ligand binding. *Cell* 72, 857–867 (1993).
30. Shimaoka, M., Lu, C., Palframan, R., von Andrian, U. H., Takagi, J. & Springer, T. A. Reversibly locking a protein fold in an active conformation with a disulfide bond: integrin αL I domains with high affinity and antagonist activity *in vivo*. *Proc. Natl Acad. Sci. USA* 98, 6009–6014 (2001).
   An engineered disulphide bridge to lock the open conformation of the αL I domain resulted in 10,000-fold increase in ligand-binding affinity to ICAM-1.
31. Huth, J. R. et al. NMR and mutagenesis evidence for an I domain allosteric site that regulates lymphocyte function-associated antigen 1 ligand binding. *Proc. Natl Acad. Sci. USA* 97, 5231–5236 (2000).
32. Shimaoka, M. et al. Structures of the αL I domain and its complex with ICAM-1 reveal a shape-shifting pathway for integrin regulation. *Cell* 112, 99–111 (2003).
   Crystal structure determination of the multiple conformations of the αL I domain with distinct ligand-binding affinity demonstrated shape-shifting pathway for activation by a downward movement of the C-terminal helix.
33. Emsley, J., Knight, C. G., Farndale, R. W., Barnes, M. J. & Liddington, R. C. Structural basis of collagen recognition by integrin α2β1. *Cell* 101, 47–56 (2000).
   The important determination of the open conformation of the α2 I domain in complex with collagen-like peptides demonstrated the significance of the conformational changes induced by ligand binding.
34. Takagi, J., Kamata, T., Meredith, J., Puzon-McLaughlin, W. & Takada, Y. Changing ligand specificities of αvβ1 and αvβ3 integrins by swapping a short diverse sequence of the β subunit. *J. Biol. Chem.* 272, 19794–19800 (1997).
35. Xiong, J. P. et al. Crystal structure of the extracellular segment of integrin αVβ3 in complex with an Arg-Gly-Asp ligand. *Science* 296, 151–155 (2002).
36. Takagi, J. & Springer, T. A. Integrin activation and structural rearrangement. *Immunological Rev.* 186, 141–163 (2002).
37. Puzon-McLaughlin, W., Kamata, T. & Takada, Y. Multiple discontinuous ligand-mimetic antibody binding sites define a ligand binding pocket in integrin αIIbβ3. *J. Biol. Chem.* 275, 7795–7802 (2000).
38. Kamata, T., Tieu, K. K., Springer, T. A. & Takada, Y. Amino acid residues in the αIIb subunit that are critical for ligand binding to integrin αIIbβ3 are clustered in the β-propeller model. *J. Biol. Chem.* 276, 44275–44283 (2001).
39. Luo, B.-H., Springer, T. A. & Takagi, J. High affinity ligand binding by integrins does not involve head separation. *J. Biol. Chem.* 178, 17185–17189 (2003).
40. Lu, C., Shimaoka, M., Ferzly, M., Oxvig, C., Takagi, J. & Springer, T. A. An isolated, surface-expressed I domain of the integrin αLβ2 is sufficient for strong adhesive function when locked in the open conformation with a disulfide. *Proc. Natl Acad. Sci. USA* 98, 2387–2392 (2001).
41. Lu, C., Shimaoka, M., Zang, Q., Takagi, J. & Springer, T. A. Locking in alternate conformations of the integrin αLβ2 I domain with disulfide bonds reveals functional relationships among integrin domains. *Proc. Natl Acad. Sci. USA* 98, 2393–2398 (2001).
42. Alonso, J. L., Essafi, M., Xiong, J. P., Stehle, T. & Arnaout, M. A. Does the integrin αA domain act as a ligand for its βA domain? *Curr. Biol.* 12, R340–R342 (2002).
43. Salas, A., Shimaoka, M., Chen, S., Carman, C. V. & Springer, T. A. Transition from rolling to firm adhesion is regulated by the conformation of the I domain of the integrin LFA-1. *J. Biol. Chem.* 277, 50255–50262 (2002).
44. Dustin, M. L. & Springer, T. A. T cell receptor cross-linking transiently stimulates adhesiveness through LFA-1. *Nature* 341, 619–624 (1989).
45. Lollo, B. A., Chan, K. W. H., Hanson, E. M., Moy, V. T. & Brian, A. A. Direct evidence for two affinity states for lymphocyte function-associated antigen 1 on activated T cells. *J. Biol. Chem.* 268, 21693–21700 (1993).
46. Constantin, G. et al. Chemokines trigger immediate β2 integrin affinity and mobility changes: differential regulation and roles in lymphocyte arrest under flow. *Immunity* 13, 759–769 (2000).
47. Vinogradova, O. et al. A structural mechanism of integrin αIIbβ3 'inside-out' activation as regulated by its cytoplasmic face. *Cell* 110, 587–597 (2002).
   A direct association of the αIIb and β3 cytoplasmic tails was demonstrated by NMR structure determination. The association was perturbed by talin head domain or activating mutations in the tail, supporting integrin activation by separation of the cytoplasmic tails.
48. Lu, C., Takagi, J. & Springer, T. A. Association of the membrane-proximal regions of the α and β subunit cytoplasmic domains constrains an integrin in the inactive state. *J. Biol. Chem.* 276, 14642–14648 (2001).
49. Kim, M., Carman, C. V. & Springer, T. A. Bidirectional transmembrane signaling by cytoplasmic domain separation in integrins. *Science* (in the press).
   FRET analysis using CFP and YFP fused to the αL and β2 cytoplasmic tails demonstrated separation of the tails in living cells on activation by chemokine and talin head domain as well as on ligand-binding to ICAM-1 in the presence of Mn²⁺.
50. Bednar, R. A. et al. Identification of low molecular weight GP IIb/IIIa antagonists that bind preferentially to activated platelets. *J. Pharmacol. Exp. Ther.* 285, 1317–1326 (1998).
51. Duggan, M. E. et al. Nonpeptide αVβ3 antagonists. 1. Transformation of a potent, integrin-selective αIIbβ3 antagonist into a potent αVβ3 antagonist. *J. Med. Chem.* 43, 3736–3745 (2000).
52. Shih, D. T., Edelman, J. M., Horwitz, A. F., Grunwald, G. B. & Buck, C. A. Structure/function analysis of the integrin β1 subunit by epitope mapping. *J. Cell Biol.* 122, 1361–1371 (1993).
53. Bazzoni, G., Shih, D.-T., Buck, C. A. & Hemler, M. A. Monoclonal antibody 9EG7 defines a novel β1 integrin epitope induced by soluble ligand and manganese, but inhibited by calcium. *J. Biol. Chem.* 270, 25570–25577 (1995).
54. Takagi, J., Isobe, T., Takada, Y. & Saito, Y. Structural interlock between ligand-binding site and stalk-like region of β1 integrin revealed by a monoclonal antibody recognizing conformation-dependent epitope. *J. Biochem. (Tokyo)* 121, 914–921 (1997).
55. Lu, C., Ferzly, M., Takagi, J. & Springer, T. A. Epitope mapping of antibodies to the C-terminal region of the integrin β2 subunit reveals regions that become exposed upon receptor activation. *J. Immunol.* 166, 5629–5637 (2001).
56. Du, X. et al. Ligands 'activate' integrin αIIbβ3 (platelet GPIIb-IIIa). *Cell* 65, 409–416 (1991).

Summary
- Members of the integrin family of adhesion molecules are non-covalently-associated α/β heterodimers that mediate cell–cell, cell–extracellular matrix and cell–pathogen interactions by binding to distinct, but often overlapping, combinations of ligands.
- Dysregulation of integrins is involved in the pathogenesis of many disease states, from autoimmunity and thrombotic vascular diseases to cancer metastasis, and so extensive efforts have been directed towards the discovery and development of integrin antagonists for clinical applications. Integrin antagonists are already well established as therapeutics for cardiovascular disease, and applications in other therapuetic areas, including inflammatory disease, seem extremely promising.
- Integrin ligand-binding function is tightly linked to molecular conformation. On activation, dramatic rearrangements occur in the overall spatial relationships of integrin domains. Understanding the structural basis of integrin activation in detail is essential for understanding the mechanism of antagonism by therapeutics, as well as for the design of second-generation antagonists with novel mechanisms of action.
- This review discusses examples of the three different classes of integrin antagonists discovered so far: α/β I-like competitive antagonists, α/β I-like allosteric antagonists and α I allosteric antagonists. These examples were chosen because they illustrate particularly well the mutually beneficial relationship between integrin drug discovery and our understanding of integrin structure and function.